ENERGY EFFICIENT RESOURCE ALLOCATION FOR VIRTUAL NETWORK SERVICES WITH DYNAMIC WORKLOAD IN CLOUD DATA CENTERS

A Dissertation
IN
Telecommunications and Computer Networking
and
Computer Science

Presented to the Faculty of the University
of Missouri–Kansas City in partial fulfillment of
the requirements for the degree

DOCTOR OF PHILOSOPHY

by
XINJIE GUAN

M. S., University of Missouri-Kansas City, Missouri, USA, 2014
B. S., Southeast University, Jiangsu, China, 2006

Kansas City, Missouri
2015

ENERGY EFFICIENT RESOURCE ALLOCATION FOR VIRTUAL NETWORK SERVICES WITH DYNAMIC WORKLOAD IN CLOUD DATA CENTERS

Xinjie Guan, Candidate for the Doctor of Philosophy Degree

University of Missouri–Kansas City, 2015

ABSTRACT

With the rapid proliferation of cloud computing, more and more network services and applications are deployed on cloud data centers. Their energy consumption and green house gas emissions have significantly increased. Some efforts have been made to control and lower energy consumption of data centers such as, proportional energy consuming hardware, dynamic provisioning, and virtualization machine techniques. However, it is still common that many servers and network resources are often underutilized, and idle servers spend a large portion of their peak power consumption.

Network virtualization and resource sharing have been employed to improve energy efficiency of data centers by aggregating workload to a few physical nodes and switch the idle nodes to sleep mode. Especially, with the advent of live migration, a virtual node can be moved from one physical node to another physical node without service disruption. It is possible to save more energy by shrinking virtual nodes to a small set of physical

nodes and turning the idle nodes to sleep mode when the service workload is low, and expanding virtual nodes to a large set of physical nodes to satisfy QoS requirements when the service workload is high. When the service provider explicates the desired virtual network including a specific topology, and a set of virtual nodes with certain resource demands, the infrastructure provider computes how the given virtual network is embedded to its operated data centers with minimum energy consumption. When the service provider only gives some description about the network service and the desired QoS requirements, the infrastructure provider has more freedom on how to allocate resources for the network service.

For the first problem, we consider the evolving workload of the virtual networks or virtual applications and residual resources in data centers, and build a novel model of energy efficient virtual network embedding (EE-VNE) in order to minimize energy usage in the physical network consists of multiple data centers. In this model, both operation cost for executing network services' task and migration cost for the live migrations of virtual nodes are counted toward the total energy consumption. In addition, rather than random generated physical network topology, we use practical assumption about physical network topology in our model.

Due to the NP-hardness of the proposed model, we develop a heuristic algorithm for virtual network scheduling and mapping. In doing so, we specifically take the expected energy consumption at different times, virtual network operation and future migration

costs, and a data center architecture into consideration. Our extensive evaluation results show that our algorithm could reduce energy consumption up to 40% and take up to a 57% higher number of virtual network requests over other existing virtual mapping schemes.

However, through comparison with CPLEX based exact algorithm, we identify that there is still a gap between the heuristic solution and the optimal solution. Therefore, after investigation other solutions, we convert the origin EE-VNE problem to an Ant Colony Optimization (ACO) problem by building the construction model and presenting the transition probability formula. Then, ACO based algorithm has been adapted to solve the ACO-EE-VNE problem. In addition, we reduce the space complexity of ACO-EE-VNE by developing a novel way to track and update the pheromone.

For the second problem, we design a framework to dynamically allocate resources for a network service by employing container based virtual nodes. In the framework, each network service would have a pallet container and a set of execution containers. The pallet container requests resource based on certain strategy, creates execution containers with assigned resources and manage the life cycle of the containers; while the execution containers execute the assigned job for the network service. Formulations are presented to optimize resource usage efficiency and save energy consumption for network services with dynamic workload, and a heuristic algorithm is proposed to solve the optimization problem. Our numerical results show that container based resource allocation provides

more flexible and saves more cost than virtual service deployment with fixed virtual machines and demands.

In addition, we study the content distribution problem with joint optimization goal and varied size of contents in cloud storage. Previous research on content distribution mainly focuses on reducing latency experienced by content customers. A few recent studies address the issue of bandwidth usage in CDNs, as the bandwidth consumption is an important issue due to its relevance to the cost of content providers. However, few researches consider both bandwidth consumption and delay performance for the content providers that use cloud storages with limited budgets, which is the focus of this study. We develop an efficient light-weight approximation algorithm toward the joint optimization problem of content placement. We also conduct the analysis of its theoretical complexities. The performance bound of the proposed approximation algorithm exhibits a much better worst case than those in previous studies. We further extend the approximate algorithm into a distributed version that allows it to promptly react to dynamic changes in users' interests. The extensive results from both simulations and Planetlab experiments exhibit that the performance is near optimal for most of the practical conditions.

APPROVAL PAGE

The faculty listed below, appointed by the Dean of the School of Graduate Studies, have examined a dissertation titled "Energy Efficient Resource Allocation for Virtual Network Services with Dynamic Workload in Cloud Data Centers," presented by Xinjie Guan, candidate for the Doctor of Philosophy degree, and hereby certify that in their opinion it is worthy of acceptance.

Supervisory Committee

Baek-Young Choi, Ph.D., Committee Chair
Department of Computer Science & Electrical Engineering

Cory Beard, Ph.D.
Department of Computer Science & Electrical Engineering

Deepankar Medhi, Ph.D.
Department of Computer Science & Electrical Engineering

Ghulam Chaudhry, Ph.D.
Department of Computer Science & Electrical Engineering

Sejun Song, Ph.D.
Department of Computer Science & Electrical Engineering

Xiaojun Shen, Ph.D.
Department of Computer Science & Electrical Engineering

CONTENTS

ILLUSTRATIONS

TABLES

ACKNOWLEDGEMENTS

I would like to express my deepest gratitude to my advisor, Dr. Baek-Young Choi, for her guidance, understanding, patience and full support during my Ph.D. study at University of Missouri-Kansas City. Not only gives many helpful advises on my research work, she also provides many invaluable opportunities and suggestions towards my long-term career goals. She is willing to share her experiences and always encourages me to grow as an independent researcher.

I would like to sincerely thank Dr. Sejun Song, for his inspiring guidance, tutoring and financial support. His insights and comments were significant supports for me to understand software defined networks and to clarify and improve the cost efficient resource allocations work presented in this dissertation.

I am grateful to other committee members of my dissertation, Dr. Cory Beard, Dr. Deep Medhi, Dr. Ghulam Chaudhry, and Dr. Xiaojun Shen for their assistances and suggestions. When I am facing questions, they are always open for discussion.

I would like to thank Dr. Hiroshi Saito, Dr. Ryoichi Kawahara for their mentoring during my internship at NTT Service Integration Laboratories. I would also like to thank my mentors Dr. Xin Wang, Dr. Jiafeng Zhu, Dr. Guoqiang Wang, and Dr. Ravi Ravindran for their great help and suggestions during my internships at Futurewei Technologies Inc.

I also would like to thank my lab mates, Daehee Kim, Hyungbae Park, Sunae Shin and Kaustubh Dhondge for the friendship and their suggestions for my research.

Last and most importantly, I would like to say thank you for my husband, Xili

Wan for his unconditional love, understanding, accompanying and support for my Ph.D. study. Thanks also go to my parents and my son for their encouragement for pursuing my Ph.D. degree.

CHAPTER 1

INTRODUCTION

As the supporting infrastructure of cloud computing services, data centers are rapidly proliferate in recent years. Nowadays, these data centers (DC) are used to deploy large portion of network services and provide large volumes of cost-efficient resources, such as virtual storage (Amazon S3 [5], Dropbox [37]), virtual platform and development tools (Microsoft Azure [100], Google Cloud Platform [91], Amazon EC2 [39]), business applications (Salesforce [97], Workday [121]). It is reported that there were more than 500,000 DCs around the world as of December 2011 [104].

With the fast growth of DCs and services deployed on them, more and more energy has been consumed for DC operating and maintainable. In 2010, between 1.1% and 1.5% of the worldwide total electricity usage was consumed by DCs [70], and their energy costs in the US doubled from 28 billion kWh to 61 billion kWh in six years, according to [1]. In addition, the large energy consumption of DCs not only increases the cost of DC operators, but also impacts our environment through carbon dioxide emission. In 2008, the carbon dioxide emission by global DCs took up to 0.3% of global carbon dioxide emission that was more than some countries, such as Argentina and Netherland [68]. This number is expected to be double in 2020 [117].

Efforts have been made for reducing DC carbon footprint from various aspects in order to save cost and protect environments. Companies, e.g., Google and Facebook

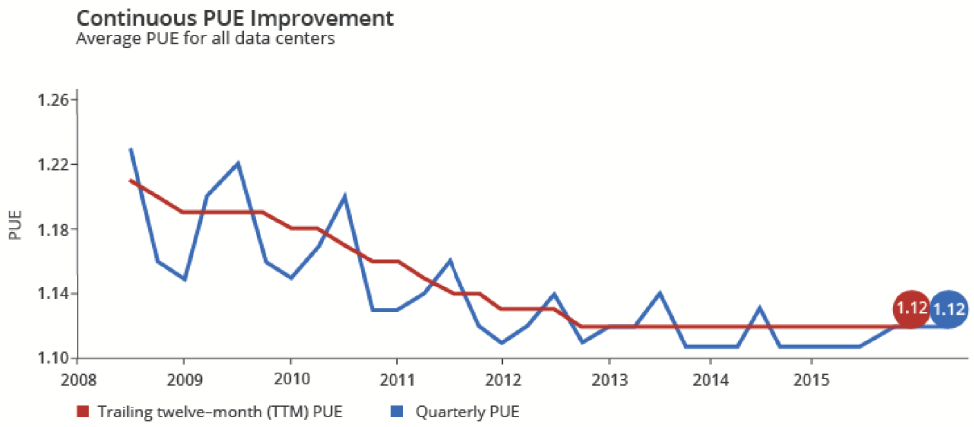

Figure 1: PUE data for all large-scale Google data centers [116]

are greening their DCs through reducing power usage for cooling and other facilities and utilizing renewable energy [51, 83]. Now their DCs have a relatively small Power Utilization Effectiveness (PUE), approximately 1.12 [51, 83]. Figure 1 [116] presents that Google improves the PUE of all their large scale data centers. On the other hand, the low PUE means most energy is used for computing that drives us to control computing energy consumption as well.

1.1 Data Centers Energy Efficiency

The power consumed for DCs mainly from three components, the computing power usage, e.g., servers, switches, storage, supporting power usage, e.g., cooling, lighting, office use, and power transfer losses. Figure 2 [116] shows the power consumption elements that are considered in Google PUE measurement.

To describe the energy efficiency of DCs, power usage effectiveness is measured

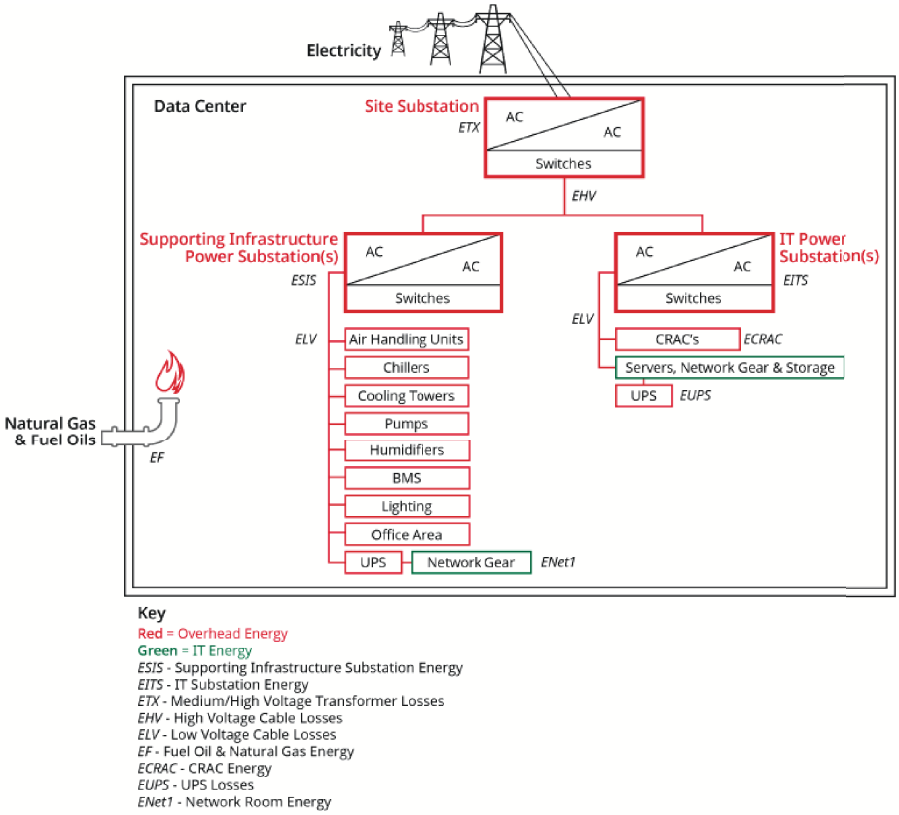

Figure 2: Power consumption elements considered by Google in their power measurement [116]

by:

$$\text{PUE} = \frac{\text{Total DC Power Consumption}}{\text{IT Equipment Power Consumption}} \tag{1.1}$$

The global average self-reported DC PUE is approximate 1.7, according to Uptime Institute's 2014 Data Center Survey [106]. Compared with private DCs, public DCs usually have a low PUE. Four approaches suggested by Google [51] to improve PUE include managing airflow [16, 81], adjusting the thermostat [14, 64], using free cooling [73, 131], and optimizing power distribution [95]. Through these approaches, Google improves their

PUE from 1.23 in 2008 to 1.12 in 2015 [116]. Now, computing energy consumption in DCs overweight energy consumption by all the other DC components. In this dissertation, we focus on minimizing the power consumption for computing, especially the CPU power consumption and network link power consumption.

1.2 Server Power Usage

Table 1: Component Peak Power Breakdown for a Typical Server [43]

Component	Peak Power	Count	Total
CPU	40 W	2	80 W
Memory	9 W	4	36 W
Disk	12 W	1	12 W
PCI slots	25 W	2	50 W
Motherboard	25W	1	25 W
Fan	10 W	1	10 W
System Total			213 W

Servers power consumption comes from multiple components such as CPU, memory, disk and so on. Fan *et al.* analyzed the power usages of a server in [43]. As shown in Table 1 [43], server power utilization is dominated by CPU and memory power usage, but power consumed by miscellaneous items, e.g., PCI slots, motherboard becomes significant when the workload of the server drops. With energy proportional computing [49], voltage or frequency can be adjusted according to a CPU workload, so that machines with less jobs consume less energy. Then, power management techniques can control power assignments to ensure that machines with light loads consume less power, while machines with heavy loads obtain enough power. However, when a server is completely idle without

doing any work, it may still consume up to 50% to 70% of its peak power [13, 127]. This 'baseline power' cannot be eliminated unless the server is turned off [27]. 'Operation cost' and 'operation energy consumption' are used to describe the power consumption for real utilization. The operation cost is approximately linear increased as the workload rises [13, 127]. On the other hand, majority servers in DCs is under utilization. Servers in DCs typically operate at 10% $\sim$ 50% of their maximum capacity most of time [43]. These large amount of under utilized servers decrease the energy efficiency because of the baseline power consumption.

1.3 Network Service Workload Variance

Traffic and workload of most network services are highly fluctuated related to human activities [8, 50, 69]. The huge differences between the peak workload and the off-peak workload of network services add the difficulties to provision resources for the service in advance. To guarantee Service Level Agreement (SLA), the provisioned resources should be enough to support the peak workload of the service. When the resources are statically provisioned based on the peak workload, a portion of resources would be idle when the workload of the service becomes low. As stated in Section 1.2, servers under utilization waste large amounts of energy.

A good news is that some traffic and workload are with patterns and could be predicted in a large time scale, such as day/night and weekday/weekend [89, 92, 98]. For example, both daily pattern and weekly pattern have been identified for PhoneFactor service in [92] and Youtube in [50]. In these studies, day time and weekdays have more

traffic and heavier workload compared with midnight to early morning and weekends. Driven by the observations, resource could be dynamic provisioned based on the predicated demand workload at a planned time, so that the idle resources can be shared by other services or switched to sleep mode.

1.4 Virtualization Techniques

As the main enabling technology for cloud computing, virtualization supports multi-tenant users to share computing, storage, and networking resources. Focusing on sizeable data centers (DCs), traditional virtualization technologies are mainly for computing and storage resources. However, as DCs for cloud computing rapidly grow in numbers and geographically dispersed DCs are interconnected, *network* resource virtualization technology becomes one of the most promising technologies for leveraging the full potential of cloud computing. Using virtual servers and sharing the same physical servers significantly cut off the operation cost, power consumption, carbon emission compared with locally hosted dedicated servers [9]. Also, live migration of virtual machines [115] allows for demanded virtual resources to be consolidated in a physical network conserving DC energy consumption.

To enable resource sharing without impacting other virtual servers sitting in the same physical server, various virtualization techniques are developed for different purposes. Basically, currently used virtualization techniques could be categorized as: full virtualization, paravirtualization, hardware-assested virtualization and OS-level virtualization.

Full virtualization fully simulates the underlaying hardware. In full virtualization, binary translation is used to trap and to virtualize instructions between the virtual hardware and the host computer's hardware. Binary translation incurs a large overhead, so that the performance of full virtualization may not be good. However, guest OS could be directly embedded without any modification. Examples of full virtualization are VMWare ESXi [40] and Microsoft Virtual Server [99].

Paravirtualization cannot directly embedded a guest OS without any modification. A thin layer named Hypervisor provides API for the communication between the guest OS and hardware. Compared with full virtualization, paravirtualization has a better performance with a lower overhead, but is harder to be implemented since the guest OS need to be tailored to run on the Hypervisor. Example of paravirtualization is Xen [85].

Hardware-assested virtualization is a type of full virtualization. In stead of binary translation and paravirtualization, hardware handles privileged and sensitive calls that automatically trapped to Hypervisor. Examples of hardware-assested virtualization are Linux KVM [79], VirtualBox [20].

OS-level virtualization or container-based virtualization is an alternative to Hypervisor based virtualization techniques. They are based on Linux container [102] and provide superior system efficiency and isolation. Unlike Hypervisor based virtualization, container based virtualization does not need to simulate the entire guest OS, but works as a thread. Therefore, container based VMs are light weighted, and could be fast deployed and migrated between different locations. One of management tool of container based virtualization, named Docker [35] is widely recognized and adopted in many companies

as well. The advent of container based virtualization and the related management tools offer a great opportunity to further improve energy efficiency and reduce cost in data centers.

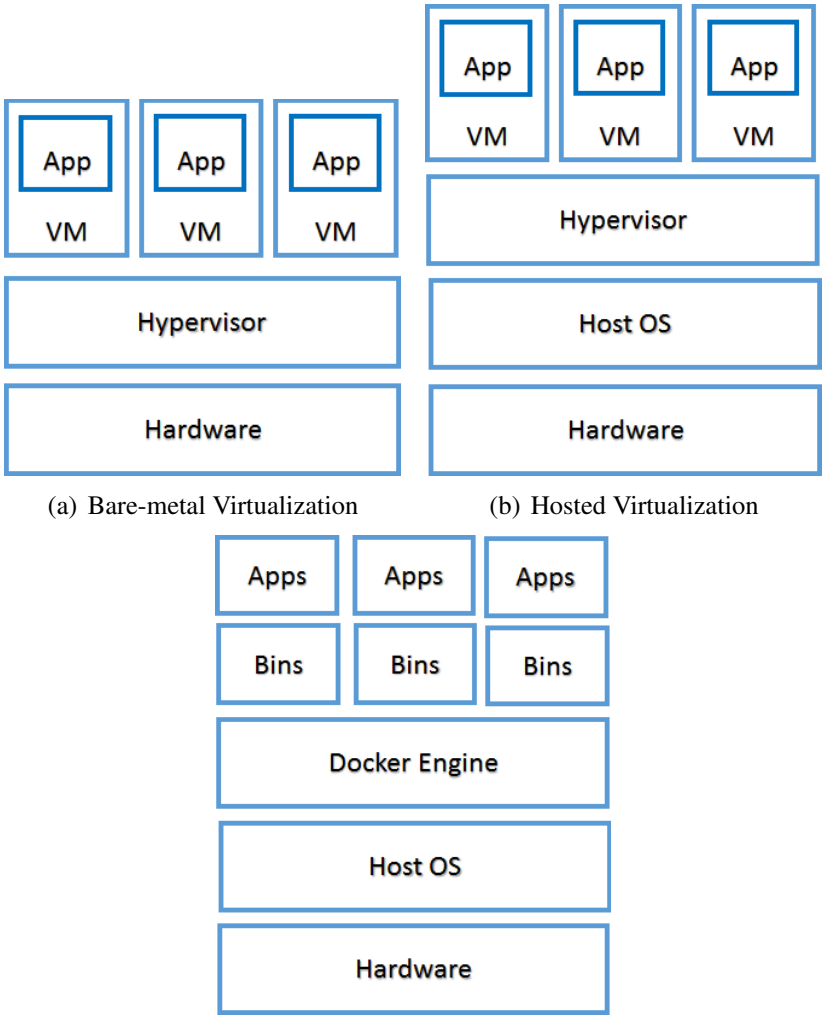

(a) Bare-metal Virtualization (b) Hosted Virtualization

(c) Container-based Virtualization

Figure 3: Architecture of three types of virtualization techniques

As shown in Figures 3, container-based virtualization does not build the guest OS, but only adds necessary bins and libraries to support the applications, while guest OS

is deployed for Hypervisor based OS. In addition, in container-based virtualization, an engine is used to coordinate among multiple containers, while Hypervisor is employed for isolation and resource mapping.

1.5 Network Virtualization

Besides vitualization of servers, network virtualization has been studied and developed for different purposes. For example, virtual networks are utilized to adopt new protocols or techniques for academic usage. In addition, they are employed to support multi-tenant environments for cloud computing and widely spread data centers. By allowing resource sharing, virtual networks saves a lot for service providers comparing with traditional dedicated DCs.

Various techniques have been developed to provision virtual resources, create and maintain virtual networks, including Virtual Local Area Networks(VLAN), Virtual Private Networks(VPN), Overlay Networks, and Programmable Networks.

VLAN partitions ports on switches so that network traffic through tagging packets on hosts. It enables host grouping even if the hosts are not under the same switch. Furthermore, it is flexible to migrate one host from one virtual network to another one by simply changing its VLAN identifier.

VPN assists the construction of logical private networks over public network infrastructure by establishing virtual end-to-end connections using tunnelling. VPN can be implemented at different network layer (layer 1, layer 2 and layer 3) using various techniques.

Overlay networks are built on top of other networks. In overlay networks, hosts are connected through logical links or tunnels, e.g., GRE tunnels, L2TP tunnels. Overlay networks typically are implemented at the application layer. Examples of overlay networks applications include most peer to peer protocols, such as Gnutella, Tor, content delivery networks, and real time media flow protocol. Note that VPNs can be categorized as overlay networks.

Programmable networks are networks in which their network devices behavior and flow control are handled independently by software rather than network hardware. Especially software defined networks separate data plane and control plane through moving routing function from network router to controllers. By using SDN infrastructures, network operators have a freedom in choosing the optimal physical servers and physical paths to support virtual nodes and virtual links without interfering other network services or functions.

Existing work, such as [38] that built FlowN, a VNE prototype on NOX OpenFlow controller, and [96] that proposed VNE architecture using BGP configurations and OpenFlow 1.3 switches, gives some guideline in implementing VNE using SDN architecture and infrastructures.

Table 2: Network Virtualization Implementation Techniques Comparison

Technique Name	Implementation Layer
VLAN	Link layer
VPN	Physical layer, link layer, network layer
Overlay networks	Application layer
Programmable networks	Network layer

1.6 Scope and Contribution of this Dissertation

This dissertation focuses improving the efficiency of cloud data centers by developing resource allocation algorithms for two different service requirements. When the service provider explicates the desired virtual network including a specific topology, and a set of virtual nodes with certain resource demands, the infrastructure provider computes how the given virtual network is embedded to its operated data centers with minimum energy consumption. We consider the evolving workload of the virtual networks or virtual applications and residual resources in data centers, and build a novel model of energy efficient virtual network embedding (EE-VNE) in order to minimize energy usage in the physical network consists of multiple data centers. In this model, both operation cost for executing network services' task and migration cost for the live migrations of virtual nodes are counted toward the total energy consumption. Two algorithms are developed towards this optimization problem.

The other is when the service provider only gives some description about the network service and the desired QoS requirements, the infrastructure provider has more freedom on how to allocate resources for the network service. We design a framework to dynamically allocate resources for a network service by employing container based virtual nodes. In the framework, each network service would have a pallet container and a set of execution containers. The pallet container requests resource based on certain strategy, creates execution containers with assigned resources and manage the life cycle of the containers; while the execution containers execute the assigned job for the network service.

In addition, the joint optimization for content placement problem has been studied to minimize the traffic from content to the final content users without increasing their experienced latency.

The main contributions of this dissertation are summarized as follows:

1) We formulate the problem of virtual network embedding that incorporates energy costs of operation and migration for nodes and links that is non-linear. To solve this problem, we introduce a technique to transform it to a linear programming problem with additional constraints. After proving the NP-hardness of this problem, we develop a heuristic algorithm named Topology and Migration-Aware Energy Efficient Virtual Network Embedding (TMAE-VNE) to minimize the energy consumption caused by both operation and future migration. This work is initially published in [56], and later extended to a journal paper [58].

2) To achieve a better solution of EE-VNE problem, we propose a novel ACO based topology migration-aware EE-VNE algorithm (ACO-EE-VNE) to minimize the energy consumption caused by both operation and migration. We develop a novel pheromone update and track scheme in the ACO algorithm, so that the space complexity of the ACO algorithm is substantially reduced. This work has been published in [59]

3) We introduce the framework for container based dynamic resource allocation mechanism. In this framework, service providers specify their demands from service

level rather than infrastructure level. Physical resources would be dynamically provisioned based on current workload of each network service/application. We formulate the dynamic resource allocation problem as an optimization problem and convert it as a linear programming problem and develop an efficient and scalable algorithm to solve the dynamic resource allocation problem that could be applied to large scale resource pools.

4) We formulate the joint traffic-latency optimization problem, and prove its NP-completeness. We then develop an efficient light-weight approximation algorithm, named Traffic-Latency-Minimization (TLM) algorithm, to solve the optimization problem with theoretical provable upper bound for its performance. To limit the frequency of updates to the origin server with local changes such as users interests shift, we also extend our TLM algorithm in a distributed manner. We provide the theoretical analysis for time complexity and space complexity of the TLM algorithm. This work is initially published in [54], and extended to a journal paper in [55].

1.7 Organization

The remainder of this dissertation is structured as follows. In Chapter 2, we review related work about optimization in virtual network embedding and resource allocation in cloud data centers. Chapter 3 addresses the energy efficient virtual network embedding

problem with evolving demands and physical resources. Chapter 4 presents how an Ant-Colony-Optimization based algorithm is developed and applied to solve the energy efficient virtual network embedding problem. Chapter 5 proposes a container based resource allocation framework with a scalable resource allocation algorithm. In Chapter 6, we identify traffic-latency optimization problem in content delivery networks and solve it with practical solutions. Finally, we summarize and conclude the dissertation and introduce the future work in chapter 7.

CHAPTER 2

RELATED WORK

With network virtualization techniques, adopting a new technique or protocol is much easier [32]. Vendors or infrastructure providers (InPs) do not need to purchase new equipment to update or deploy new techniques or protocols. An existing network could be flexibly expanded without involving much configuration work. In addition, network virtualization allows a physical network to be shared and divided into several isolated virtual networks (VNs) that consist of virtual machines (VMs) and their specified connectivities. Each VN serves a different group of users with different requirements of computing, storage, and network resources. Small institutions could have an economic option by renting VNs from an infrastructure provider rather than building and maintaining their private networks. Therefore, due to its benefits, network virtualization has been highlighted and studied from many aspects, such as resource discovery [53], admission control [94], resource scheduling [12], security issues [82], and resource allocation that is also known as virtual network embedding (VNE) [31, 66, 77, 130, 132].

In this chapter, we first investigate existing work about network virtualization, and resource allocation, then we briefly discuss about content distribution optimization that assigns storage resources to content delivery services and determines content placement in cloud.

2.1 Virtual Network Embedding (VNE)

Network virtualization allows physical nodes and links to be shared by multiple VNs. It improves the physical resource usage efficiency, reduces the cost for service providers, and simplifies the update and deployment of new techniques or protocols [32]. As one of the essential problems in the network virtualization area, VNE has been widely studied to achieve different goals [47]. It maps VNs coming over time to a physical network. In a real application, an InP receives a set of VN requests from the Service Providers (SP). Each VN asks for slices of resources, including computational and network resources, to provide value-added services, such as video on demand and voice-over-IP. By properly embedding the VNs, certain optimization goals are expected to be achieved without violating resource limitations.

Various VNE models have been proposed with different optimization goals or constraints. Many schemes aim to increase the VN acceptance ratio that is the number of successfully mapped VN requests to the number of total VN requests [33], or balance the workload on physical nodes or links [132]. [33] modeled the VNE problem with a specified location preference of the virtual nodes as a mixed integer programming problem and presented a deterministic algorithm as well as a random algorithm to solve the problem. [132] designed an algorithm that identifies the physical node or links with max stress and balances the workload of those nodes or links through reconfiguration.

In all of the above mentioned research, VNE has been completed in two stages. In the first stage, all the virtual nodes have been mapped to physical nodes that satisfy the desired demands; while in the second stage, the algorithms compute a proper physical

path for each virtual link in the virtual network. It is possible that a feasible mapping cannot be found for a virtual link, since the link capacities are not considered during the mapping of the virtual nodes. In this case, the above mentioned algorithms have to be backtracked to the first stage and map the virtual node again, which could be time consuming.

To improve the mapping efficiency, one-stage VNE algorithms have been proposed where the related virtual links are mapped right after mapping a virtual node [29, 62, 77, 87, 111]. In [62], constraints on delay, routing, and location were taken into consideration in the VNE problem, and the multicommodity flow integer linear program is used to solve the improved model. Trinh, T. et al. [111] tried to increase the profit of the infrastructure provider and save the cost of subscribers by applying a careful overbooking concept. The topology of the physical networks and virtual networks are modeled as a directed graph in [77], and the authors present a heuristic VNE algorithm that maps nodes and links at the same stage based on the subgraph isomorphism. [29] is inspired by Google's PageRank algorithm. It argued that virtual network topologies and virtual nodes' positions have a significant impact on VNE's efficiency and acceptance ratio. Virtual optical networks mapping to an optical network substrate was studied in [87]. The authors formulated the problem as integer linear programming formulations and designed a greedy randomized algorithm to solve it. [48] proposed a pre-cluster method to partition a virtual network into clusters. In this method, multiple virtual nodes within one VN are mapped to the same physical node if there are enough available resources, so that the traffic inside a VN could be minimized.

In [124], evolving VNs and physical networks are investigated. The authors also suggested migrating embedded virtual nodes or virtual links to accommodate more VN requests. Driven by this observation, [22] tried to minimize the VNE cost when the substrate network evolves. They compared the cost differences between re-embedding the virtual nodes or virtual links and migrating them. They solved the proposed problem with a heuristic algorithm. The purpose of [42] is to minimize the reconfiguration cost and balancing the physical link workload. A virtual node or link lying on a congestion physical link would be migrated to another physical node or link. The evolvement or changes of a virtual network are random and unexpected in [22, 42, 124].

In practice, however, many changes of VN workloads are periodic due to day/night time zone effects or weekend effects [109, 120, 128] and can be fairly well predicted [89, 98]. Meanwhile, making the data center energy efficient and protecting the environment attracts much attention. VNE targeting energy efficiency has been recognized and studied in [6,19,46]. Botero, J.F. et al. [19] saved the energy consumption by reducing the number of inactive physical nodes and physical links. Fischer, A. et al. [46] described the way to modify existing VNE algorithms towards energy efficiency without maintaining their other performance by considering energy as a factor when mapping. Energy efficiency is also considered in [6] that partitions and embeds virtual DCs to the substrate network that consists of multiple DCs, so that the inter DC traffic can be reduced and DCs with relative low PUE are used. The migration of virtual nodes and links have not been performed in [6, 19, 46], which would lead to a lower acceptance ratio compared with VNE algorithms that allow migration. In addition, in both [19] and [46], multiple virtual nodes from the

same VN could be consolidated on the same physical node to save energy; however, this may impact the resilience of the virtual networks. On the other hand, in our model, virtual nodes in the same VN are ensured to be mapped to different physical nodes for resilience consideration.

The above mentioned existing work has been summarized and compared in Table 3. All of the aforementioned work only targets a snapshot optimization where the resource limitations and demand requirements are considered at one time. Differing from these existing VNE solutions, our work is unique in that we holistically aim to optimize the energy efficiency of VNE over the entire life cycle of virtual networks. We achieve this goal by not only considering the embedding for the current moment but also scheduling possible migrations for the future at the time we map a virtual network. Thus, we can successfully minimize operation energy costs as well as possible migration costs. In addition, most previous work models the physical network as a graph with an arbitrary topology. This is not precise to describe intra DC networks that are usually organized in a hierarchical topology. We consider the practical topology of physical networks in the real world. In our model, a physical network may consist of multiple DCs, and the network inside each DC is hierarchical.

2.2 Meta-Heuristic Algorithms in VNE Optimization

In the above mentioned work, heuristic algorithms are developed in [6, 46] towards different optimization objectives, while [19] utilized CPLEX or GPLK based exact algorithms to solve their proposed optimization problems. CPLEX or GPLK based exact

Table 3: Comparison of VNE Studies

	Stage	Static or Dynamic	Objective	Algorithm
[33]	Two	Static	Increase acceptance ratio	Heuristic
[132]	Two	Dynamic	Balance load	Heuristic
[62]	One	Static	Minimize cost	MILP
[111]	One	Static	Increase profit and reduce cost	MILP
[77]	One	Static	Minimize cost	Heuristic
[29]	One	Static	Maximize revenue	Heuristic
[87]	One	Static	Minimize cost	Heuristic
[124]	Two	Dynamic	Increase profit and reduce cost	Heuristic
[22]	One	Dynamic	Minimize cost	Heuristic
[42]	One	Dynamic	Minimize reconfiguration cost and balance workload	Heuristic
[19]	Two	Static	Minimize energy consumption	Heuristic
[46]	One or Two	Static	Minimize energy consumption	Heuristic
[6]	One	Static	Minimize energy consumption	Heuristic

algorithms are expected to achieve the optimal solutions for the small scale of the problem. However, the time consumed by these exact algorithms increase significantly as the problem size grows. On the other hand, heuristic algorithms run in polynomial time, but can only search in a very limited solution space, resulting in a relative low quality of the solution compared with the solutions obtained by the exact algorithms.

Heuristic algorithms are developed in [6,46] towards different optimization objectives, while Botero [19] utilized a mixed integer programmer solver based exact algorithm to solve their proposed optimization problems. Exact algorithms can achieve the optimal solutions in small scales but are time consuming, especially when the problem size expands; while heuristic algorithms run in polynomial time but cannot approach the optimal

solutions in large scale problems.

Meta-heuristic algorithm offers new methods of solving large scale NP-hard optimization problems. It is usually inspired by natural biological behavior and includes probabilistic global searching based on evolutions and iterative operations. As a representative meta-heuristic algorithm, ACO has been utilized in various large scale NP-hard combinatorial optimization problems, e.g., [114]. In [23,41], ACO has been applied to the VNE problem to minimize the cost of VNE. They proved that the ACO based algorithm achieve a better performance than some existing heuristic algorithms. Chang *et al.* [26] aimed to minimize the energy consumption of migration using ACO based algorithm. However, they only considered the energy consumption in one time snapshot while we minimize the energy consumption in the VN's entire life cycle. However, [41] focuses on reducing the cost of physical links, while we want to improve the energy efficiency considering both the node energy consumption as well as link energy consumption. In addition, we minimize the energy efficiency of the entire life cycle of virtual network requests rather than in different time snapshots as in [6, 19, 46]. By doing this, the total energy consumption could be further saved; however, the hardness and the scale of the problem is increased as well. In our previous work [56], a heuristic algorithm was proposed that reduced the energy consumption and improved the acceptance ratio compared with the existing algorithms. However, as most other heuristic algorithms, it has a low approximation ratio and is inadequate in facing a large solution space.

2.3 Resource Allocation

To save the cost on building and maintaining a private data center, service providers move their service and data to cloud infrastructure providers. To further save cost and improve efficiency, dynamic scaling of resource management for web application and big data computing have been studied, such as [78, 118]. Jobs are dispatched to specific servers with web application or hadoop running in that system. Applications are organized in a multi-tier structure and tasks are distributed through a front-end dispatcher [122].

To provider more complicated services/applications, e.g. game hosting, resources are required to be allocated in application level. [122] targeted energy efficient resource allocation at VM level. By embedding and migration the entire VMs, [122] improve energy efficiency for applications that require specific environment setting. In addition, VN level resource allocation has been studied for different objectives, such as increasing acceptance ratio, improving energy efficiency [57, 58]. In these virtual machine or virtual network embedding studies, they all based on VM technologies that isolate VMs at the hardware abstraction layer, e.g., using Hypervisor based virtualization.

As an alternative of hypervisor based virtualization, container based virtualization has been proposed in [102], and attracts many attentions in recent years. As a management tool of container based virtualization, [35] has been recognized and widely used to deploy many network services. [91, 100] also start to support container based virtualization in their cloud services. Due to its light weight size, prompt deployment and shipping [44], with container based VM, it is possible to have an application level adaptive resource allocation mechanism.

However, current hypervisor VM placement models and mechanisms assume 1) physical resources are strictly allocated for each VM, 2) the amount of VM and capacity of VM are static. While, in container based virtualization, 1) resource could be shared based on their priority, e.g. in docker [35], 2) dynamic change the number and capacity of containers, 3) the size of containers could be different based on environments of physical machines. Considering the different requirements, a novel framework and theoretical model are necessary for building an adaptive resource allocation mechanism using container based virtualiztion techniques.

2.4 Optimal Content Distribution

Content distribution algorithms aim to optimize the system performance with limited resources expressed in various metrics. It is worth noting that those content distribution techniques can be based on a P2P structure as well as on a server/client structure. [60] investigated content distribution techniques in both CDNs and P2P networks that are utilized to decrease the traffic load in backbone networks or to optimize content users' experience by shorter end-to-end paths and delays. The motivations of existing content distribution techniques based on CDNs or P2P networks range from improving final users' experience to compressing access cost such as link traffic. Based on the differences on the motivations, most of the content distribution algorithms could be categorized as 'Latency-Minimization' (**LM**) and 'Traffic-Minimization' (**TM**).

LM algorithms mainly focus on the optimization of the total communication delay

from servers to clients, which is the performance perceived by clients. The average number of autonomous systems (ASes) has been utilized to indicate latency incurred in CDNs in [67]. The authors of [67] also proposed heuristic algorithms to minimize the average number of ASes traveled for requests. [10,11,71] attempted to reduce clients' access costs for retrieving contents from peers or within the access network. The access cost is related to the distance between content users and replicas [10, 71], or it can be a general concept involving all the costs to complete content transmissions [11]. In addition to the communication and access latency, the computational cost is studied and reduced using clustering algorithms in [28]. The authors in [30] studied the download latency under a competitive P2P environment, where source peers have a limited capacity of parallel connections. They attempted to achieve minimum download time by dynamically changing the source set of peers under a pull-based model. Similar schemes are employed in grid computing including where distributed resources are shared through a high speed network. In [15], data are replicated in nearby caches to final user rather than distant source to reduce data transmission time. In [110], LSAM proxy multicast push web pages to affinity groups for aggregated requests to offload the central server and backbone networks. Moreover, efficient prefetching algorithms are designed in [34,93] to indicate the most probable disk blocks and push those blocks to user nodes in advance in order to speed up data access.

TM algorithms are designed to lower the traffic volume consumed for contents delivery, so to cut down the expenditure for cloud services. In [4], the authors saved the traffic cost through considering the router level and AS level topologies and utilizing multicast streams. Recently, [18] addressed the issue of reducing the traffic volume for large

videos in CDNs. They developed heuristic algorithms for specific topologies by using cache clusters, assuming many system parameters were constant. The study in [61] adopted various forms of local connectivity and storage for multimedia delivery in a neighbor assisted system to reduce access link traffic. [65] studied the influence of server allocation in ISP-operated CDNs to the transmission bandwidth consumption and suggested the properties of nodes' topological locations that impact cache placement effectiveness in multiple network topologies. Unified linear programming is utilized to optimal content placement under multiple constraints in [74]. A matrix based k-means clustering strategy is proposed in [125] to reduce total data movement in scientific cloud workflows. This is where the replication and distribution are constrained by enforcement policies, such as some scientific data are restricted from moving.

Other than the LM and TM algorithms, a few recent works focus on content delivery problems over cloud-based storage. [119] decreased the storage cost by calculating and maintaining a minimal number of replicas under certain availability requirements. [24, 101] tried to optimize the content providers' investment by content delivery over multiple cloud storage providers. [21, 76] designed and implemented frameworks to assist replica placement over cloud storage services, in order to make it possible to optimal content delivery over cloud under diversity requirements.

Our work differs from the previous LM and TM algorithms that we collectively consider content providers' expenditures on traffic volume over cloud storage and content users' experiences. Our aim is to address the optimization problem of traffic consumption

and latency for large and diverse sizes of contents by a push-pull hybrid content distribution strategy, where push means replicating objects on certain servers in advance, and pull means only delivering contents that are requested by the content users.

The push-pull strategy has been implemented for content distribution earlier. [129] analyzed a P2P pull-based streaming protocol to understand the fundamental limitations and design an effective protocol to achieve better throughput. [45] investigated theoretic bounds for pull-based protocol under a mesh network and explained the performance gap. The push-pull strategy is also utilized in data aggregation fields to minimize global communication cost in [25]. However, those push and pull hybrid protocols are designed for P2P networks or sensor networks without considering the storage of nodes. Therefore, they are not suitable for content distribution over cloud storage where the storage space impacts the content providers investment.

We focus on the environments of cloud based content delivery where the content placement can be actively controlled considering traffic volume while the latency can be controlled under storage constraints. We develop an efficient light-weight approximation algorithm with a provable performance bound, and time and space complexity analysis. We further design a distributed version of the algorithm in which proxy servers can determine object distribution by exchanging local information without requiring global knowledge.

CHAPTER 3

ENERGY EFFICIENT VIRTUAL NETWORK EMBEDDING FOR GREEN DATA CENTERS USING DATA CENTER TOPOLOGY AND FUTURE MIGRATION

In this Chapter, we study energy efficient virtual network embedding considering practical DC topologies and future migration. Unlike existing work, we focus on improving energy efficiency of virtual network embedding through planning future migration as well as initial embedding.

By migrating some virtual nodes or links to other physical nodes or links at a planned time based on predicated VN workloads, idle servers and network elements can be turned off to save energy. Figure 4 depicts an example where two VNs from cloud customers A and B are embedded onto two physical DCs during the day time due to their resource needs. At night, however, the smaller workloads permit the infrastructure provider to combine them onto one DC or rack saving the operating costs of servers and switches. For example, web servers could run on multiple physical servers during the busy hours to ensure the performance but aggregated to a less number of physical servers at night so that some idle physical servers could be turned off to save energy. This motivates us to design a VNE scheme that saves energy and supports energy efficient DCs by aggregating the workload to a less number of servers and turning off idle servers.

Furthermore, in most existing VNE schemes, the physical networks to embed VN requests are modeled with random graphs. DCs are, however, typically organized in a hierarchical fat tree architecture, as depicted in Figure 5. We consider this hierarchical

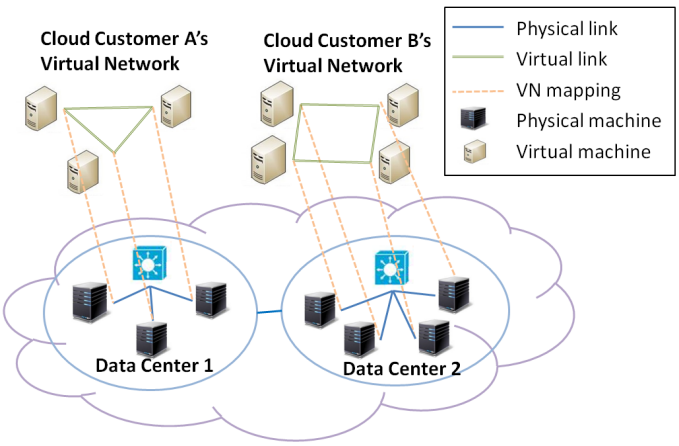

(a) A VNE in Green DC during day time

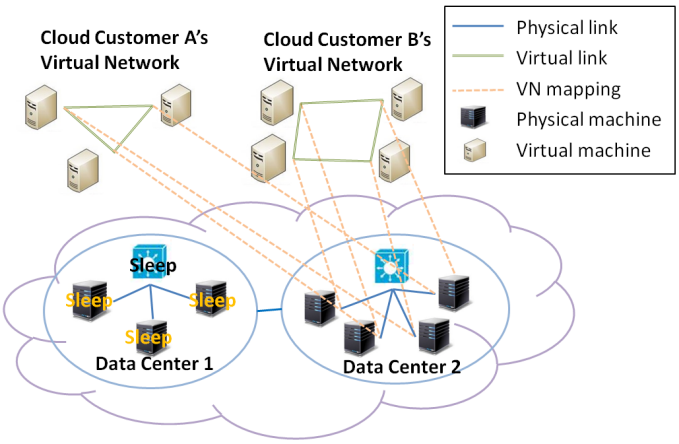

(b) A VNE in Green DC during night time

Figure 4: An example of VNE for green DCs

structure when modeling the VNE problem, so that VN embedding can minimize the energy consumption used by intermediate switches as well as servers, as shown in Figure 6. We build a novel model of virtual network embedding in order to minimize energy usage in data centers for both computing and network resources by taking practical factors into consideration.

The main contributions of the chapter are as follows.

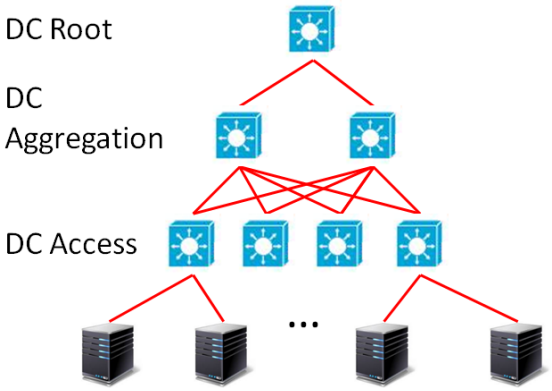

Figure 5: A typical hierarchical fat tree data center architecture

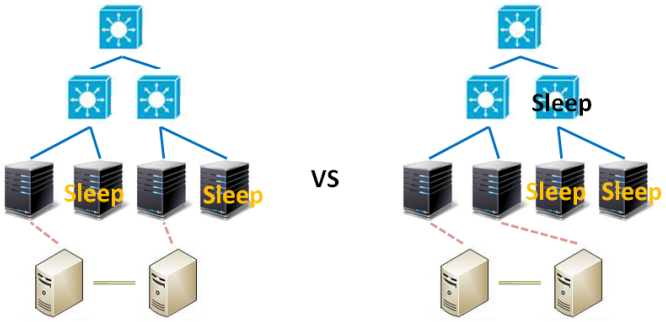

Figure 6: Topology awareness reduces energy consumption (right)

- We formulate the problem of virtual network embedding that incorporates energy costs of operation and migration for nodes and links that is non-linear. To solve this problem, we introduce a technique to transform it to a linear programming problem with additional constraints.

- After proving the NP-hardness of this problem, we develop a heuristic algorithm

named Topology and Migration-Aware Energy Efficient Virtual Network Embedding (TMAE-VNE) to minimize the energy consumption caused by both operation and future migration. To the best of our knowledge, this work is the first to optimize energy consumption over the VN's entire life cycle, considering time varying resource demands of virtual network requirements. In addition, we consider a practical intra-DC architecture to further improve energy efficiency.

- We conduct extensive evaluations and comparisons with two state-of-the-art algorithms using various inter-DC topologies. The results show that the proposed algorithm substantially saves energy consumption and allows high acceptance ratios.

The remainder of this chapter is organized as follows. We formally model the VNE problem with dynamic VN requests, physical nodes with sleep/awake modes, and realistic DC network topologies in Section 3.1. The proposed algorithm is described in Section 3.2. A motivating example is discussed in Section 3.3. The performance evaluations and comparisons of the proposed algorithm with existing algorithms using multiple DC topologies are presented in Section 3.4. The concluding remarks of this chapter are given in Section 3.5.

3.1 Problem Formulation

Table 4: Notations Used

Notation	Explanation
$G^p(N^p, L^p)$	A physical network with a set of physical nodes N^p and a set of physical links L^p
$G^v(N^v, L^v)$	A virtual network with a set of virtual nodes N^v and a set of virtual links L^v
G^p_{inter}	A physical network that connects data centers
L^p_{inter}	A set of inter-DC physical links
D	The number of DCs
$c^p(i)$	Total computational resources of a physical node i
$c^p(i,t)$	Available computational resources of a physical node i at time t
$c^v(u,t)$	The desired computational resources to embed the virtual node u at time t
$w^p(i,j)$	weight of physical link (i,j)
$b^p(i,j)$	Total bandwidth resources of the physical link between i and j
$b^p(i,j,t)$	Available bandwidth resources of the physical link between i and j at time t
$b^v(u,w,t)$	Desired bandwidth to map the virtual link between u and w at time t
$E_{base}(i)$	Baseline energy consumption of the physical node i
C_{opr}	Total operation energy consumption for embedding VN requests
C_{mgr}	Total energy consumption of necessary migrations for embedded VN requests
$s(u,t)$	State information of virtual node u at time t
$x(i,u,t)$	Binary variable if virtual node u is embedded to physical node i at t or not
$S_{status}(i,t)$	Sleep or awake status of physical node i at time t
$f(i,j,u,w,t)$	If virtual flow between virtual node u and w goes through the link between physical node i and j at time t

We model the energy efficient VNE problem as an optimization problem aiming to minimize the energy consumed for embedding VN requests. Specifically, the total energy consumption consists of the energy consumed for operation and migration under a group of constraints, including computational and network resource limitations, binary limitations, and flow constraints. We further transform the proposed VNE problem to a linear program problem by introducing two auxiliary variables.

3.1.1 Notations

In this section, we model the VNE problem that minimizes the energy consumption with practical DC topologies and migration awareness. Notations used in the Chapter 3 are listed in Table 4.

Assume a physical network $G^p(N^p, L^p)$ consists of multiple DCs $G_1^p(N_1^p, L_1^p)$, $G_2^p(N_2^p, L_2^p)$, $\cdots$, $G_D^p(N_D^p, L_D^p)$. Here, D is the number of DCs in a physical network. A DC d includes a group of physical nodes N_d^p and physical links L_d^p. We have

$$G^p = G_1^p \bigcup G_2^p \bigcup \cdots \bigcup G_D^p \bigcup G_{inter}^p$$

$$N^p = N_1^p \bigcup N_2^p \bigcup \cdots \bigcup N_D^p$$

$$L^p = L_1^p \bigcup L_2^p \bigcup \cdots \bigcup L_D^p \bigcup L_{inter}^p$$

where G_{inter}^p is the network that connects DCs, and L_{inter}^p is the set of all inter DC links. Each physical node $i \in N^p$ is equipped with limited computational resources $c^p(i)$[1], while each physical link between two adjacent physical nodes i and j has limited bandwidth $b^p(i, j)$.

[1]Here, we consider a general computational resources. In real applications, it could be CPU capacity or available storage size

An infrastructure provider receives VN requests and assigns proper computational and network resources satisfying the specific demands of each VN request. In detail, a VN request can be modeled as a weighted graph $G^v(N^v, L^v)$, where N^v and L^v are the sets of virtual nodes and virtual links, respectively.

Based on the observation that users' workloads often change predictably with time, such as day and night times [128], we assume VN resource workloads are different in the time intervals. We denote the minimal desired computational resource at time t for a virtual node $u \in N^v$ as $c^v(u,t)$, and the minimal desired bandwidth resource at time t for a virtual link in L^v as $b^v(u,w,t)$. For the simplicity of our discussion, we only consider demands of two different times (t and $t+1$ for day and night times, respectively, for example) for each VN request in the illustrating example and evaluation sections. However, the idea of scheduling and mapping can be naturally extended to handle more time intervals. For a certain virtual node u of VN request v, its requested computational resource $c^v(u,\cdot)$ is specified for the day and night times as shown below.

$$c^v(u,\cdot) = \begin{cases} c^v(u,t), & \text{during day time} \\ c^v(u,t+1), & \text{during night time} \end{cases} \tag{3.1}$$

The requested bandwidth between virtual nodes u and w, $b^v(u,w,\cdot)$ is specified for the day and night times as:

$$b^v(u,w,\cdot) = \begin{cases} b^v(u,w,t), & \text{during day time} \\ b^v(u,w,t+1), & \text{during night time} \end{cases} \tag{3.2}$$

After embedding some VN requests, the available computational resources of a physical node i are the residual computational resources after reserving resources for

already embedded VN requests:

$$c^p(i,t) = c^p(i) - \sum_{\forall v \uparrow i} c^v(u,t) \tag{3.3}$$

Here, $v \uparrow i$ indicates that virtual node v is embedded on physical node i. Due to the different demands of VN requests for day and night times, the available resources change over time too.

Similarly, the available bandwidth of a physical link between two adjacent physical nodes i and j is defined as:

$$b^p(i,j,t) = b^p(i,j) - \sum_{\forall (u,w) \uparrow (i,j)} b^v(u,w,t) \tag{3.4}$$

Here, $(u,w) \uparrow (i,j)$ indicates that the virtual link between virtual node u and w passes through the physical link between physical nodes i and j.

Our goal is to embed a group of VN requests with minimal energy consumption that consists of operational energy cost C_{opr}, and migration energy cost C_{mgr} under resource limitations, which is defined as follows;

$$min \sum_{t} (C_{opr}(t) + C_{mgr}(t)) \tag{3.5}$$

In addition, we assume that physical nodes support the sleep and awake mode in the physical network. Especially, there is no energy consumption if a physical node is turned to the sleep mode. For an awake node, a baseline energy is consumed for maintaining basic functions [127], while for each newly embedded virtual node, an additional power is consumed for performing the work on this virtual node.

3.1.2 Operation Energy Consumption

We model the operational energy consumption including energy costs for nodes and links as:

$$\begin{aligned} C_{opr}(t) &= \textit{Energy cost for nodes + Energy cost for link bandwidths} \\ &= \sum_{i}\sum_{u}\sum_{t=0}[\alpha_{o_1}E_{base}(i)S_{status}(i,t) + \alpha_{o_2}c^v(u,t)]x(i,u,t) \\ &\quad +\alpha_{o_3}\sum_{i,j}\sum_{u,w,u>w}\sum_{t=0} w^p(i,j)b^v(u,w,t)f(i,j,u,w,t) \end{aligned} \tag{3.6}$$

Here, a binary variable $x(i,u,t)$ is used to indicate whether or not a virtual node u is embedded to physical node i at time t.

$$x(i,u,t) = \begin{cases} 1, & \text{if virtual node } u \text{ is assigned to physical node } i \text{ at time } t \\ 0, & \text{otherwise} \end{cases} \tag{3.7}$$

The operation cost of embedding a virtual node u to physical node i at time t consists of a possible baseline energy consumption $E_{base}(i)$ for waking up node i if its status $S_{status}(i,t-1)$ at time $t-1$ is asleep and an operation cost for executing virtual node u's tasks $c^v(u,t)$ at time t.

$$S_{status}(i,t) = \begin{cases} 1, & \text{if physical node } i \text{ is asleep at the beginning of time } t \\ 0, & \text{otherwise} \end{cases} \tag{3.8}$$

On the other hand, link operation cost is determined by traffic volume, $b^v(u,w,t)$ on the virtual link (u,w) at time t, and the weight, $w^p(i,j)$ of the physical links (i,j) that is different for inter or intra DC links. We use network flow $f(i,j,u,w,t)$ to determine whether a physical link (i,j) is used to embed a virtual link u,w. When $f(i,j,u,w,t)$

is equal to 1, virtual link (u, w) passes through the physical link (i, j). Otherwise, $f(i, j, u, w, t)$ is equal to 0. Coefficients α_{o_1}, α_{o_2}, and α_{o_3} are used to balance the weight among different parts of the operation cost.

3.1.3 Migration Energy Consumption

Even though migrating embedded virtual nodes could save energy, it may introduce additional overhead, such as the cost for moving system resources and maintaining additional links when the migration is processed. [115] describes the processes of the virtual router's live migration and its related overhead. We model the migration energy cost at time t as shown below.

$$\begin{aligned} C_{mgr}(t) &= \textit{Cost due to size of system resource + Cost due to bandwidth usage} \\ &= \alpha_{m_1} \sum_{i_1,i_2,i_1 \neq i_2} \sum_{u} \sum_{t=1} s(u,t) E_{len}(i_1,i_2) x(i_1,u,t-1) x(i_2,u,t) \\ &+ \alpha_{m_2} \sum_{i_1,i_2,i_1 \neq i_2} \sum_{a,b} \sum_{u,w,u>w} \sum_{t=1} b^v(u,w,t-1) x(i_1,u,t-1) x(i_2,u,t) \\ & \quad f(a,b,u,w,t-1) w^p(a,b)) \end{aligned} \tag{3.9}$$

Here, we formulate the migration cost as the summation of duplicating the virtual nodes' status and maintaining duplicated links before migration is completed. In Equations (3.9), $s(u, t)$ is the coefficient indicating the cost of duplicating execution status for virtual node u at time t. $E_{len}(i_1, i_2)$ is the weight of a physical path between physical nodes i_1 and i_2. The product of $x(i_1, u, t-1)$ and $x(i_2, u, t)$ indicates that the virtual node u was embedded on physical node i_1 at time $t-1$ and migrated to physical node i_2 at time t. $b^v(u, w, t-1)$

is the coefficient for maintaining the physical link (a, b) that is used for embedding the virtual link (u, w). Coefficients α_{m_1}, α_{m_2}, and α_{m_3} are used to balance the weight among different parts of the migration cost.

3.1.4 Transformation of the Optimization Objective

Due to the existence of the products of variables, such as $x(i_1, u, t-1)x(i_2, u, t)$, the objective function is a non-linear problem that is hard to solve. We transform it to a linear program problem by introducing two auxiliary binary variables: $m(i_1, i_2, u, t-1)$ and $g(i_1, i_2, a, b, u, w, t)$. Here we replace $x(i_1, u, t-1)x(i_2, u, t)$ with $m(i_1, i_2, u, t-1)$ and replace $x(i_1, u, t-1)x(i_2, u, t)f(a, b, u, w, t-1)$ with $g(i_1, i_2, a, b, u, w, t)$. Intuitively, $m(i_1, i_2, u, t-1)$ indicates if a virtual node u has migrated from physical node i_1 to i_2 at time t; while $g(i_1, i_2, a, b, u, w, t)$ represents if a physical link (a, b) belongs to the physical path that embedding virtual link (u, w), and one end of the virtual link has migrated from physical node i_1 to i_2 at time t. Constraints (3.12) and (3.13) are added to ensure the converted problem is equivalent with the original one.

The original objective function is as follows:

$$
\begin{aligned}
min \quad & (\sum_{i}\sum_{u}\sum_{t=0}[\alpha_{o_1}E_{base}(i)S_{status}(i,t) + \alpha_{o_2}c^v(u,t)]x(i,u,t) \\
& +\alpha_{o_3}\sum_{i,j}\sum_{u,w,u>w}\sum_{t=0} w^p(i,j)b^v(u,w,t)f(i,j,u,w,t) \\
& +\alpha_{m_1}\sum_{i_1,i_2,i_1\neq i_2}\sum_{u}\sum_{t=1} s(u,t)w^p(i_1,i_2)x(i_1,u,t-1)x(i_2,u,t) \\
& +\alpha_{m_2}\sum_{i_1,i_2,i_1\neq i_2}\sum_{a,b}\sum_{u,w,u>w}\sum_{t=1} b^v(u,w,t-1)x(i_1,u,t-1)x(i_2,u,t) \\
& f(a,b,u,w,t-1)))w^p(i,j)
\end{aligned}
\tag{3.10}
$$

The transformed objective function is as follows:

$$
\begin{aligned}
min \quad & (\sum_{i}\sum_{u}\sum_{t=0}[\alpha_{o_1}E_{base}(i)S_{status}(i,t)+\alpha_{o_2}c^v(u,t)]x(i,u,t) \\
& +\alpha_{o_3}\sum_{i,j}\sum_{u,w,u>w}\sum_{t=0}w^p(i,j)b^v(u,w,t)f(i,j,u,w,t) \\
& +\alpha_{m_1}\sum_{i_1,i_2,i_1\neq i_2}\sum_{u}\sum_{t=1}s(u,t)w^p(i_1,i_2)m(i_1,i_2,u,t) \\
& +\alpha_{m_2}\sum_{i_1,i_2,i_1\neq i_2}\sum_{a,b}\sum_{u,w,u>w}\sum_{t=1}b^v(u,w,t-1)g(i_1,i_2,a,b,u,w,t) \\
& w^p(i,j)))
\end{aligned} \tag{3.11}
$$

The following two constraints are introduced to ensure the equivalence of the converted problem and the origin problem.

$$0 \leq x(i_1,u,t-1)+x(i_2,u,t)-2m(i_1,i_2,u,t) \leq 1 \tag{3.12}$$

$$0 \leq m(i_1,i_2,u,t)+f(a,b,u,w,t-1)-2g(i_1,i_2,j,a,b,u,w,t) \leq 1 \tag{3.13}$$

3.1.5 Constraints

The optimization goal is subjected to the constraints on computational and network resources.

$$\sum_{u} c^v(u,t)x(i,u,t) \leq c^p(i,t), \forall i,t \tag{3.14}$$

$$\sum_{u,w} f(i,j,u,w,t)b^v(u,w,t) \leq b^p(i,j,t), \forall i,j,t \tag{3.15}$$

Constraint (3.14) ensures that for each physical node i at any time t, the total required computational resources of virtual nodes that mapped to i would not exceed the available computational resources on i. Constraint (3.15) guarantees that for each physical

link (i, j), the total amount of bandwidth required by the virtual links would not exceed the available bandwidth on (i, j).

Constraint (3.16) is employed to ensure that each virtual node u must be embedded to a physical node i.

$$\sum_{i} x(i, u, t) = 1, \forall u, t \tag{3.16}$$

Considering the resilience as in an existing VNE work, it is not allowed that two virtual nodes from the same VN are embedded to the same physical node. Therefore, we have

$$\sum_{u} x(i, u, t) \leq 1, \forall i, t \tag{3.17}$$

Finally, flow conservation is used to make sure that the net flow of a physical node must be zero except for the physical node that embeds a virtual node.

$$\sum_{j} f(i, j, u, w, t) - \sum_{j} f(j, i, u, w, t) = x(i, u, t) - x(i, w, t), \forall i, u, w, t \tag{3.18}$$

Through solving the transformed optimization problem (3.11) under a group of constraints (3.12)-(3.18), we could obtain the optimal solution of the topology and migration aware energy efficient VNE by using IBM ILOG CPLEX or other math tools for linear programming problems. However, due to the large solution space, time spent to solve the problem grows exponentially when the size of the problem increases. Thus, an efficient algorithm is necessary for computing the optimal embedding for VN requests.

3.2 Topology and Migration Aware Energy Efficient VNE

We first study the complexity of the formulated optimization problem, and prove the NP-hardness of the TMAE-VNE problem. We next propose a heuristic algorithm

to determine scheduling to maximally save the total energy consumption in a scalable manner.

3.2.1 Hardness of TMAE VNE problem

The optimization problem formulated in Section 3.1 can be shown to be NP-hard, as a standard VNE problem which is known to be NP-hard [7] can be reduced to this in polynomial time. A standard VNE problem is defined as below.

Standard VNE problem: Given an undirected graph $G^p = (N^p, L^p)$, a set of vertices $i \in N^p$ and a set of edges $(i, j) \in L^p$, where $i, j \in N^p$ has been assigned a value $c^p(i)$ or $b^p(i, j)$, respectively. Given another undirected graph $G^v = (N^v, L^v)$, a set of vertices $u \in N^v$ and a set of edge $(u, w) \in L^v$, where $u, w \in N^v$ has been assigned a value $c^v(i)$ or $b^v(i, j)$, respectively.

The problem is to determine whether or not we can find a set of valid mappings from L^v to L^p. In each mapping from edge $(u, w) \in L^v$ to $(i, j) \in L^p$, two conditions are satisfied 1) $c^p(i) \geq c^v(u)$, and $c^p(j) \geq c^v(w)$; 2) $b^p(i, j) \geq b^v(i, j)$.

We convert our TMAE-VNE problem to a decision problem and restate it as below. Later we demonstrate that the standard VNE problem could be reduced to this problem.

TMAE-VNE problem: Given an undirected weighted graph G^p that consists of a set of subgraphs $G_1^p(N_1^p, L_1^p)$,$G_2^p(N_2^p, L_2^p)$,$\cdots$, $G_D^p(N_D^p, L_D^p)$ and a set of edges L_{inter}^p connecting subgraphs. Each vertex $i \in N_d^p$ and each edge $(i, j) \in L_d^p \bigcup L_{inter}^p$, where $i, j \in \bigcup_d N_d^p$ has been assigned a value $c^p(i, t)$ or $b^p(i, j, t)$, respectively at time t. Given another undirected graph $G^v = (N^v, L^v)$. Each vertex $u \in N^v$ and each edge $(u, w) \in$

L^v, where $u, w \in N^v$ has been assigned a value $c^v(i,t)$ or $b^v(i,j,t)$, respectively at time t.

In addition, an embedding to a node $i \in \bigcup_d N_d^p$ brings additional cost $C_{opr}(i,t)$; and embedding on a edge $(i,j) \in L_d^p \bigcup L_{inter}^p$ products additional cost $C_{opr}(i,j,t)$. Migrations between nodes and edges result in additional costs $C_{mig}(i,t)$ and $C_{mig}(i,j,t)$, respectively. The total energy cost could be computed according to Equations [3.5], [3.6], and [3.9].

A valid one-to-one mapping for each node $u \in N^v$ to a $i \in N^p$ and each $(u,w) \in L^v$ to $(i,j) \in L^p$ should satisfy two conditions: 1) $c^p(i,t) \geq c^v(u,t)$, and $c^p(j,t) \geq c^v(w,t)$; 2) $b^p(i,j,t) \geq b^v(i,j,t)$. The problem is to determine whether or not we can find a set of valid mappings with a cost smaller than a constant value κ.

The standard VNE could be reduced to a TMAE-VNE problem, by setting $c^p(i) = c^p(i,t)$, $b^p(i,j) = b^p(i,j,t)$, $c^v(i) = c^v(i,t)$, and $b^v(i,j) = b^v(i,j,t)$ for all t. In addition, let $C_{opr}(i,t) = C_{opr}(i,j,t) = 1$ and $\kappa = n + l$, where n is the size of N^v and l is the number of the edges in G^p. The reduction can be completed in polynomial time. After this reduction, if we could find a solution for a standard VNE, it would be also a solution for the TMAE-VNE problem and vice versa. In addition, a mapping could be validated in polynomial time if it is a solution for the TMAE-VNE problem. Thus, the TMAE-VNE problem is NP-complete.

3.2.2 The Proposed Heuristic Algorithm

We use a type of a single phase algorithm where for each virtual node, its DC and a physical node are assigned followed by its corresponding virtual link embedding. We first determine the set of DCs to place a virtual node at each time phase t. We then look into these DCs and find the most proper physical nodes to embed the virtual node in each time phase. Since the number of DCs are much less than the number of physical nodes, we could check all the set of DCs with enough resources, and finally, find a best set that consumes the least energy. On the other hand, the energy cost of inter DC migrations significantly overweighs that of intra DC migrations. Therefore, we first check sets of DCs with enough available resources and determine optimal embedding in the DC granularity, then we look into each physical node in the selected DCs.

We next consider the order of embedding each virtual node to reduce energy consumption. Due to the limitation of available resources, a physical node may not embed multiple virtual nodes. In addition, different virtual nodes cost different amounts of energy due to different connectivities and the network workload. Thus, the order of embedding virtual nodes impacts total energy consumption. We determine the embedding order for each virtual node based on the possible saved energy if this virtual node is embedded first. For each virtual node u, we pick two embeddings with the least and the second least energy costs. The cost difference δ_u between these two costs indicates possible energy saving if the virtual node u's embedding with the least cost is applied. Thus, we prefer to first embed the virtual node with the largest cost difference.

The detailed algorithm is shown in Algorithm 1. For simplicity, we only consider

two time phases, time t_{day} and t_{night} in the algorithm. In each of these time phases, the workloads of the physical networks and VNs are different. However, our algorithm could be easily extended for multiple time phases.

Algorithm 1 Topology and Migration-Aware Energy Efficient VNE (TMAE-VNE)

Input: physical network available resources $[G^p(N^p, L^p), \{c_i^p, i \in N^p\}, \{b_{ij}^p, i, j \in N^p\}]$; VN requested resources $[G^v(N^v, L^v), \{c_u^v : u \in N^v\}, \{b_{uw}^v : u, w \in N^v\}]$

Output: VNE for G^v at [t, $t+1$]

1: **while** there is at least one unembedded virtual node **do**
2: **for** each unembedded virtual node u **do**
3: $List_{DC}^u$:= FindFeasibleDCSets(DC, u)
4: **for** each element $[DC_d, DC_{d'}]$ in $List_{DC}^u$ **do**
5: Estimate the total energy consumption if embedding u to DC_d at time t and $DC_{d'}$ at time $t+1$ according to Equations (3.5), (3.6) and (3.9) based on usage, distance to embedded virtual node and other factors
6: Record the energy consumption as $C_u(DC_d, DC_{d'})\}$
7: **end for**
8: Compute $\delta_u := SecondMin\{C_u\} - Min\{C_u\}$
9: **end for**
10: virtual node w:= $max_u\{\delta_u\}$
11: Find $Min\{C_w\}$ and corresponding $[DC_d, DC_{d'}]$ with minimal energy consumption in $C_w(DC_d, DC_{d'})$
12: Assign w to a physical node $i \in DC_d$ during time t according to first fit police while considering topology
13: Assign w to a physical nodes $j \in DC_{d'}$ during time $t+1$ that first fit w
14: Assign virtual links whose two ends have both embedded using shortest path that satisfy the bandwidth constraints
15: Update available resources in G^p
16: **end while**

Algorithm 2 Find Feasible DC Sets: FindFeasibleDCSets()

Input: physical network available resources $[G^p(N^p, L^p), \{c_i^p, i \in N^p\}, \{b_{ij}^p, i, j \in N^p\}]$, a virtual node and requested resources $[u, c_u^v, b_u^v]$

Output: $List_{DC}^u$

1: **for** each DC_d, $d \in \{1, 2, \ldots, D\}$ **do**
2: Count $DC_d\{n^p(s_{aw}, t), n^p(s_{as}, t), v^p(s_{aw}, t\}$
3: **end for**
4: **for** each time interval t for embedding **do**
5: **for** each $DC_d, d \in \{1, 2, \ldots, D\}$ **do**
6: **if** $n^p(s_{aw}, t) > 0$ and $v^p(s_{aw}, t) \geq c^v(u, t)$ **then**
7: $List_{DC}^{awake}(t) := List_{DC}^{awake}(t)$.append$(DC_d)$
8: **else if** $n^p(s_{as}, t) > 0$ **then**
9: $List_{DC}^{asleep}(t) := List_{DC}^{asleep}(t)$.append$(DC_d)$
10: **end if**
11: **end for**
12: **end for**
13: $U_t = (List_{DC}^{awake}(t)) \bigcup (List_{DC}^{asleep}(t))$
14: $U_{t+1} = (List_{DC}^{awake}(t+1)) \bigcup (List_{DC}^{asleep}(t+1))$
15: **for** each DC_d in U_t **do**
16: **for** each DC'_d in U_{t+1} **do**
17: $List_{DC}^u$=$List_{DC}^u$.append(DC_d, DC'_d)
18: **end for**
19: **end for**

As demonstrated in Algorithm 1, the physical network, the VNs along with their topologies and available/required resources are listed as input. In steps 1-3, we count $n^p(s_{aw}, t)$ and $n^p(s_{as}, t)$, the number of physical nodes that are awake or asleep, respectively, and $v^p(s_{aw}, t)$, the maximum available resources on a single awake physical node.

This information will help to quickly filter out DCs without enough resources. Then for each unmapped virtual node u, we call FindFeasibleDCSets(DC,u) to calculate and return all feasible DCs for u, $List^u_{DC}$ satisfying the computational resource requirements.

In the function FindFeasibleDCSets, as presented in Algorithm 2, we check each DC_d for each time phase t to see 1) if DC_d has any awake physical node at time t; 2) if $v^p(s_{aw}, t)$ is larger than the required resources of the virtual node at time t; 3) if DC_d has any asleep physical node at time t. If conditions 1) and 2) stand, d will be added into $List^{awake}_{DC}(t)$; or if 3) stands but not 1) or 2), DC_d will be appended into $List^{asleep}_{DC}(t)$. The union U_t of $List^{awake}_{DC}(t)$ and $List^{asleep}_{DC}(t)$ contains all the DCs that have enough computational resources to embed u at time t. The Cartesian product of set U_t and U_{t+1} contains all the feasible DC sets that u could be embedded into without violating computational resource limitations.

For each element $(DC_d, DC_{d'})$ in $List^u_{DC}$, we could roughly estimate the energy consumption $C_u(DC_d, DC_{d'})$ by embedding u in DC_d at time t and in $DC_{d'}$ at time $t + 1$ using Equations (3.6) and (3.9). Each virtual node u may have multiple feasible DC sets with different estimates of energy consumption. We pick the two DC sets with the smallest estimated energy consumption and compute the difference δ_u between their consumptions. Virtual nodes are embedded based on δ and the virtual node w with largest δ_w will be embedded first. Different policies could be employed, e.g., first fit, load balance, or threshold, when embedding virtual nodes to physical nodes. After embedding w, each virtual link connecting w and its embedded virtual neighbors will be embedded to a physical link with the shortest path under resource constraints. Finally, the resources

usage is updated before embedding the next virtual node.

By calling Algorithm 2 whose time complexity is $O(m)$, where m is the number of physical nodes, the time complexity of Algorithm 1 is $O(n^2m)$, where n is the number of virtual nodes in the virtual network. It is because we need to go through each physical node for the amount of available resources. However, since the number of virtual nodes are quite small compared with the number of physical nodes, e.g., only 12 DCs are involved in B4 [63], this algorithm is efficient and reasonable in practice.

3.3 A Simple Comparative VNE Example

In this section, we discuss an example that compares the proposed TMAE-VNE with other existing schemes such as Topology Aware VNE (TA-VNE) [29] and Migration Aware VNE (MA-VNE) [22]. TA-VNE embeds virtual nodes based on the static rank that is determined by available resources and network topology. MA-VNE and TMAE-VNE are also topology-aware as they consider the distance between physical nodes while embedding or migrating virtual nodes or links. TMAE-VNE, on the other hand, schedules migrations according to predictable changes of physical networks or the workload of VNs before embedding VN requests. Therefore, migrations over an unnecessary long distance could be avoidable. In addition, TMAE-VNE could recognize the different energy usage between inter and intra DC links. Thus, it is especially suitable for networks of multiple DCs. TMAE-VNE also explores an efficient DC architecture and is aware of switch usage. The comparison of the three algorithms is summarized in Table 5.

We compare the algorithms with a simple VNE example shown in Figures 7, 8,

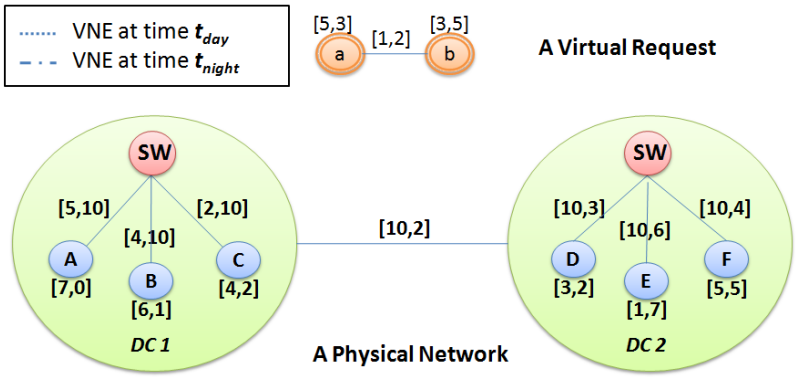

Figure 7: Topology Aware VNE (TA-VNE): no feasible embedding available

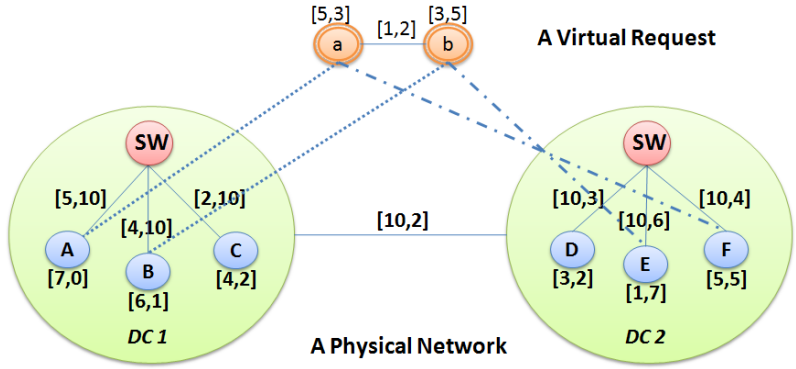

Figure 8: Migration Aware VNE (MA-VNE): total energy cost 86 units

and 9. We want to embed a VN request (with virtual nodes a and b) to a physical network that consists of two DCs. Each DC has a gateway switch, labeled as 'SW' and is connected to three physical nodes. We use a pair of numbers $[c^p(t_{day}), c^p(t_{night})]$ to indicate the 'available' resource of a physical node or link during time t_{day} and t_{night}. For a VN request shown on the top, we specify the amount of 'required' resources of the virtual node (or link) at time t_{day} and t_{night} by $[c^v(t_{day}), c^v(t_{night})]$. We assume that the operation energy consumption for a physical link between two DCs is 10 units, while energy consumption for a link within a single DC is 5 units. We also assume that the baseline energy for waking

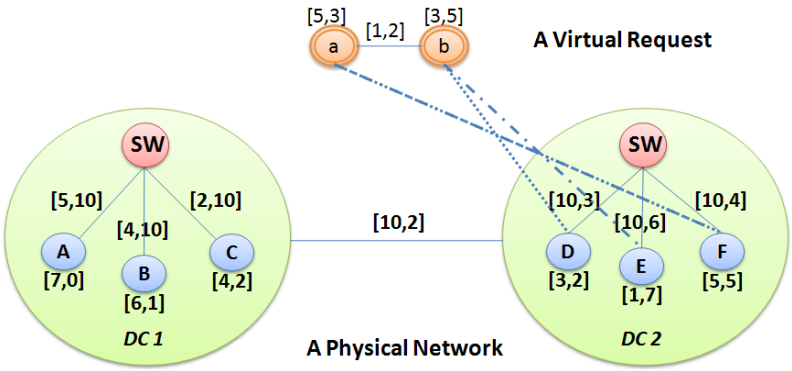

Figure 9: Topology and Migration-Aware Energy Efficient VNE (TMAE-VNE): total energy cost: 52 units

up a sleeping physical node is 10 units, while additional 5 units of energy are consumed for each embedded virtual node. We further set the coefficient of the duplicating execution cost as 1.

As shown in Figure 7, TA-VNE cannot find a feasible mapping according to Equations (3.5), (3.6), and (3.9). However, MA-VNE can embed virtual nodes a and b to physical nodes A and B at t_{day}, respectively, and migrate to physical nodes F and E at t_{night}, respectively, as in Figure 8. The total energy cost is 86 in the example, since the operation energy consumption is $40\ (= 5+10+5+5+10+5)$ and the migration energy cost is $46\ (= 23 + 23)$. Meanwhile, as depicted in Figure 9, the proposed TMAE-VNE can find the optimal solution. Node a is embedded to node F at both t_{day} and t_{night}, and node b is embedded to node D at t_{day} and E at t_{night}. The total energy cost is 52 including $40\ (= 5+10+5+5+10+5)$ for operation and $12\ (= 0+12)$ for migration. TMAE-VNE incurs less migration cost than MA-VNE as it plans migrations in advance for $t + 1$.

Table 5: Algorithms Comparison

	Topology Consideration	Migration Consideration	DC Architecture	Multiple DCs
TA	Node rank	✗	✗	✗
MA	Migration distance	When physical network evolves	✗	✗
TMAE	Inter/Intra DC topology	Physical/virtual workload changes	✓	✓

3.4 Evaluations

We compare the performance of TMAE-VNE with two existing algorithms, the Topology Aware VNE (TA-VNE) [29] and Migration Aware VNE (MA-VNE) [22], with respect to energy consumption and acceptance ratio using various parameter settings.

3.4.1 Setting

We generate a physical network that consists of DCs and links between DCs. The inter-DC network is randomly generated using NetworkX [86], and the DCs are highly connected through this inter-DC network. Networks within a DC are generated in a hierarchical architecture. Since we are focusing on VNE, we use the simplest DC architecture; however, TMAE-VNE could be easily extended for more complicated architectures, such as [3] to improve the scalability. A root switch connects with all aggravate switches. Each aggregate switch is connected with a group of edge switches, and each edge switch is connected with a group of physical nodes. The number of physical nodes in a DC is randomly determined.

The status of each physical node is randomly determined to be awake or asleep with an equal probability of 0.5. Each physical node is randomly assigned a value between [20, 35] to indicate its maximum available resource following uniform distribution. To examine the impact of the available resources on energy consumption, we randomly deduct a portion of available resources of each physical node to simulate the initial resource usage. The deducted portion is randomly decided following uniform distribution between $[0, \theta]$. We vary the lower bound of this portion θ between [0.1, 0.9] and examine its impact in Figure 11.

We validate our algorithm through three sets of simulations comparing with the optimal solution solved by IBM ILOG CPLEX, and two existing algorithms TA-VNE and MA-VNE using topology generated by NetworkX as well as a real topology of B4.

TA-VNE computes a rank for each physical node based on its available computational and network resources. It also calculates a rank for each virtual node based on its required resources and connectivity. Intuitively, the virtual node with a higher rank has more neighbors or demands more resources compared with the virtual node that has a lower rank. On the other hand, a physical node with a higher rank possesses more resources than a physical node with a lower rank. Therefore, TA-VNE embeds virtual nodes to physical nodes based on the nodes' ranks, so that the virtual node v with the highest rank will be mapped to a physical node i with the highest rank. In addition, it validates if i could meet all the demands of v.

Note that TA-VNE determines a static VNE decision for a VN request. Even though, the substrate network or the mapped VNE may vary later, v is always mapped

to i. As illustrated in Section 3.1, static VNE methods may not find the most efficient solution or even a feasible solution. Unlike TA-VNE, MA-VNE provides a dynamic VNE solution. When the substrate network evolves, MA-VNE may migrate a virtual node v from a physical node i to another physical node j to save costs and increase the acceptance ratio. In addition, delays are considered, so that v will be migrated to j only if the delay between i and j satisfies some constraints.

We summarize the parameters used in this chapter in Table 6.

Table 6: Parameter Setting

Parameter	Values
Probability of sleep/awake status	0.5
Range for physical capacity	[25, 30]
Portion of available physical resources	[0.1, 0.9]
Number of DCs	[2, 5] or [1, 13]
Size of each DC	[3,6] or [5,10]
Number of hierarchy layers in each DC	3
Size of VNs	[3,6] or [3,10]
Amount of virtual resource request	[3,5]

3.4.2 Comparison with the Optimal Solution

We first validate our algorithm by comparing it with the optimal solution solved by IBM ILOG CPLEX. Due to the hardness of the problem, we use small physical networks and VN requests. The number of DCs in this set of evaluations changes from 2 to 5, while the number of physical nodes in a DC is randomly decided between 3 to 6. We also use NetworkX to generate a random topology for each VN request. The number of virtual nodes in each VN request is randomly selected from 3 to 6 following uniform distribution.

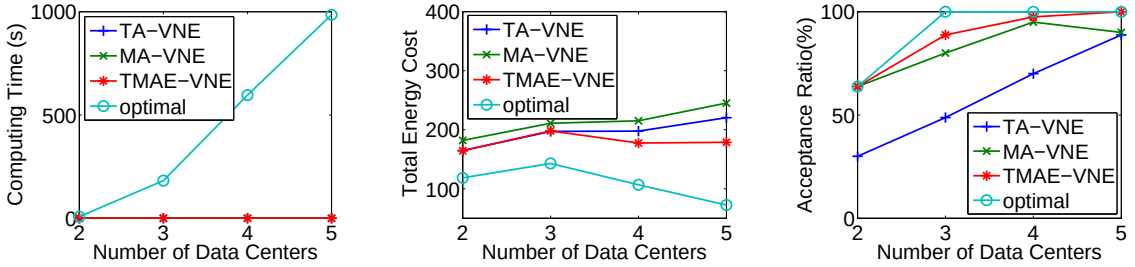

(a) Execution time (b) Total energy cost (c) Acceptance ratio

Figure 10: Comparison with optimal solution

Each virtual node requires a random amount of resources between [3,5].

As presented in Figure 16(a), the average computing time of embedding each VN by using CPLEX increases exponentially from 7.8 s to 985.03 s when the number of DCs in the physical network rises from 2 to 5, while the computing time of TA-VNE, MA-VNE, and the proposed TMAE-VNE are stable around 0.01 s even when the size of the problem increases. Although there is some distance between the proposed TMAE-VNE and the optimal solution in the total cost (Figure 16(b)) and the acceptance ratio (Figure 16(c)), TMAE-VNE always outperforms TA-VNE and MA-VNE. As the problem size increases, the distance between the total costs computed by the optimal solution and that computed by the heuristic algorithms becomes larger as shown in Figure 16(b). In addition, as shown in Figure 16(c), when the physical network expands, the acceptance ratios of all the four methods increase as there are more available resources.

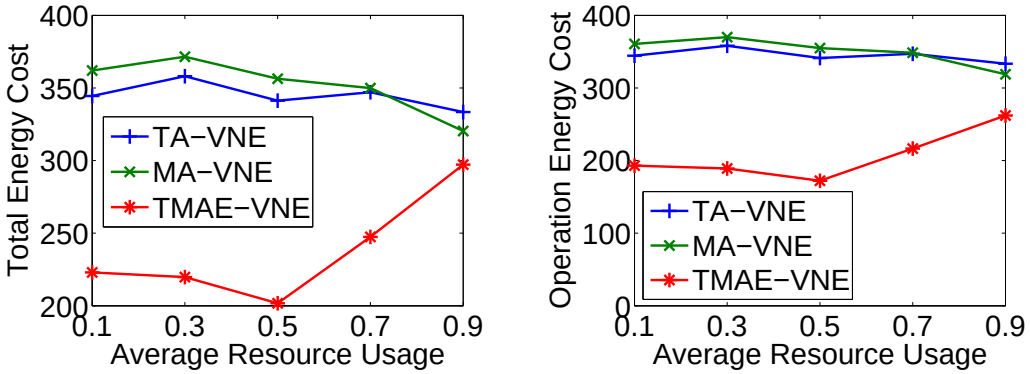

(a) Total energy cost

(b) Operation energy cost

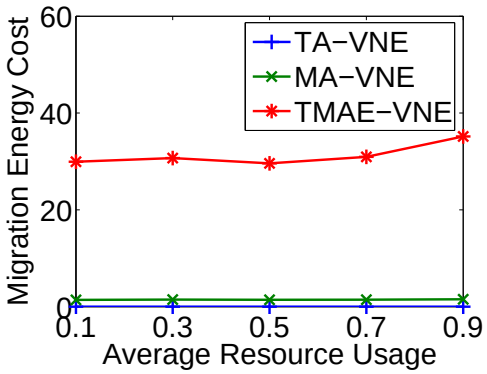

(c) Migration energy cost

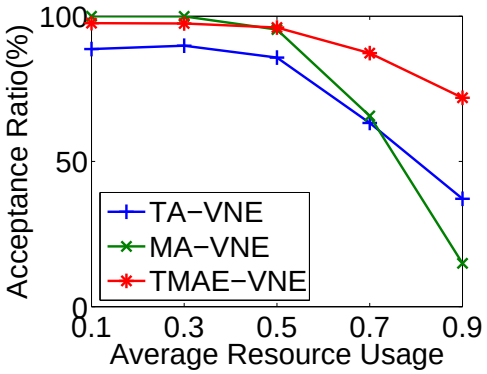

(d) Acceptance ratio

Figure 11: Comparison for varied resource usage ratio

3.4.3 Comparison with Two Existing Algorithms

Using larger scale DCs, we compare our TMAE-VNE algorithm with two existing algorithms. The number of physical nodes in a DC is randomly decided between 5 and 10, and the number of virtual nodes in each VN request is randomly selected from 3 to 10 following uniform distribution.

We examine the impact of the initial usage rate of each physical node in Figure 11

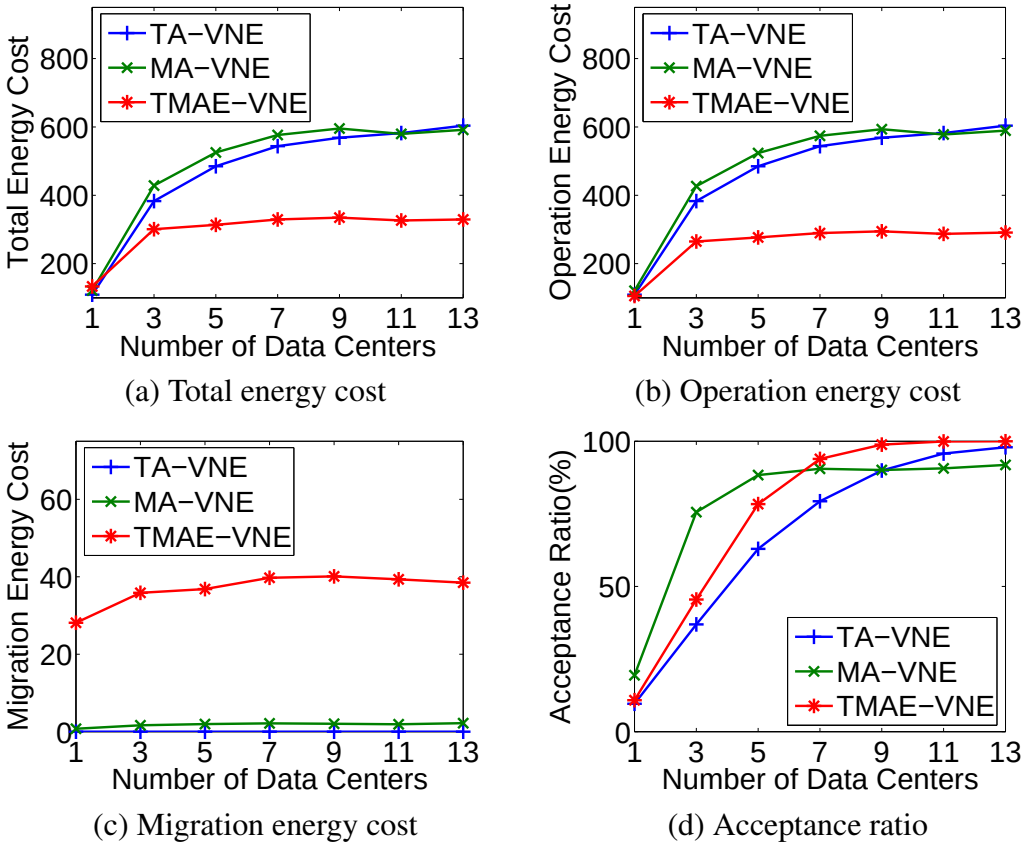

(a) Total energy cost

(b) Operation energy cost

(c) Migration energy cost

(d) Acceptance ratio

Figure 12: Comparison for varied number of DCs

on the total energy cost, operation energy cost, migration energy cost, and VNE acceptance ratio. The average initial usage rate varies between [0.1, 0.9]. A smaller rate means more available resources on a single physical node.

As demonstrated in Figure 11, TMAE-VNE achieves the largest acceptance ratio and the smallest total energy consumption. When the initial usage rate increases from 0.1 to 0.9, the acceptance ratio of TMAE-VNE drops from 97.6% to 71.9%. However, it is still 33.2% or 57% higher than TA-VNE (only 37.1%) or MA-VNE (only 14.9%),

respectively. The migration energy cost and operation energy cost slightly increase when the initial usage rate grows. Since the initial usage rate is larger, physical nodes with sufficient available resources are spread around the physical network. However, TMAE-VNE always consumes the least cost. It even cuts up to 40% energy consumption compared to MA-VNE.

We also check the impact of the number of DCs in the physical network in Figure 17. Here, the number of DCs varies from 1 to 13. When the number of DCs increase, the total number of physical nodes that are possible to have enough capacity rises too. However, since the network expands, the length of a physical path that embeds a virtual link may become longer. Therefore, the total energy consumption increases when the number of DCs increases from 1 to 3. When the physical network grows from 3 to 13, the available resources become even more, so that TMAE-VNE could always find mappings consuming less energy. This leads to the stable energy usage when the number of DCs is from 3 to 13 or even a little drop from 9 to 11.

As shown in Figure 17, the acceptance ratio rises when the number of DCs increases as there are more physical nodes in the entire physical network. At the same time, migration energy costs and operation energy costs rise when the number of DCs increases from 1 to 5 and keep stable when there are more than 7 DCs. TMAE-VNE still consumes the least energy all the time. The acceptance ratio of TMAE-VNE is slightly lower than MA-VNE when the number of DCs is less than 7, but it grows quickly when there are more DCs in a physical network. This is because we determine the order for each virtual node based on energy savings, while MA-VNE determines the order based

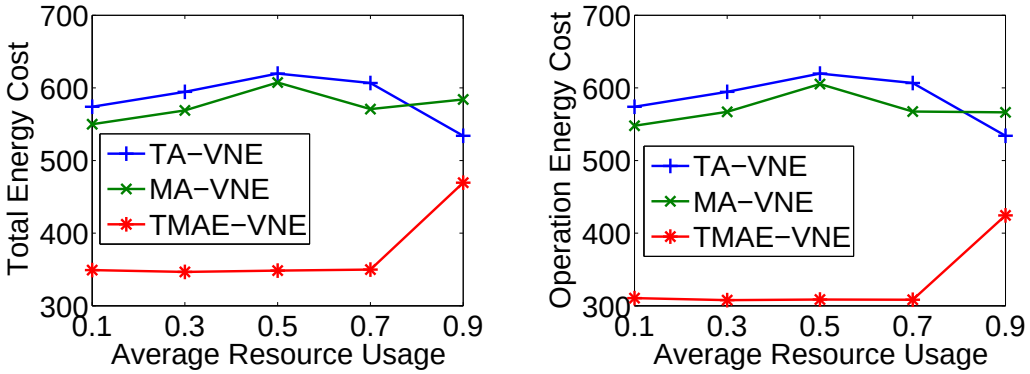

(a) Total energy cost

(b) Operation energy cost

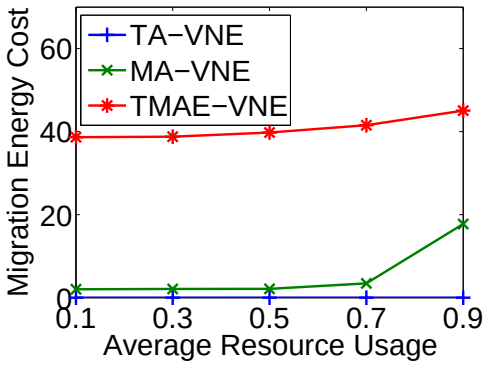

(c) Migration energy cost

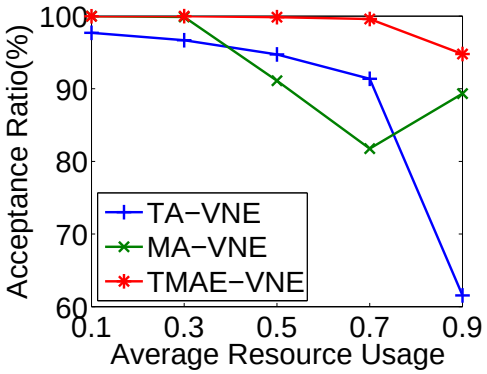

(d) Acceptance ratio

Figure 13: Comparison for varied number of DCs under B4 topology

on the required resources of a virtual node. When the number of available physical nodes is small, MA-VNE ensures the virtual nodes that require more resources are mapped first, then it embeds the virtual nodes with a small requirement to fill the gap. However, our TMAE-VNE could always achieve minimal energy consumption and a high acceptance ratio as the physical network expands.

We also validate the efficiency of the TMAE-VNE algorithm using a real topology of B4 that is a globally-deployed software defined network operated by Google [63]. B4

has 12 DCs covering 3 continents.

We checked the impact of the initial resource usage rate in the B4 network in Figure 13. As shown in Figure 13(a) TMAE could reduce up to 44% of the total energy consumption compared with TA-VNE by finding a good balance between the operation energy cost and the migration energy cost. In addition, TMAE also increases the acceptance ratio up to 33%. In addition, MA-VNE has the lowest acceptance ratio when the available resources in the physical network is relative low. This is because that MA-VNE only migrates the virtual nodes or links when their embedded physical nodes or links do not have enough physical resources, and MA-VNE puts some limitations on the migration distance. However, when the available resources in the physical network are extremely (0.9), the acceptance ratio is around 90% that is better than the case that the initial resource usage is relative low (0.7). It is because, when the available resources are extremely low, most virtual nodes have to be migrated, and the constraint cover set would be larger.

3.5 Summary

We have modeled and proposed an efficient and practical virtual network embedding algorithm (TMAE-VNE) that takes energy consumption, future migration, and practical intra/inter DC topologies into consideration to minimize the energy consumption caused by both operation and migration of virtual networks. Since computing and network demands of a virtual network change over time and are often predictable (such as during day/night times and weekday/weekends), by considering future resource migration at the time when the different resource amounts are demanded, we have shown more physical

nodes and links can be put into a sleep mode leading to greater energy savings. Understanding hierarchical fat tree DC architectures further allows us to optimize the network resource usages. We have performed extensive comparisons with prior VNE algorithms using practical intra and inter-DC topologies, and we have validated that the proposed algorithm significantly saves energy consumption, while achieving high acceptance ratios under various scenarios.

CHAPTER 4

ANT COLONY OPTIMIZATION BASED ENERGY EFFICIENT VIRTUAL NETWORK EMBEDDING

Efforts have been done to lower energy consumption by data centers, such as, proportional energy consumption hardware, dynamic provisioning, and virtualization techniques. Especially, Energy efficient virtual network embedding (EE-VNE) has been studied to improve the utilization of network resources and save energy consumption in data centers in Chapter 3. However, the problem has been proved to be NP-hard. Especially, when considering multiple data centers with evolving virtual network resources requirements, it becomes much more challenging to approach an optimal solution in a reasonable amount of time.

Exact optimization algorithms with CPLEX/GLPK have been adapted to solve the EE-VNE problem, e.g., [19]. However, as the size of the problem increases, their computation time increases dramatically. In Chapter 3, we proposed a topology and migration aware energy efficient VNE model that aims to maximize energy savings for virtual network requests during their entire life cycle rather than a time snapshot. Considering the entire life cycle of virtual network requests further reduces the energy consumption in VNE. However, it significantly expands the solution space compared with existing VNE problems and leads to exponential increasing execution time. A heuristic algorithm has been developed to solve the energy efficient VNE problem. It outperforms existing algorithms in energy savings and acceptance ratios, but still cannot achieve the optimal

solution as we examined with simulations in Section 4.2.

A meta-heuristic method is a sophisticated tool to solve a wide group of hard problems [17]. It provides us an alternative way to obtain near optimal solutions in a reasonable time, especially for NP-hard problems. It has been applied to a wide group of difficult problems [17]. Compared to heuristic algorithms and exact algorithms, meta-heuristic algorithms could obtain high quality solutions of difficult optimization problems in a reasonable time [108]. Driven by this, we propose an Ant Colony Optimization (ACO) based algorithm to solve the EE-VNE problem to minimize the energy consumption of virtual networks during their entire life cycle rather than a time snapshot. In our model, we consider large scale physical networks and evolved virtual network requests, and include both the operation cost and migration cost for embedded nodes and links.

In addition, we design an efficient method to track and update the pheromone to tackle the EE-VNE problem on a large scale. Specifically, we only track and update the pheromone on the trails that are touched by the ants. This way, the space complexity of tracking and updating the pheromone is reduced from $O(n^4m^2)$ to $O(m^2n_{ant}n_{it})$ where n is the number of physical nodes; m is the number of virtual nodes; n_{ant} is the number of ants; and n_{it} is the number of maximum iterations. Our extensive evaluation results show that our ACO-EE-VNE could reduce energy consumption up to 52% and double the acceptance ratio compared with existing virtual network embedding algorithms.

The contributions achieved in Chapter 4 are as follows.

- We propose a novel ACO based topology migration-aware EE-VNE algorithm (ACO-EE-VNE) to minimize the energy consumption caused by both operation and migration that provides high quality solutions without taking too much time. In doing so, we consider data center network topologies and dynamic resource demand over time.

- We develop a novel pheromone update and track scheme in the ACO algorithm, so that the space complexity of the ACO algorithm is substantially reduced.

- We conduct extensive comparisons with three state-of-the-art algorithms as well as an exact optimization algorithm using CPLEX with various inter-DC topologies. The results prove that the proposed algorithm significantly saves energy consumption and allows high acceptance ratios within a reasonable amount of execution time.

The remainder of this chapter is organized as follows. We convert the EE-VNE problem presented in Section 3.1 to an ACO construction graph and propose the ACO based topology migration-aware EE-VNE algorithm in Section 4.1. We validate the performance of ACO-EE-VNE algorithm through evaluations and comparisons with existing algorithms in Section 4.2, and present the concluding remarks of this chapter in Section 4.3.

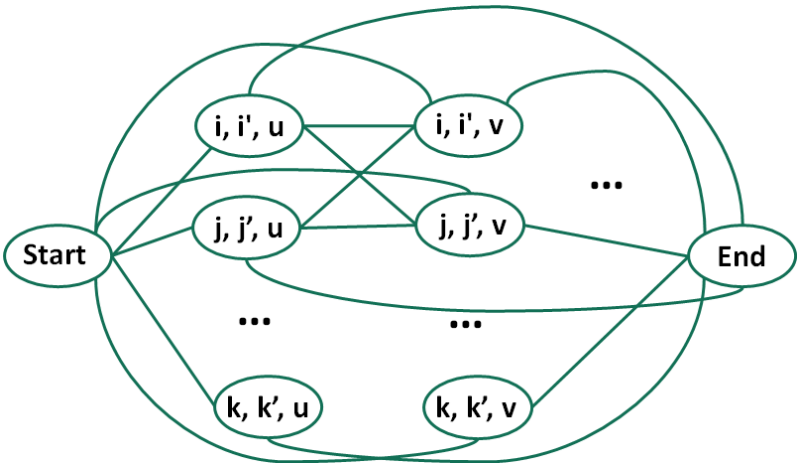

Figure 14: Construction graph for ACO model

4.1 Ant Colony Optimization Based Model and Solution

In this section, we establish a construction graph similar to [36] to model our EE-VNE problem as an ACO problem. We then design the strategies for the pheromone and heuristic factor assignment on the tuples and links in the graph. Based on the construction graph, and heuristic and pheromone strategies, we develop an ACO based EE-VNE algorithm. Furthermore, to deal with the large scale EE-VNE problem, we propose a novel way to track and update the pheromone on the links in the graph. Notations used in this section are listed in Table 7.

4.1.1 ACO Model

In order to map the VNE problem to a problem that could be solved by ACO, we build a construction graph $G^{ACO}(N^{ACO}, L^{ACO})$. In the graph, the embedding from virtual nodes to physical nodes at different times are represented as tuples in the graph.

Table 7: Notations Used

Notation	Explanation
$G^{ACO}(N^{ACO}, L^{ACO})$	ACO Construction graph with a set of vertices N^{ACO} and a set of links L^{ACO}
(i, i', u)	A vertex in ACO graph indicating that virtual node u is embedded to physical node i at time t and i' at time $t+1$
$\tau_{i,i',u,j,j',v}$	Pheromone on the trail between ACO vertices (i, i', u) and (j, j', v)
τ_0	Initial pheromone that is identical for every trail
$\tau_{i,i',u}$	Pheromone factor of a vertex (i, i', u)
ξ	Pheromone evaporation coefficient
Δ_τ^k	Amount of pheromone laid by the kth ant
g_{best}	Energy consumption of the global best solution
g_k	Energy consumption of the solution found by the kth ant
$\rho_{i,i',u}^k$	Transition probability of ant k travels to vertices (i, i', u) when it has a partical solution S_k
$C_{i,i',u}$	Total energy consumption of the assignment (i, i', u)

The link between any two tuples A and B indicates the likelihood that an artificial ant would move toward the tuple B when it is standing at tuple A. This likelihood is computed based on both heuristic factor and a historical factor, pheromone. Pheromone would be updated based on the energy consumption of solutions in previous iterations, and it would eventually evaporate in time.

Construction graph: The vertex set N^{ACO} of G^{ACO} consists of the tuple vertex

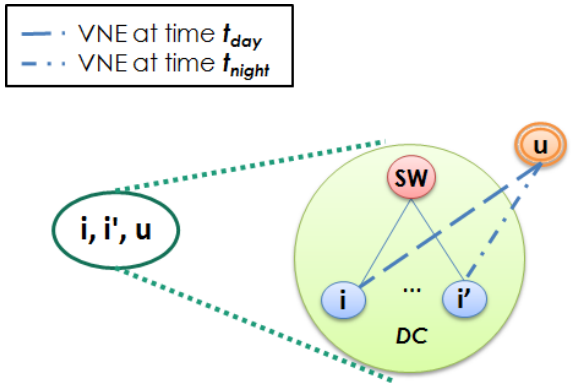

Figure 15: A tuple (i, i', u) in the ACO construction graph represents a mapping in the EE-VNE problem that virtual node u is assigned to physical node i at time t and physical node i' at time $t + 1$.

(i, i', u), the nest of ants denoted by $Start$ vertex, and the food denoted by end vertex as shown in Figure 14. Each tuple (i, i', u) represents a mapping from a virtual node u to physical nodes i, i' at different time snapshots as presented in Figure 15. Each vertex in N^{ACO} is associated with a cost that corresponds to the energy consumption of the node mapping including the node operation energy cost and the node migration energy cost. L^{ACO} is the edge set of the complete graph on N^{ACO}. A link in L^{ACO} that connects vertices (i, i', u) and (j, j', v) is associated with a cost that corresponds to the link energy consumption including the link operation cost and link migration cost. If virtual nodes u and v are not directly connected in a VN request, the cost of the link between vertices (i, i', u) and (j, j', v) is set to infinite.

A trail from the nest $Start$ to the food end corresponds to a feasible solution to the EE-VNE problem. In this graph, ants want to find a trail from the nest $start$ to the food end with the minimum total cost that corresponds to the energy consumption of

embedding a virtual network.

Constraints: Each virtual node must be exactly mapped to one physical node at each time slot, and each physical node cannot embed more than one virtual node for a single VN request at any time. In addition, the mapping is subjected to resource limitations on physical nodes and links.

Pheromone trails: The pheromone trail between any two vertices (i, i', u) and (j, j', v) refers to the desirability of embedding virtual node u to physical nodes (i, i') while virtual node v is embedded to physical nodes (j, j'), or vice versa. The initial value of pheromone τ_0 on each trail is identical when constructing the graph. Each iteration, pheromone on each trail evaporates as:

$$\tau_{i,i',u,j,j',v} = max\{\tau_0, (1-\xi)\tau_{i,i',u,j,j',v}\} \tag{4.1}$$

where ξ is the evaporation coefficient. Meanwhile, ant k lays pheromone on the trails between any pair of vertices in its corresponding as

$$\tau_{i,i',u,j,j',v} = \tau_{i,i',u,j,j',v} + \xi\Delta_\tau^k \tag{4.2}$$

Δ_τ^k is the amount of pheromone laid by the kth ant. Here, we model Δ_τ^k as the ratio between the energy consumption of the global best solution g_{best} to the energy consumption of the solution g_k found by the kth ant.

$$\Delta_\tau^k = \frac{g_{best}}{g_k} \tag{4.3}$$

We denote the set of already traveled vertices by the kth ant as partial solution S_k. For the kth ant, the pheromone factor $\tau_{i,i',u}$ of a vertex (i, i', u) depends on the quantity of

pheromone on the edges between the vertex (i, i', u) and the vertices in S_k:

$$\tau_{i,i',u} = \sum_{(j,j',v) \in S_k} \tau_{i,i',u,j,j',v} \tag{4.4}$$

Heuristic information: The ratio between the minimum possible node energy consumption $2\chi_{op}$ to the energy consumption $C_{i,i',u}$ of mapping the virtual node u are utilized as the heuristic factor $\eta_{i,i',u}$

$$\eta_{i,i',u} = \frac{\chi_{opr}}{C_{i,i',u}} \tag{4.5}$$

$$\chi_{opr} = \sum_{t} \alpha_{o_2} c^v(u, t) \tag{4.6}$$

We use the operation power consumption χ_{opr} of a physical node multiply the length of the operation time duration 2, as the minimum possible node embedding energy consumption, and compute the energy consumption $C_{i,i',u}$ as the sum of node operation energy consumption $C_{opr}(i, i', u)$, defined in Equ. (3.6) and node migration energy consumption $C_{mgr}(i, i', u)$, defined in Equ. (3.9).

$$C_{i,i',u} = C_{opr}(i, i', u) + C_{mgr}(i, i', u) \tag{4.7}$$

Based on the heuristic factor $\eta_{i,i',u}$ and pheromone factor $\tau_{i,i',u}$ of each vertex, each ant selects vertices randomly within the candidate set with respect to the transition probability $\rho_{i,i',u}$ when the kth ant has a partial solution S_k, i.e.,

$$\rho^k_{i,i',u} = \frac{[\eta_{i,i',u}]^\alpha [\tau_{i,i',u}]^\beta}{\sum_{(j,j',v) \in S_{cand}} [\eta_{j,j',v}]^\alpha [\tau_{j,j',v}]^\beta} \tag{4.8}$$

4.1.2 ACO-VNE

Based on the model described in Section 4.1.1, a trail from the nest $start$ to the food end corresponds to a solution of the EE-VNE problem. Each ant moves from

Algorithm 3 Ant Colony Optimization based EE-VNE (ACO-EE-VNE)

1: Build the construction graph $[G^{aco}(N^{aco}, L^{aco})]$, initialize the global best solution $g_{global} = +\infty$
2: Compute the heuristic factor for each node in N^{aco}
3: **while** the maximum number of iteration is not reached **do**
4: Initialize a group of n_{ant} ants
5: **for** Each ant **do**
6: Call Algorithm 4 to compute the mapping results g_{ant}
7: Update the pheromone matrix on the trails that have been touched using Eq. (4.2)
8: **end for**
9: Compute the local best solution g_{local} in this iteration
10: **if** $g_{local} < g_{global}$ **then**
11: Update global best solution $g_{global} = g_{local}$
12: **end if**
13: Evaporate pheromone using Eq. (4.1)
14: **end while**

one vertex to another vertex using a decision policy based on the heuristic factor and pheromone until it eventually arrives at the food. In order to converge toward the optimal solution, the algorithm runs for multiple iterations and in each iteration, multiple ants move independently toward the food. The ants in previous iterations lay pheromone for ants in later iterations, while the pheromone laid on each link evaporates in each iteration. The detailed procedure of the ACO algorithm is presented in Algorithm 3 and Algorithm 4.

Note that in ACO, the pheromone on links between any two vertices are kept for computing transition probability. The space complexity of tracking the pheromone is $O(n^4m^2)$, where n is the number of physical nodes, and m is the number of virtual nodes. This consumes huge amounts of memory for large scale physical networks. Actually, ants only visit a portion of the graph, and most of the links in the graph are not touched.

Algorithm 4 Ant Colony Optimization based EE-VNE - Solver

1: Randomly choose a start vertex based on the transition probability matrix
2: Put the selected vertex into $trail$, label corresponding physical node and virtual node as mapped
3: Put the virtual nodes that are not embedded and adjacent to the mapped virtual node in set $S_{neighbor}$
4: **for** Virtual node in $S_{neighbor}$ **do**
5: Find the candidate vertices and compute their transition probability
6: Select a vertex based on Roulette algorithm
7: **if** The mapping is not valid **then**
8: Continue
9: **end if**
10: Put the selected vertex into S_{trail}, label corresponding physical node and virtual node as mapped
11: Update $S_{neigbhor}$ by removing embedded virtual node and adding its unmapped neighbors
12: **end for**
13: **return** the solution of embedding $trail$

Therefore, we do not need to track the pheromone on every link, but only the portion of links that were touched by the ants, as shown in Algorithm 3. When computing the transition probability matrix (Algorithm 4) which includes untouched links, the pheromone of these untouched links are the initial value assigned in the Algorithm's input. The space complexity of only tracking the pheromone of touched links has been reduced to $O(m^2 n_{ant} n_{it})$, where n_{ant} is the number of ants in each iteration and n_{it} is the number of iterations.

4.2 Evaluations

To validate the performance of the ACO-EE-VNE algorithm, we compare it with three existing algorithms, the Topology Aware VNE (TA-VNE) [29], Migration Aware

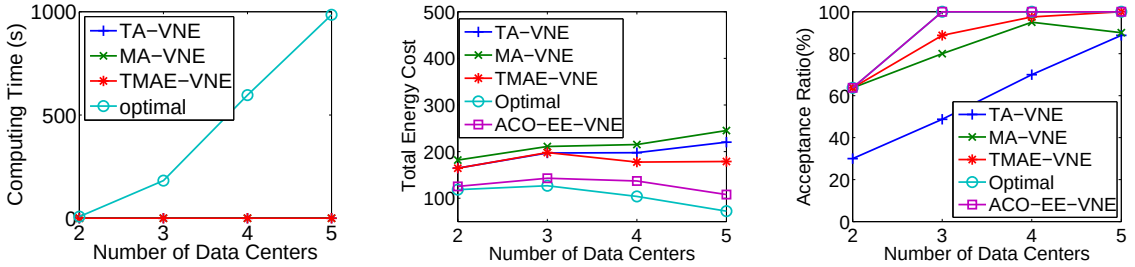

(a) Execution time (b) Total energy cost (c) Acceptance ratio

Figure 16: Comparison with optimal solution

VNE (MA-VNE) [22], and topology and migration aware energy efficient VNE (TMAE-VNE), and CPLEX based exact algorithm with respect to energy consumption and acceptance ratio using various parameter settings.

TA-VNE [29] calculates the rank for each physical node and each virtual node based on its available computational and network resources, or required resources and connectivity, respectively. Later, the physical node with the highest rank would be utilized to embed the virtual node with the highest rank if the physical node could meet all the demands of the virtual node.

Note that TA-VNE embeds virtual nodes based on their demands on peak workloads and makes a static VNE decision for each VN request. MA-VNE and TMAE-VNE, may embed a virtual node to different physical nodes at different times to save costs and increase the acceptance ratio. MA-VNE migrates virtual nodes when the physical network evolves and the physical node cannot serve the virtual node embedded on it due to resource limitations. TMAE-VNE schedules possible migrations for the future as well as the embedding for the current moment while mapping a virtual network.

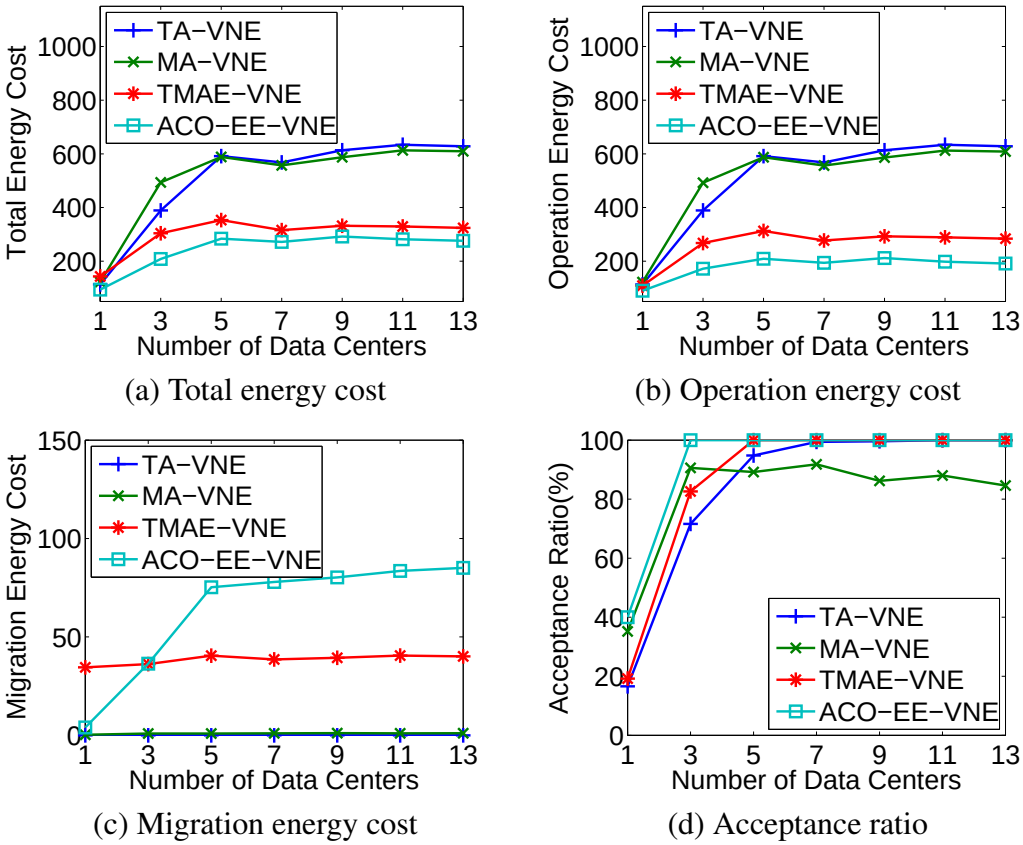

(a) Total energy cost

(b) Operation energy cost

(c) Migration energy cost

(d) Acceptance ratio

Figure 17: Comparison for varied number of DCs

We follow the similar setting used in Chapter 3.4. The topologies of inter-DC network and virtual networks are generated by NetworkX [86], while the intra-DC topologies are generated in a hierarchial architecture. We randomly determined the status of each physical node to be awake or asleep with an equal probability of 0.5, and the maximum available resource of each physical node is randomly assigned between [20, 35] following uniform distribution. The parameters used in this chapter are summarized in Table 8.

Table 8: Parameter Setting

Parameter	Values
Probability of sleep/awake status	0.5
Range for physical capacity	[25, 30]
Portion of available physical resources	[0.1, 0.9]
Number of DCs	[2, 5] or [1, 13]
Size of each DC	[3,6] or [5,10]
Number of hierarchy layers in each DC	3
Size of VNs	[3,6] or [3,10]
Amount of virtual resource request	[3,5]

4.2.1 Comparison with the Optimal Solution

We first investigate the performance of heuristic algorithms and our proposed ACO-based meta-heuristic algorithm through comparisons with the exact algorithm based on IBM ILOG CPLEX. In the case of small scale problem, CPLEX-based algorithm can give the optimal solution. We use it as the baseline in the comparison. However, its search time grows exponentially as the problem scale increases. Therefore, we use small physical networks and VN requests in this simulation. Here, the number of DCs changes from 2 to 5, while the number of physical nodes in a DC is randomly selected between 3 to 6.

As presented in Figures 16(a) and (b), the heuristic algorithms cannot achieve the optimal solution in the total cost and the acceptance ratio. Especially, when the problem size increases, the distances between the optimal solution and the heuristic algorithms become larger. The proposed ACO based algorithm outperforms three heuristic algorithms, and is quite near the optimal solutions obtained by the CPLEX based algorithm. On the other hand, the average time for computing VNE of using CPLEX raises exponentially

from 7 s to 985 s when the number of DCs increases from 2 to 5 as shown in Figure 16. The computing time of the ACO based algorithm only slightly increases to 233 s, which is around 23.65% of the execution time of the CPLEX based algorithm. From the observation in Figure 16, ACO based algorithm could obtain the near optimal solution within a limited time.

4.2.2 Comparison with three Existing Algorithms

We also compare our ACO based algorithm with three existing heuristic algorithms on the total energy cost, operation energy cost, migration energy cost, and VNE acceptance ratio with varied problem size in Figure 17. The number of physical nodes in a DC is randomly decided between 5 and 10, and the number of virtual nodes in each VN request is randomly selected from 3 to 10 following the setting in [56].

As shown in Figure 17(d), the acceptance ratio rises as the number of DCs increases from 1 to 13 for all four algorithm. ACO-EE-VNE always achieves the highest acceptance ratio and the smallest total energy consumption. When the number of DCs rises from 1 to 5, the acceptance ratio of the ACO based VNE increases from 40% to 100%. It is almost double the acceptance ratio of the three heuristic algorithms. On the other hand, when the physical network expands, a longer physical path may be used to embed a virtual link. In Figure 17(a)(b)(c), the total energy consumption increases as the number of DCs rises from 1 to 3. However, when the physical network grows even larger from 3 to 13, the energy usage of all the four algorithms is relatively stable. ACO-EE-VNE could also find a good trade-off between the operation cost in Figure 17(b) and the migration

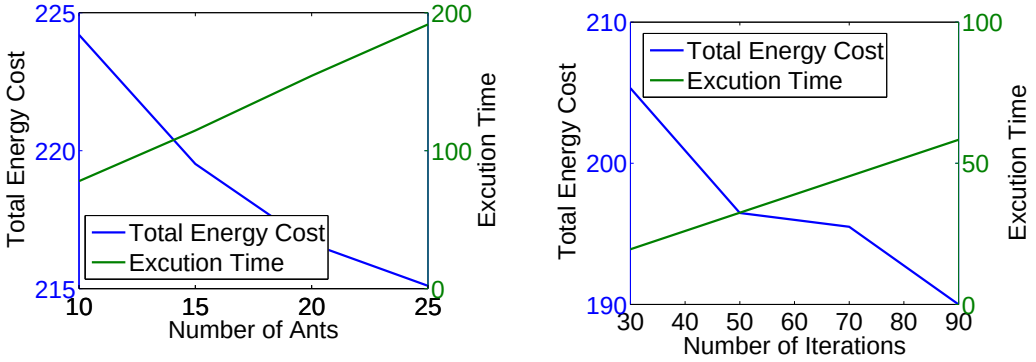

(a) Impact of number of ants (b) Impact of iteration times

Figure 18: Impact of parameters in ACO

cost in Figure 17(c). As demonstrated in Figure 17(a), during each VN request's entire life time including its initial embedding and migrations in different times, ACO-EE-VNE cuts up to 52% total energy consumption compared with TA-VNE and MA-VNE, and saves up to 32% total energy consumption compared with TMAE-VNE.

We further check the impact of the number of ants in each iteration on the energy saving and execution time in Figure 18(a) and the impact of the number of iterations in Figure 18(b). Figure 18(a) shows that the more ants, the better the solution the ACO algorithm could reach. However, the execution time increases from 77 s to 191 s when running with a single thread. Figure 18 demonstrates that running the ACO for iterations could improve the quality of the solution, but adds more execution time.

4.3 Summary

We investigated energy efficient virtual network embedding considering both operation and migration energy consumption. Driven by the motivation that heuristic algorithms usually have a low approximation ratio and the time complexity of an exact algorithm increases exponentially as the problem scales, we designed an ACO based meta-heuristic algorithm to minimize the energy consumption of the entire life cycle of virtual networks within a limited execution time.

We built a construction graph to model the energy efficient problem into an ACO problem. We formulated a proper heuristic factor and pheromone trail specifically for our energy efficient ACO problem. Due to the extremely large scale of the VNE problem, we improved the way that tracks and updates pheromone trails in the constructed graph, so that the execution memory consumption could be saved from $O(n^4m^2)$ to $O(m^2n_{ant}*n_{it})$, where n_{ant} is the number of ants in each iteration and n_{it} is the number of iterations. Extensive comparisons with prior heuristic VNE algorithms and a CPLEX based exact algorithm have been performed. Through these comparisons, it was validated that the proposed ACO based algorithm achieved a near optimal solution within an acceptable execution time under various scenarios.

CHAPTER 5

ENERGY AWARE CONTAINER BASED RESOURCE ALLOCATION FOR VIRTUAL SERVICES IN GREEN DATA CENTERS

Recently, an alternative to Hypervisor based virtualization techniques attracts many attentions from industry. These techniques based on Linux container [102] provide superior system efficiency and isolation. The container based VMs are light-weight, so that could be promptly deployed and migrated between different physical machines. In addition, Docker [35] that is a management tool for Linux container based virtualization, has been invented recently. It enables layering of network application libraries and bins that improves the memory efficiency of containers by sharing the libraries between multiple network services. Due to its benefits, Docker has been widely recognized in industry and adopted by many big companies, such as Groupon, Paypal [84].

Deploying a network service through embedding Hypervisor based VMs with fixed numbers and fixed capacities has a less success rate when the available physical resources are less and in fragments. An illustration example is presented in Figures 19 and 20. A network service is going to be deployed with the physical resources in a data center with 5 physical machines. Each physical machine only has a small amount (4 units) of available resources. However, a cloud user has no idea about data center usage and asks for 4 VMs with 5 units of resources to deploy certain network application as drawn in Figure 19. In this example, this VM placement request cannot be satisfied, since the remaining resources on each physical machine are not enough to embed any VM.

On the other hand, considering the usage status in the data center, we can divide the application workload and assign the workload to 5 containers. Each container is allocated 4 units resources to satisfy the QoS requirements of the application. Then these containers can be fitted into the physical machines and the application is successfully deployed as shown in Figure 20.

Driven by this motivation, we aim to design a dynamic resource allocation framework. Unlike tradition VM based resource provisioning, service providers do not need to specify or dedicate a fixed amount of VMs to deploy an application using the proposed framework. Based on the workload of the application and resource usage status in the physical networks, The number of container based-VMs and the demands of each VMs could be dynamically determined to minimize the deployment cost and improve the acceptance ratio. In addition, we consider using Docker like container management tool, to layer application supporting libraries and bins to improve memory efficiency.

The contributions of this chapter are as follows:

- we introduce the framework for container based dynamic resource allocation mechanism. In this framework, service providers specify their demands from service level rather than infrastructure level. Physical resources would be dynamically provisioned based on current workload of each network service/application. Based on our knowledge, we are the first one to study resource allocation mechanism using container based virtualization techniques.

- To save cost for service providers, and improve resource usage efficiency, we formulate the dynamic resource allocation problem as an optimization problem and

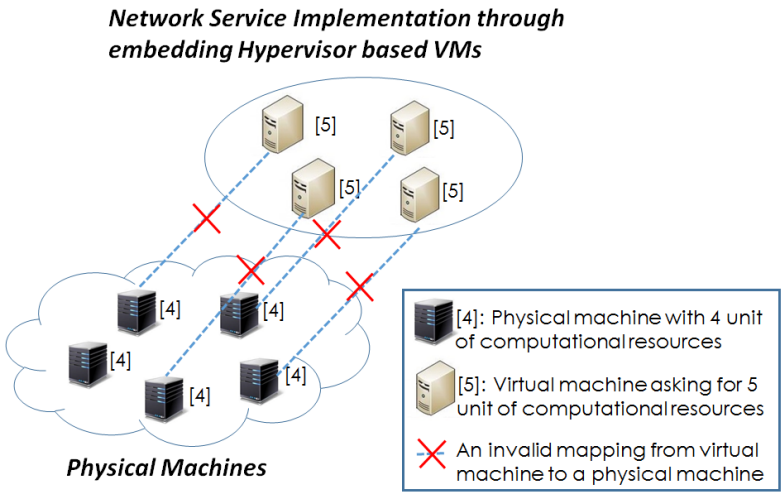

Figure 19: Hypervisor based virtual machines cannot be embedded due to resource limitation

develop an efficient and scalable algorithm to solve the dynamic resource allocation problem that could be applied to large scale resource pools. The benefits of the proposed framework and algorithm are validated through evaluations.

The rest of this chapter is organized as follows. Section 5.1 presents the details of the framework for container based dynamic resource allocation. In Section 5.2, we formulate the dynamic resource allocation problem and propose an efficient algorithm to solve the problem. Evaluations are shown in Section 5.3. Finally, we conclude this chapter in Section 5.4.

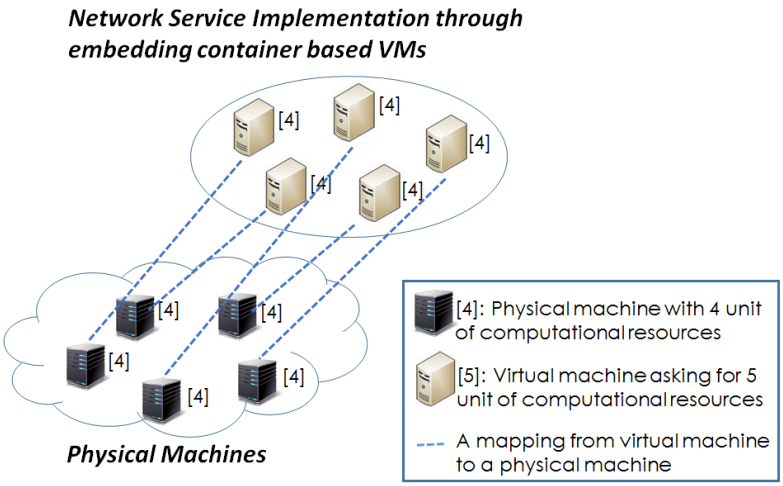

Figure 20: Container based virtural machines have been successfully allocated with available resources

5.1 Adaptive Resource Allocation Framework Using Container-Based Virtualization

We present our framework of adaptive distributed resource allocation mechanism using container-based VMs. In our framework, we introduce a new scheduler and two kinds of containers, pallet container and execution container, which decouple the resource management and task execution for each application. Unlike Hypervisor based VM placement, the number of execution containers and their demands on physical resources are dynamically determined based on not only the applications' workload but also resource usage status in the data center.

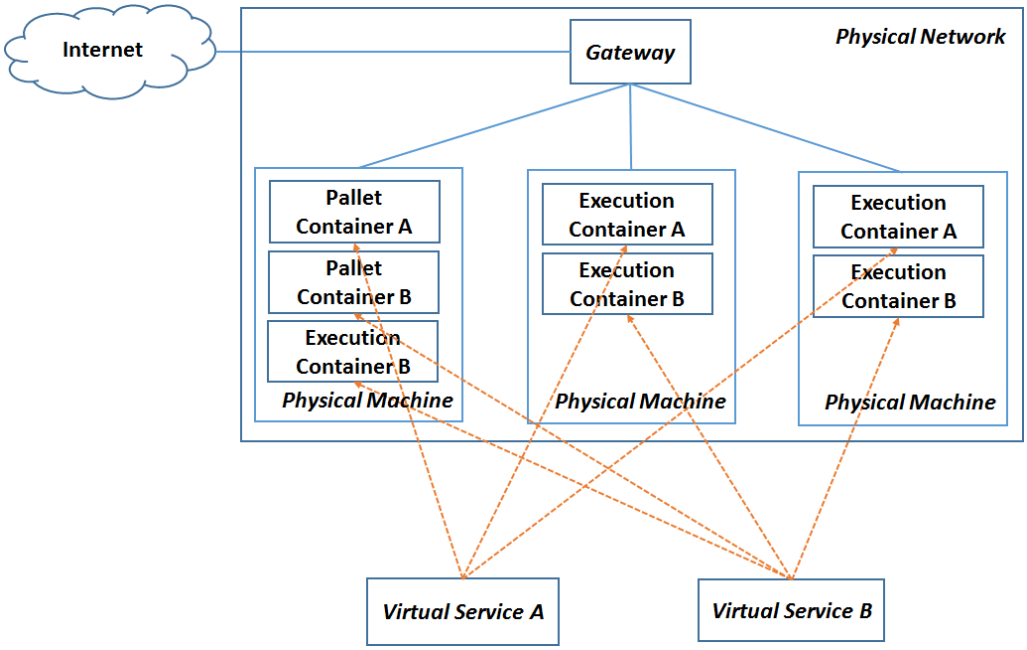

Figure 21: Overview of adaptive resource allocation framework

Figure 21 illustrates the overview for adaptive distributed resource allocation framework using container based virtualization. As shown in Figure 21, when deploying an application or service in the DC, resources are allocated to the application or service as containers distributed on multiple physical machines. Especially, each application or service has a pallet container and one or multiple execution containers. A **pallet container** has four main functions including making resource allocation decisions, requesting resources for execution containers, tracking task status on execution containers, and managing the life cycle of execution containers. **Execution containers** complete all the tasks of the application.

When activated by a scheduler, pallet containers analyze the amount of resources

needed to serve current workload without violating SLA. Based on the estimated amount of resources, it gradually queries and requests available resources from a small scale to large scales. Then it starts execution containers and dispatchs tasks to each container. Based on diversity requirements of different applications, the aim of allocating resources and building execution containers could be load balancing, or reducing latency. Driving by these aims, pallet containers determine the number of execution containers, the demands of each execution container on physical resource, and the amount of tasks dispatched to them. We discuss the detail of these algorithms in Section 5.2,.

Execution containers work mainly on completing the assigned tasks. It also reports to pallet container about the status of task execution comparing with expected status. If it is behind schedule, pallet container could try to allocate more resources for this container, or balance its workload among active execution containers or migrate this container to another physical machine with enough resources.

Both pallet container and execution containers are located on physical machines. Figure 22 depicts the architecture in a physical machine. As shown in this figure, on a bare physical machine, a host operation system is installed and configured. Upon the host OS, a **container engine** is running for resource isolation and security of the containers running simultaneously on the host OS. The container engine maintains the operating environment for containers, assists the execution of commands to build, run containers and preserves the isolation between containers. In the container engine, a scheduler is used to manage pallet containers life cycle. When receives a service request, the scheduler creates a pallet container and assigns resources to the pallet container based on the service's requirements

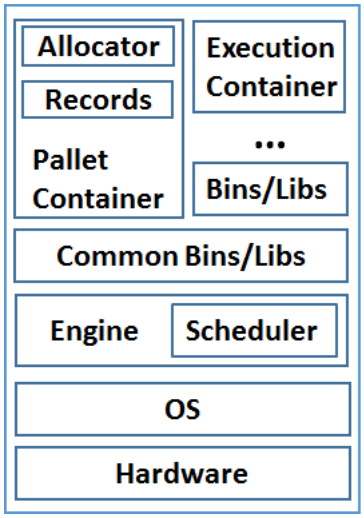

Figure 22: Components in a physical machine

and the resource usage status. It may forward the application activate request to other schedulers, if the application's demands on resources cannot be satisfied with resources on this physical machine.

Some common supporting libraries and bins are installed in advance and shared by the containers that need these functions. In addition, the libraries and bins can be built in layers to save the time and memory space of embedding containers using those libraries and bins.

Figure 23 illustrates a main work flow of deploying an application in a data center. When the request of deploying a new application or active an inactive application (step (1) and (2)), the container scheduler of this service initiates a pallet container for the application and assigns some resources for the pallet container (step (3)). The pallet container analyzes requirements of the application, makes resource allocation decisions. The pallet

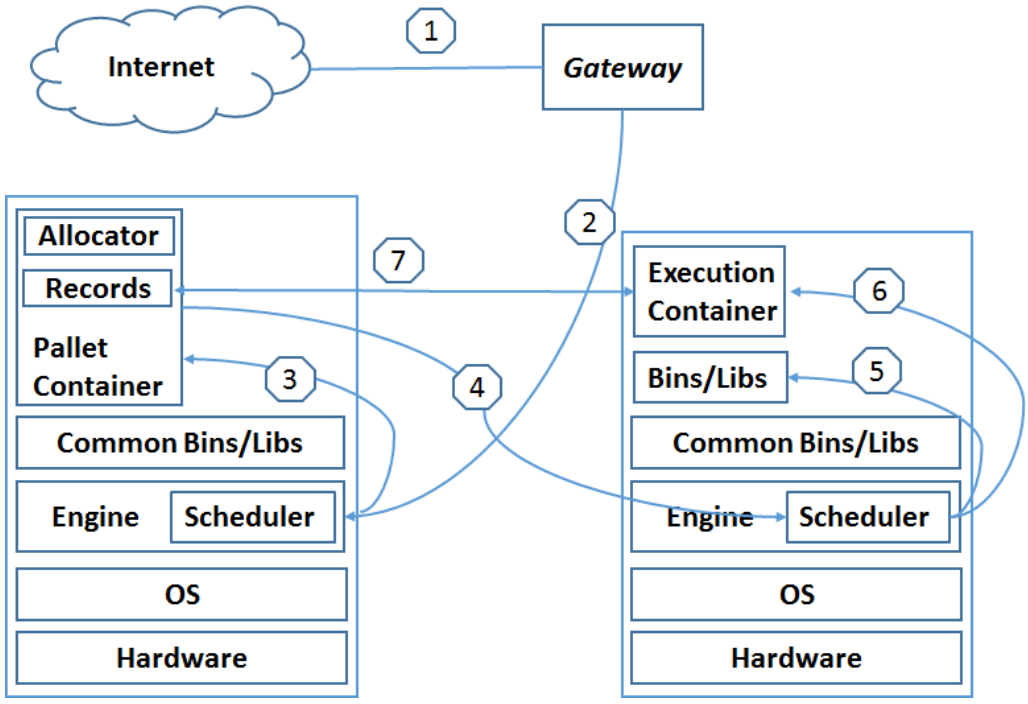

Figure 23: Work flow of adaptive resource allocation for activating an application

container requests resources on local or other physical machines for containers based on the decision (step (4)). If the request has been approved by the scheduler, resources are provisioned and execution containers are created (step (5) and (6)). Tasks are assigned to the execution containers according to the resource allocation decisions. Later, execution containers work on the tasks and update execution status to the pallet container (step (7)). Based on real time workload of the application, the pallet container may dynamically adjust the number, location and assigned resources of execution containers. When the application is deactivated, pallet container is terminated and its used resources would be collected by the scheduler.

Using this framework, the allocated resources for each application could be shrank or expend based on the application's requirements, real time workload and the status of available resources in the data center. The resource allocation decision is made by each pallet container in a distributed manner to be scalable. Besides the demands on scalable, the resource usage efficiency over the entire data center is desired to be improved too. To achieve the goal, we model resource allocation strategy on pallet containers as an optimization problem and present a solution to the problem in Section 5.2.

5.2 System Model and Algorithm

5.2.1 System model

We model the adaptive container based resource allocation problem as an optimization problem aiming to increase the efficiency of physical resource utilization while satisfying QoS requirements from applications.

We consider a physical network that consists of multiple regions based on their geographic locations and connectivity. For example, a rack could be defined as a region, or a data center could be defined as a region. Physical nodes[1] in the same regain are connected with physical links and could reach each other in a limited number of hops. We use $G^p(N^p)$ to denote the physical network that consists of a set of regions $G_1^p(N_1^p), G_2^p(N_2^p), \cdots, G_D^p(N_D^p)$. Here, D is the number of regions in the physical network. A region d contains a group of physical nodes N_d^p. We have

$$G^p = G_1^p \bigcup G_2^p \bigcup \cdots \bigcup G_D^p$$

[1]Here, we consider a general physical node. In real applications, it could be a physical machine or a component offering certain physical resource utilized in cloud applicants.

Each physical node $j \in N^p$ is equipped with limited available resources c_j^p. Here, we use computational resources as an example to model resource allocation problem. We further assume that physical nodes are identical in capacity and price in the physical network. However, they may equip with different libraries or bins in advance to support different applications.

As described in Section 5.1, various applications, e.g., big data type computing, online video, and other applications are deployed in the physical network and share the same physical resources in cloud. Some basic image, database and other necessary service data are replicated in specific physical nodes in advance. As explained in Section 5.1, the pallet container creates and manages execution containers for the requested job. The requested job could be further divided into independent tasks, each of which are executed in a executive containers. The pallet containers request physical resources to build executive containers for tasks. These assignments of physical resources respect specific demands of each request including job integrity, time limitation and priority.

In detail, we model each application as a tuple $G_i^v(\alpha_i, w_i, T_i)$. Since we assume physical nodes are identical in a data center, we use w_i to represent the total workload that is the time that the job i could be completed by dedicating 1 unit of resource on a single physical node. We further assume that the time is inverse proportional reduced when increase the amount of physical resources used to execute the task. α_i denotes the ratio that the workload of an atomic operation for the job i to the total workload of i. Considering atomic operation, a job cannot be arbitrary divided. Integrity requirements are used to make sure that a task is not smaller than an atomic operation. Therefore, each

execution container should be assigned the task with workload larger than $w_i * \alpha_i$. T_i specifies the latency requirement of the job i. Assume all the containers are started and terminated at the same time, to ensure the job i finished within required time latency, the minimum required capacity for the resource should be at least C_i^v.

$$C_i^v = \frac{w_i}{T_i} \tag{5.1}$$

We use the widely accepted energy consumption model used in existing work. Total energy consumption for a physical node j consists of baseline power P_s and operation power P_o. The operation power is proportional to the workload W_j assigned to the physical node j.

$$P_s + P_o * W_j \tag{5.2}$$

Even when a physical node is completely idle, it still consumes certain amount of baseline power up to 70% of its peak power for maintaining memory, disk and other basic operations [126]. Using awake physical machines could save energy by avoiding additional baseline power consumption.

When some virtual applications have been deployed in a data center, the remaining physical resources on physical nodes are chopped into fragments. The size of containers can be dynamically adjusted based on available resources that makes it more possible to fit into the physical machines with limited resources than Hypervisor based VMs. However, to deploy each execution container, additional energy and physical resources[2] are consumed for embedding necessary bins/libraries. Therefore, it is possible that using many

[2]Note that the energy and resources consumed by maintaining containers' bins/libraries are much smaller than maintaining Hypervisor based VMs [88].

active physical machines consumes more energy than waking up a few inactive physical machines. In addition, we consider existing libraries and bins on the physical machines and library layering of containers to further save memory space and energy consumption.

Pallet containers request physical resources independently to minimize the total energy consumption for their individual service or application. Here, the total energy consumption includes execution energy consumption and communication energy consumption between the pallet container and execution containers.

$$U_{exe} + U_{com} \tag{5.3}$$

U_{exe} represents the execution energy consumption that consists of the baseline power consumption for waking up an inactive physical node, the container maintenance consumption, e.g. building and maintaining the supporting bins/libraries, and the actually power spent for executing assigned tasks.

$$U_{exe} = \sum_{j}((P_s * s_j + P_o * c_{ij}^b) * x_{ij} + P_o * p_{ij} * w_i) \tag{5.4}$$

s_j indicates the sleep/awake status of a physical machine j. c_{ij}^b is the power consumption for building a container for application i on physical machine j. We use a binary variable x_{ij} (Equation (5.5)) to represent if a container for the service/application i is embedded on a physical server j. p_{ij} is the portion of job i assigned to the physical machine j, and w_i is the total workload of job i.

$$x_{ij} = \begin{cases} 1, & \text{if a container for the service } i \text{ is assigned to} \\ & \text{physical node } j \\ 0, & \text{otherwise} \end{cases} \tag{5.5}$$

The communication energy consumption U_{com} describes the energy consumed for data exchanges between the pallet container and each execution container, and is proportional to the distance between two containers. We model the communication cost for a service/application as:

$$U_{com} = \sum_{j} l_{jk} * f_{jk} \tag{5.6}$$

l_{jk} is the length of the overlay link between k and j if f_{jk} amount of traffic passes through this overlay link. Note the amount of total received traffic of the pallet container k is the sum of f_{jk}

We want to minimize the utility function Equation (5.3) by determining where to place the containers x_{ij} and how much workload p_{ij} to be executed on the container. When requesting the physical resources, the pallet container aims to minimize the utility function:

$$\begin{aligned} & Min\{U_{exe} + U_{com}\} \\ = \; & Min\{\sum_{j}((P_s * s_j + P_o * c_{ij}^b) * x_{ij} + P_o * p_{ij} * w_i) + \sum_{j}\sum_{k} l_{jk} * f_{jk}\} \end{aligned} \tag{5.7}$$

while satisfying a set of constraints as followings:

$$\forall j \in N^p : p_{ij} * w_i < c_j^p \tag{5.8}$$

$$\forall j \in N^p : f_{jk} < b_{jk}^p \tag{5.9}$$

$$\forall j \in N^p : \sum_{j} p_{ij} = 1 \tag{5.10}$$

$$\forall i \in G_i^v, j \in N^p : 0 \leq p_{ij} \leq 1 \tag{5.11}$$

$$\forall i \in G_i^v, j \in N^p : |p_{ij} * w_i - \alpha_i| \geq 0 \tag{5.12}$$

$$\forall i \in G_i^v : \sum_j p_{ij} * w_i \geq C_i^v \tag{5.13}$$

$$\forall i \in G_i^v, j \in N^p : x_{ij} \geq p_{ij} \tag{5.14}$$

$$\sum_j f_{jk} - \sum_j f_{kj} = \sum_j p_{ij} * b_{ij} - \sum_j y_{ij} * b_{ij}; \tag{5.15}$$

Constraint (5.8) guarantees that the assigned resources will not exceed the available resources on a physical node j. Constraint (5.10) ensures every portion of the task has been allocated. Constraint (5.11) checks the lower bound and upper bound of partitions. Constraint (5.13) exams if the minimum required resources are allocated to the job i so that i could be completed within desired time. Constraint (5.14) builds the relationship between variable x_{ij} and p_{ij}. Flow conservation (5.15) checks flow balance on each link. Here b_{ij} is the amount of traffic between the execution container on physical node j and the pallet container for application i. We assume b_{ij} proportional to the amount of workload p_{ij} on physical node j.

5.2.2 Algorithm

When a large number of services/applications with varying workloads and demands are deployed in a data center, a centralized manager that takes charge of all the resource allocation and container management work may have some problem in scalability and security. To deal with this problem, pallet container for each service/application would compute in distributed manner to acquire resources and manage containers. They do not have a comprehensive global view about the data center. They only try to minimize its own energy consumption based on their limited knowledge. However, through the utility function Equation 5.7, the number of fragments is expected to be reduced and the

global resource utilization could be improved. In addition, the pallet container start with searching its local region, and incrementally extend the searching area to nearby regions. The distributed resource allocation algorithm is shown in Algorithm 5.

Algorithm 5 Energy Efficient Container Placement (EE-CP)

Input: physical network topology in region(s) $G_r^p(N_r^p)$; Resource allocation request $G_i^v(c_i^v, w_i^v, t_i)$; A set of neighbor region IDs set_n
Output: Allocation decision x_{ij}, p_{ij} for job i

query physical nodes in N_r^p for current available resources and workload C_j
solve the objective function (5.7) under constraints (5.10) - (5.15)
if there is a feasible solution $\{x_{ij}, p_{ij}\}$ **then**
  for physical node j that $x_{ij} == 1$ **do**
    send a resource request to physical node j for the amount of $p_{ij} * c_i^v$ resources
    receive response from physical node j, and record the results x_{ij}^r in set_r
  end for
  for every result $result_j$ in set_r **do**
    if $result_j$ is accept **then**
      build an execution container on physical node j, and a connection between j and the pallet container
      record x_{ij} and p_{ij} into $directory_i$
      $N_r^p = N_r^p - j$,$C_j - p_{ij} * c_i^v$
    else
      record p_{ij} into set_u
      $N_r^p = N_r^p - j$
    end if
  end for
end if
if set_r is not null, and set_u is not null **then**
  $N_r^p = N_r^p \bigcup set_n$, set_n = $\bigcup$ set_n's neighbors
  call EE-CP(N_r^p, G_i^v, set_n)
end if

As shown in Algorithm 5, a pallet container only checks physical nodes in the region that it is located about their available resources, and solves the optimization problem based on the physical nodes' available resources and the workload of this application.

It then sends resource requests to selected physical nodes based on the solution. If the request has been approved, an execution container will be built on the selected physical node, and the physical node would be marked as used. If the request has been rejected, this physical node would be marked as infeasible and this part of workload would be recorded into a new set. When all the portion of the job has been processed, and there are still some tasks that have not be successfully mapped, the search will be extended to a larger scale including nearby regions.

5.3 Evaluations

Table 9: Parameter Setting

Parameter	Values
Probability of sleep/awake status	0.8
Range for physical capacity	[25, 30]
Portion of available physical resources	[0, 0.5]
Size of each Hypervisor based VM	25
Size of each library	2.5
Number of physical nodes	[5, 40]
Number of Hypervisor based VM	[3, 8]
Total workload of each application	[50,80]

We compare the performance of adaptive container based resource allocation and static Hypervisor based VM placement, with respect to total energy cost and acceptance ratio using various parameter settings.

We randomly generate the substrate network including a group of physical machines and overlay links between physical machines using NetworkX [86]. The status of

each physical node is randomly determined to be awake with an probability of 0.8. Each physical node is randomly assigned a value between [20, 35] to indicate its maximum available resource following uniform distribution. To examine the impact of the available resources on energy consumption, we randomly deduct a portion of available resources of each physical node to simulate the initial resource usage. The deducted portion is randomly decided following uniform distribution between $[0, \theta]$. Here we set θ as 0.5. In addition, we randomly set the type for each physical server. The type of the server indicates of the differences between available libraries of the physical machines and the required libraries of the application. When the type of physical server and the type of the application is n, the necessary libraries that need to be deployed for the container is $n *$ average size of each library. We assume the average size of each library is 2.5, and the size of a VM is 25. Parameters used in this chapter is summarized in Table 9.

We first validate our algorithm by comparing it with the optimal solution of VM placement. The number of physical nodes in this set of evaluations changes from 5 to 40, while the number of virtual nodes to be embedded is fixed to 5. The total workload of each application is randomly determined between [50,80].

As presented in Figure [24](a), the VM with fixed requirements on computational and network may not be able to be embedded into the physical network when the number of available physical nodes is small, while container based resource allocation could always properly allocates enough resources for the application. The container based resource allocation also outperforms VM placement in total cost as shown in Figure [24](b).

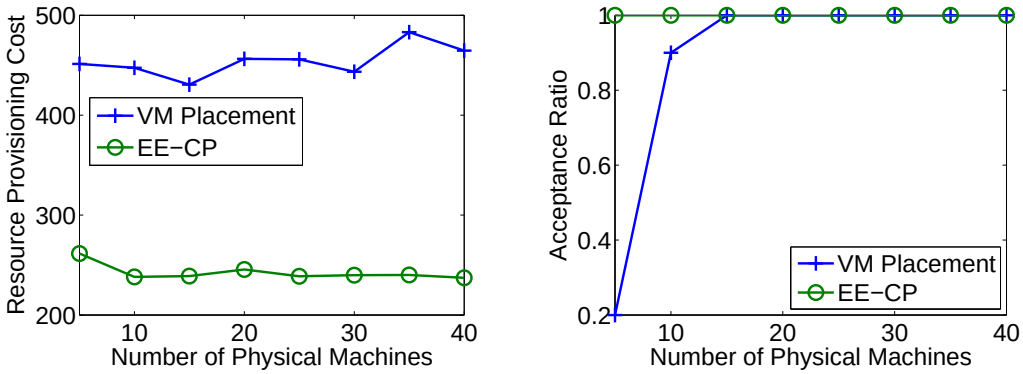

(a) Total energy cost (b) Acceptance ratio

Figure 24: Comparison for varied number of physical machines

The total cost of provisioning resources for VMs is around 450, while the cost for container based resource allocation is around than 250. This cost saving mainly comes from the memory size savings.

We also examine the impact of the number of VMs in Figure [25](a) and (b). Here, we vary the number of VMs from 3 to 8. The more VMs to be embedded for the application, the more redundant memory to be used for building the guest OS, and the more total cost for the VM embedding. As presented in Figure [25](a), when the number of VMs increases from 3 to 8, the total cost increases from 376 to 612. However, when to satisfy the QoS requirement of the same application but with a smaller number of VMs, each VMs would demand more physical resources. This would increase the difficulties to embed the VMs, especially when the physical resources are limited. Figure [25](b) draws when the number of VMs is 3, the acceptance ratio is only 45%. To ensure the acceptance ratio more than 95%, this work should be spread to at least 5 VMs. Container

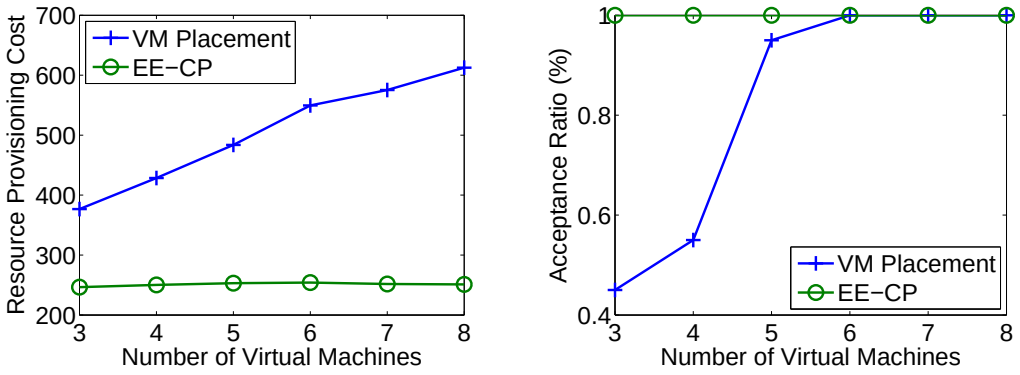

(a) Total energy cost (b) Acceptance ratio

Figure 25: Comparison for varied number of virtual machines

based resource allocation could dynamically adapt the number of containers and adjust the size of each container. Therefore, it could achieve a relative high acceptance ratio with minimum total cost.

5.4 Summary

We have designed a framework for dynamic resource allocation for container based VMs and proposed a resource allocation algorithm to minimize the provisioning cost while preserving applications requirements on QoS. In our framework, a pallet container tracks application execution status and adaptively manages allocated resources based on applications real time workload. Multiple execution containers are managed by the pallet container and cooperate toward the applications' jobs. We consider the awake/sleep status of physical nodes, and available libraries and bins on each physical nodes to minimize the baseline cost and reduce the redundant cost to build the guest OS.

Comparisons with static Hypervisor based VM placement shows that the dynamic container based VMs has a smaller cost with a higher acceptance ratio.

CHAPTER 6

ACHIEVING OPTIMAL CONTENT DELIVERY USING CLOUD STORAGE

While traditional Content Distribution Networks (CDNs), such as Akamai [2] and Limelight Networks [75], can be expensive for moderate-size content providers, and building and managing a CDN infrastructure is becoming increasingly difficult [21], the advent of cloud-based content storage and delivery services provides an economical alternative for those content providers. By outsourcing the tasks of maintaining and delivering a large number of contents to cloud storage providers, content providers, who are also the cloud users, can significantly cut down their expenditures on building and managing a storage infrastructure ([5, 21, 52]). This economic variation of content placement and delivery attracts a renewed interest on content distribution strategies.

As with traditional CDNs, content providers that use cloud storage are committed to satisfy content users' demands within a reasonable response time. In order to reduce this latency, content providers can disseminate objects on cloud storage servers dispersed in a network near their users. On the other hand, while emphasizing the content users' experience as an overriding concern, content providers also need to consider the expenditure of cloud storage services that is charged on the occupied storage space and traffic volume according to cloud storage providers' polices, such as Amazon Simple Storage Service (S3) [5] and Google Cloud Storage [52]. While replicating objects on cloud servers can lower the cost caused by content delivery traffic by cutting down repetitive transmissions,

it, however, raises the cost of additional storage space on cloud servers. This opens a new challenge to design algorithms that could optimize latency as well as cloud storage cost through replicating contents on proper locations.

Various algorithms have been proposed to optimize content delivery that can be mainly categorized as Latency-Minimization (LM) algorithms and Traffic-Minimization (TM) algorithms, according to their optimization aims. The LM algorithms focus on the optimization of latency; while the TM algorithms concern on the optimization of traffic consumed by the delivery of contents in backbone networks.

In Chapter 6, we argue that considering the traffic volume together with latency performance under the constraint on storage cost is crucial for economic and efficient content delivery service for content providers using cloud services. We have first formulated the joint traffic-latency optimization problem, and proved its NP-completeness. We then develop an efficient light-weight approximation algorithm, named Traffic-Latency-Minimization (TLM) algorithm, to solve the optimization problem with theoretical provable upper bound for its performance. To limit the frequency of updates to the origin server with local changes such as users interests shift, we also extend our TLM algorithm in a distributed manner. We provide the theoretical analysis for time complexity and space complexity of the TLM algorithm, that are $O(mnlog(n))$, and $O(mn)$ respectively, where m is the number of proxy servers and n is the number of objects. Unlike most previous works, our algorithm employs fixable and practical conditions that relax many assumptions on parameters such as object size, object request probability, the storage capacity, and the number of requests. Simulation results and experiments show that the

performance is near optimal for most of the practical conditions.

The remainder of the chapter is organized as follows. We formulate our network model and traffic-latency optimization problem, and prove the hardness of the problem in Section 6.1. We describe our proposed approximation algorithm TLM in both a centralized and a distributed manners, as well as its analysis in Section 6.2. The performance evaluations and comparisons of TLM with prior algorithms are presented in Section 6.3. The concluding remarks are given in Section 6.4.

6.1 Problem Formulation

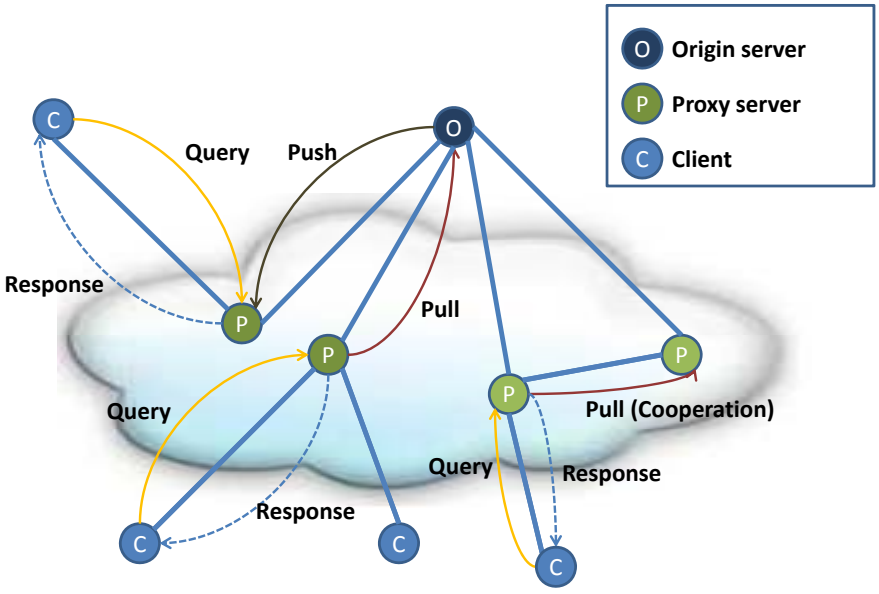

Figure 26: Push vs. pull: The origin server pushes some objects to proxy servers. Content user queries objects from the proxy server. A proxy server will pull from the origin server or another cooperative proxy server if it doesn't have the requested objects.

Table 10: Notation Used

Notation	Explanation
m	The number of proxy servers
n	The number of objects
i	Index of proxy servers, also indicates the service area for server i, $i = 1, 2, \ldots, m$
c_i	The maximum storage space on proxy server i
j	Index of objects, $j = 1, 2, \ldots, n$
d_{ij}	The distance from proxy server i to its nearest replica of object j
λ_i	Total number of requests in area i
p_{ij}	Probability that object j will be queried in area i
s_j	Size of object j
x_{ij}	Decision variable for pushing object i to proxy server j
α	Coefficient to balance the weight for latency and data traffic
κ_{ij}	Cost for pulling object j to respond the requests for object j in area i
Δ_{mn}	Total cost for a simple pull strategy with m proxy servers and n objects, $\Delta_{mn} = \sum_{i=1}^{m} \sum_{j=1}^{n} \kappa_{ij}$
f_{ij}	Cost saved by pushing object j to proxy server i. f_{ij} could be positive or negative
F_{mn}	Total cost for push-pull strategy with m proxy servers and n objects, including latency and data traffic cost

As a traditional content distribution network consists of a central origin server and multiple proxy servers, a content distribution network over a cloud storage is comprised of an origin server and multiple proxy servers on a cloud network. The proxy servers are connected with the origin server and/or other proxy servers, as illustrated in Figure 26. In order to shorten the latency experienced by the final content users, some objects are replicated on a proxy server, also called a replica, in advance near the users. Moreover, in order to improve the content users' experience, proxy servers may cooperate with each

other so that they can download objects from others rather than from the origin server. The proxy servers that are connected by a direct overlay link can communicate with each other, called neighbors. We assume that the origin server has a sufficient capacity to store all n objects whose sizes are $s_1, s_2, \ldots, s_n$. However, the storage capacity on each proxy server i $(i = 1, 2, \ldots, m)$ is limited due to the cost on the cloud storage space, which makes it impossible to replicate all n objects on each proxy server i, $(i = 1, 2, \ldots, m)$. Thus, we need a salient distribution strategy to decide if it is better to replicate object j on proxy server i in advance. Notations used in Sections 6.1 and 6.2 are summarized in Table 10.

6.1.1 The Push-Pull Model

In our model, each proxy server takes charge of one area of service, which can be assigned according to geographic locations or domains as in [123]. Content users in area i will directly request and download objects from the proxy server i. For simplicity of our discussion, we denote a proxy as if there is only one proxy server per one area. In practice, an origin server may be a server farm, and more than one proxy server may be in charge of one area. In such a case, the sum of proxy servers' storage space for area i can be used as c_i. Notice that cloud storage requires multiple replication based on predefined replication factor. The available storage space will be the actual storage size divided by the replication factor. Here, we assume that the same replication factor will be applied for all the contents, and use c_i as the available storage space for distinct contents. The issue of necessary number of proxy servers in an area has been studied in [112,113]. Additionally,

servers in a data center are typically clustered and situated in a close location, resulting in little difference in delay to a user from any of the servers in a farm.

In satisfying content users' requests, two typical schemes can be considered for content distribution, a push-based scheme and a pull-based scheme. In a *push-based scheme*, objects are replicated into proxy servers prior to requests until a proxy server's storage limitation is reached. This distribution procedure is referred to as a *push*. When requests arise for those pushed objects, a proxy server will directly serve the content users without involving other cloud servers. On the other hand, no object is replicated into the proxy servers in advance under a *pull-based scheme*. When proxy servers receive queries for the un-pushed objects, they will forward the query and download the requested objects from the nearest source that could be either the origin server or another cooperative proxy server. This procedure is specified as a *pull*. By disseminating objects in advance, a push-based scheme shortens the retrieval latency of object j; while a pull-based scheme reduces traffic volume by eliminating object downloads that would never be requested. In order to optimize both latency cost and traffic cost, we consider a content delivery scheme that is the combination of a push-based scheme and a pull-based scheme. This *push-pull scheme* is expected to properly determine which objects should be pushed and which should be pulled, so that both the push-based scheme and pull-based scheme are used to their best advantages. We formulate the push-pull scheme in Section 6.1.2 as an optimization problem and solve it with our Traffic-Latency-Minimization (TLM) algorithm in Section 6.2.

6.1.2 The Push-Pull Optimization Problem

We point out that we focus on the performance within a distribution cloud network and do not compute the latency and traffic costs between a proxy server and the final content users. In fact, those costs will not be impacted by the content distribution strategies, since each content user is directly served by a fixed proxy server according to the users' location. Therefore, our problem is to minimize the total cost, that includes the latency cost and the traffic cost between cloud servers, to satisfy all the requests from content users.

From the content providers' point of view, the overriding concerning is to ensure the content users' experience; however, it is also significant to reduce costs for maintaining and delivering contents. Therefore, the costs for content delivery over cloud storage should include latency cost, which is related to the experience of final content users, and the traffic cost that is the main characteristic to estimate the expenditure for cloud service.

The latency in area i to obtain object j corresponds with the distance d_{ij} between proxy server i and its nearest replica of j. d_{ij} could be either spacial, such as the number of hops as used in [67, 71] or temporal, such as the average round trip time that can be predicted with the methods proposed in [80, 105]. The latency from a proxy server to different users may vary depending on a user's access network and the path. However, in this chapter, we focus on the latency from the location of a requested objects to the proxy server that directly serve a final user, and omit the latency from this proxy server to the final user. The related discussion about latency from proxy servers to final users can be found in [65].

When a request is raised for object j in area i, if j has already been pushed into the proxy server i, proxy server i can respond immediately without involving any extra latency. However, if object j has not been replicated on proxy server i in advance, proxy server i needs to pull object j from either the origin server or another cooperative proxy server that results in an additional latency cost d_{ij} for each request for object j in area i. Assume the total number of requests for object j in area i is the product of λ_i, which is the total number of requests in area i, and p_{ij}, which is the probability that object j will be queried in area i, then the expectation of the total latency cost in area i is $d_{ij}p_{ij}\lambda_i$ for un-pushed object j. We highlight that the request patterns are heterogeneous depending on the area, which means we introduce various λ_i and p_{ij} in a different service area i. It is more practical than the assumption of a fixed request pattern used in previous studies such as [10, 67].

On the other hand, s_j that is the size of object j is utilized to estimate the traffic cost. Furthermore, if object j has been pushed to the proxy servers, the amount of s_j is appended to the traffic cost for each replica of object j. Otherwise, the amount of s_j is added for each query for object j.

We use a matrix X to present an allocation of replicas with the push-pull strategy, and each element x_{ij} in X indicates whether object j should be pushed to a proxy server i or not.

$$x_{ij} = \begin{cases} 1, & \text{Object } j \text{ is pushed on proxy server } i \\ 0, & \text{Object } j \text{ is not pushed on proxy server } i \end{cases} \tag{6.1}$$

Now, the expectation of accumulated latency in a cloud storage networks using

the push-pull strategy can be represented as:

$$\sum_{i=1}^{m}\sum_{j=1}^{n}(1-x_{ij})d_{ij}\lambda_i p_{ij} \tag{6.2}$$

and the total traffic volume for this network can be formulated as:

$$\sum_{i=1}^{m}\sum_{j=1}^{n}(x_{ij}s_j+(1-x_{ij})s_j\lambda_i p_{ij}) \tag{6.3}$$

As we consider the costs of both latency and traffic, we use a coefficient α to balance the influence of latency and traffic costs to satisfy various application and performance requirements. Then, our objective is to minimize this weighted total cost of latency and traffic for this network when using the push-pull strategy under the storage constraints.

$$\sum_{i=1}^{m}\sum_{j=1}^{n}(1-x_{ij})d_{ij}\lambda_i p_{ij}+\alpha\sum_{i=1}^{m}\sum_{j=1}^{n}(x_{ij}s_j+(1-x_{ij})s_j\lambda_i p_{ij}) \tag{6.4}$$

subject to storage constraints:

$$\sum_{j=1}^{n}x_{ij}s_j\le c_i,\qquad i=1,2,\ldots,m \tag{6.5}$$

To solve this optimization problem, we simplify Eq. (6.4) and obtain

$$\min(\sum_{i=1}^{m}\sum_{j=1}^{n}(d_{ij}\lambda_i p_{ij}+\alpha s_j\lambda_i p_{ij}-x_{ij}(d_{ij}\lambda_i p_{ij}+\alpha s_j\lambda_i p_{ij}-\alpha s_j))) \tag{6.6}$$

Eq. (6.6) can be further derived as:

$$\min\sum_{i=1}^{m}\sum_{j=1}^{n}(\kappa_{ij}-x_{ij}f_{ij}) \tag{6.7}$$

where $\kappa_{ij}=d_{ij}\lambda_i p_{ij}+\alpha s_j\lambda_i p_{ij}$ and $f_{ij}=d_{ij}\lambda_i p_{ij}+\alpha s_j\lambda_i p_{ij}-\alpha s_j$. Note that κ_{ij} denotes the weighted total cost for un-pushed object j in area i, and f_{ij} represents the relative saved cost by pushing object j to proxy server i.

When λ_i that is the number of requests in area i, popularity p_{ij} for object j in area i, distance d_{ij} from the nearest replica of object j to the proxy i and size s_j for object j are determined, the weighted total cost of the simple pull strategy by which no object is replicated on the proxy server in advance, will not be impacted by the replica allocation. Therefore we denote $\Delta_{mn} = \sum_{i=1}^{m} \sum_{j=1}^{n} \kappa_{ij}$ as the weighted total cost for a simple pull cloud storage network with m proxy servers and n objects when every request is responded to by pulling. Then, the optimization problem described in Eq. (6.4) is equivalent to

$$\max \sum_{i=1}^{m} \sum_{j=1}^{n} (x_{ij} f_{ij}) \tag{6.8}$$

subject to storage constraints:

$$\sum_{j=1}^{n} x_{ij} s_j \leq c_i, \qquad i = 1, 2, \ldots, m \tag{6.9}$$

where f_{ij} is utilized to signify the cost saving by pushing object j to proxy server i. In addition, f_{ij} could be positive or negative. $f_{ij} > 0$ means that pushing object j to proxy server i can reduce the weighted total cost, while $f_{ij} < 0$ suggests that pushing object j to proxy server i will increase the cost. When $f_{ij} = 0$, pushing object j to proxy server i cannot save the weighted total cost, but takes up additional storage space on proxy server i that results in increased cloud storage cost. Thus, we only consider the object j with a positive f_{ij} as a candidate to be pushed on proxy server j.

Consider the special cases of Eq. (6.4). When α is set to 0, it is reduced to a simple latency minimization problem when α is set to 0. It is reduced to a simple traffic minimization problem, when α is set to a large number, such as 100 or 1000, assuming that latency cost and traffic cost are with the same order of magnitude.

6.1.3 Hardness of the Problem

As we presented in Section 6.1.2, our aim is to optimize the weighted total cost of latency and traffic under the storage constraints by solving the optimization problem Eq. (6.4) subject to Eq. (6.5), named the *push-pull optimization problem*. As we illustrated in Section 6.1.2, Eq. (6.4) is equivalent to Eq. (6.8) that we named the *push-pull equivalent problem*. We demonstrate the NP-completeness of the push-pull equivalent problem by using the well-know Knapsack problem and considering a special case of the push-pull equivalent problem, so that we prove the hardness of the push-pull optimization problem. Before we present the NP-completeness of the push-pull equivalent problem, we first restate this push-pull equivalent problem as well as the push-pull optimization problem and the Knapsack problem.

Push-pull optimization problem: Given a set of n objects with varying sizes $s_1, s_2, \ \ldots, s_n$, varying locations and the probability that they will be queried, the problem is to figure out whether there is any allocation X, with which the weighted total cost of a push-pull strategy over cloud storage is less than a constant value F, and the total size of the objects pushed to proxy server i is smaller than $c_i, i = 1, 2, \ \ldots, m$ as in Eq. (6.5) or not.

Push-pull equivalent problem: Given a set of n objects with varying sizes $s_1, s_2, \ \ldots, s_n$, varying locations and the probability that they will be queried, the problem is to figure out if there is a group of object j, by pushing which to certain proxy server i, the amount of the weighted total cost of a simple pull network over cloud storage can be saved more than a constant value $F - \Delta_{mn}$, and the total size of objects pushed to the proxy server i is smaller than $c_i, i = 1, 2, \ \ldots, m$ as in Eq. (6.9), where Δ_{mn} is the weighted total cost

of the simple pull network with m proxy servers and n objects.

Knapsack problem: Assume a set of n items with varying weights $w_1, w_2, \ldots, w_n$, and values $v_1, v_2, \ldots, v_n$. The problem is to determine whether or not there is any subset of these n items so that the total weight of this subset is no more than a given limit W while the total value is larger than V.

We consider a special case of the push-pull equivalent problem, where we have only one proxy server 1 with the storage capacity c_1. We need to determine the group of objects to be pushed on the proxy server 1 so that the weighted total cost can be saved more than a constant $F - \Delta_{mn}$. Because the original push-pull problem equivalent is more complex than this special case, if the special case is proved to be NP-complete, the original problem is NP-complete, and the original push-pull optimization problem is NP-complete as well.

First, it is easy to prove that the special case of the push-pull equivalent problem belongs to NP. Any object allocation can be examined if it is a feasible solution that the weighted total cost is saved more than $F - \Delta_{mn}$ and it meets the storage constraint in polynomial time. Next, we prove that the Knapsack problem, that is a well known NP-complete problem, can be reduced to the special case of the push-pull equivalent problem in polynomial time. By letting weight w_j correspond to size s_j of object j and value v_j correspond to the cost saving f_{1j} of pushing object j to proxy server 1, this means $w_j = s_j$ and $v_j = f_{1j}$. Let the weight limitation W correspond to storage constraint c_1 while the value limitation V corresponds to the weighted total cost saved by pushing object $(F - \Delta_{mn})$, where $W = c_1$ and $V = (F - \Delta_{mn})$, the Knapsack problem is reduced

to our push-pull problem. Therefore, if the solution of the Knapsack problem is known, the corresponding set of objects is a solution of the push-pull equivalent problem as well as the solution for the push-pull optimization problem.

6.2 Approximation Algorithm

In this section, we develop an approximation algorithm toward an optimal solution of the push-pull optimization problem, and then we establish a theoretical efficiency bound and produce a performance analysis for this approximation algorithm.

As we demonstrated in Section 6.1.2, the weighted total cost of a push-pull network over cloud storage is equal to the weighted total cost of a simple pull network subtracting the cost saved by pushing a group of objects. Thus, we can solve the push-pull optimization problem by determining a group of objects, so that the weight total cost saved can be maximized by pushing them to proxy servers in advance.

One naïve heuristic algorithm could be choosing the objects in the decreasing order of f_{ij}, which is the amount of saved weighted total cost for pushing object j to proxy server i. However, this does not best utilize the storage toward the maximum saved weighted total cost in Eq. (6.8), or in other words, the minimum weighted total cost in Eq. (6.4).

Instead, we design an approximation algorithm that selects objects that can maximize saving the weighted total cost while occupying a small storage space. We first compute

$$r_{ij} = f_{ij}/s_j \tag{6.10}$$

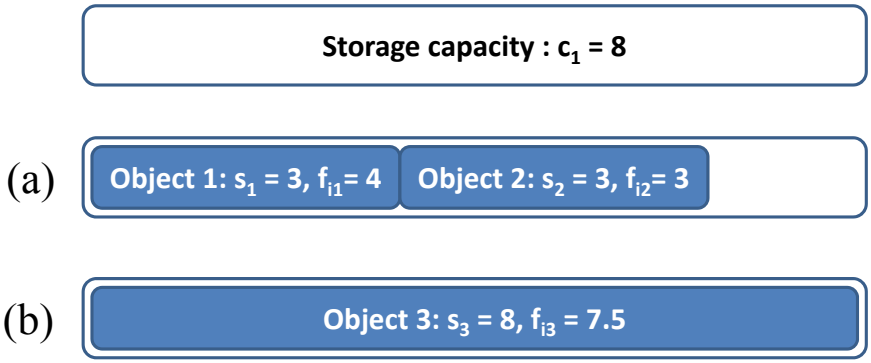

Figure 27: $r_{i1} = 1.33; r_{i2} = 1; r_{i3} = 0.94$. Pushing object 1 and 2 with the lowest ratio r_{i1} and r_{i2}(case (a)) is worse than pushing object 3 (case (b)).

, which is the ratio of the push-pull cost saved for pushing object j to proxy server i and the size of object j. Then, the objects with the highest ratio will be pushed to proxy server i while the space is allowed within the storage constraint as in Eq. (6.5).

We observe that using only the ratio r_{ij} to determine whether pushing object j to proxy server i may not be a good solution in some scenarios, as illustrated in Figure 27. In this occasion, a proxy server i has an available storage amount of $c_i = 8$, and there are three objects, (object 1,2, and 3) with decreased r_{ij} ($r_{i1} = 1.33, r_{i2} = 1, r_{i3} = 0.94$). Proxy server i cannot replicate all the three objects due to the storage limitation. Therefore, the problem turns into the selection of objects to be replicated. Suppose the sizes and the push-pull cost differences for objects 1, 2, and 3 are $(s_1 = 3, f_{i1} = 4)$, $(s_2 = 3, f_{i2} = 3)$, and $(s_3 = 8, f_{i3} = 7.5)$, respectively. If we push objects according to the ratio of push-pull cost differences to the size, object 1 and object 2 will be replicated to proxy server i in advance. However, under this case, 2 units of spare room in the cache

will be left, which is not enough for other objects to be replicated in this proxy server. Therefore, the weighted total cost is $\Delta_{mn} - 7$ according to Eq. (6.8) and Eq. (6.10), where $\Delta_{mn} = \sum_{j=1}^{3} \kappa_{ij}$. On the other hand, if object 3 is chosen to be pushed, all the space has been efficiently used, and the weighted total cost is $\Delta_{mn} - 7.5$ that is smaller than pushing object 1 and object 2.

This problem can be addressed by comparing the weighted total cost of objects with the highest r_{ij} that can be pushed, subject to a storage constraint with the cost of the first object that cannot be pushed. By adding this comparison, the weighted total cost of the modified algorithm will be bounded less than $\Delta_{mn} - \frac{1}{2}\sum_{j \in OptSet} f_{ij}$, while the optimal total cost is $\Delta_{mn} - \sum_{j \in OptSet} f_{ij}$. Based on this observation, we propose an approximation algorithm, named the Traffic-Latency-Minimization (TLM) algorithm as depicted in Algorithm 6.

As described in Algorithm 6, we first calculate f_{ij}, the saved weighted cost by pushing object j to proxy server i and r_{ij}, the ratio of f_{ij} and the object size s_j for each object j. We further compute the weighted total cost for a simple pull network over cloud storage with these m proxy servers and n objects. Then, we sort the objects in descending order according to their r_{ij} and push the objects with positive r_{ij} until the storage limitation of proxy server j has been reached. When there is not enough space for object j in proxy server i, we compare the saved weighted total cost of all already pushed objects with the possible saved cost of pushing object j, if pushing object j can save more, we remove pushed objects on proxy server i until there is enough space to replicate object j; otherwise, we do nothing and move to the next object.

Algorithm 6 TLM approximation algorithm - runs on origin server

for every proxy server $i \in \{1, 2, \ldots, m\}$
  Calculate f_{ij} and r_{ij} for each object $j \in \{1, 2, \ldots, n\}$;
  Sort r_{ij} in descending order and record corresponding indices in array h;
  Calculate total cost of system $TotalCost = TotalCost + \sum_{j=1}^{n} \kappa_{ij}$;
  Keep a record of the weighted total cost for a simple pull system $\Delta_{mn} = \Delta_{mn} + \sum_{j=1}^{n} \kappa_{ij}$;
  for $index \in \{1, 2, \ldots, n\}$
    $j = h[index]$;
    if ($r_{ij} > 0$ AND $s_j \leq$ available storage on i)
      Put j into $PushSet_i$;
      $TotalCost = TotalCost - f_{ij}$;
    else if ($r_{ij} > 0$ AND $s_j >$ available storage on i)
      if ($\Delta_{mn} - f_{ij} < TotalCost$ AND $s_j \leq c_i$)
        Keep removing the last element in $PushSet_i$ till there is enough room for j;
        Update $TotalCost$;
        Put j into $PushSet_i$;
      end if
    else if $r_{ij} \leq 0$
      Break;
    end if
  end for
end for

Next, we prove the bounded quality of our approximation algorithm.

Theorem 1. *The upper bound of the TLM approximation algorithm is* $\Delta_{mn} - \frac{1}{2} \sum_{j \in OptSet} f_{ij}$, *if the optimal total cost is* $\Delta_{mn} - \sum_{j \in OptSet} f_{ij}$.

Proof. Suppose a list of objects j, $j = 1, 2, \ldots, n$ are sorted in a descending order according to r_{ij} the ratio of f_{ij}, saved weighted total costs if pushing object j on proxy server i and object size s_j. In the list, object 1 has the largest ratio r_{i1}, which means

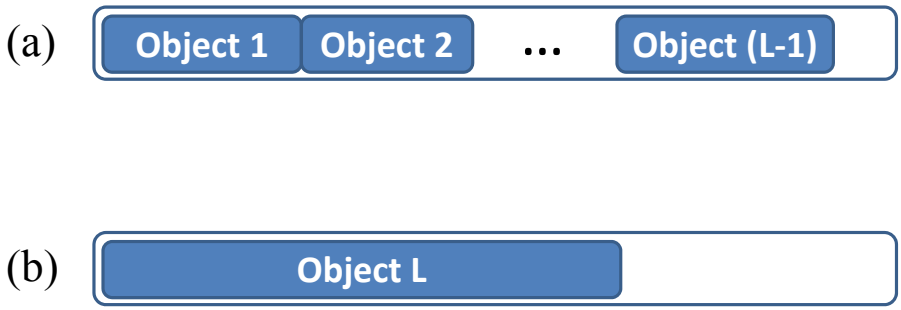

Figure 28: In TLM, either object $1, \ldots, L-1, (L > 1)$ or object L can be pushed to a proxy server.

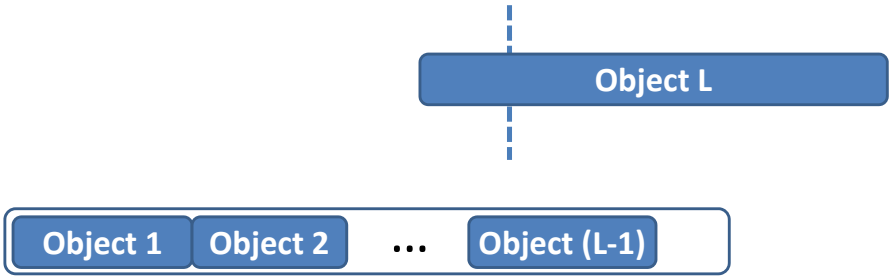

Figure 29: The upper bound of optimal solution

pushing object 1 to proxy server i reduces the most cost per bit up to s_1 bits; while object n has the smallest ratio r_{in}, which indicates pushing object n reduces the least of the cost per bit when taking up to s_n bits space. Without loss of generality, we only consider the objects with ratios r_{ij} larger than 0, which means the optimal solution is to push all of these objects in order to minimize total weighted cost of the system. However, the total size of those objects can be larger than the storage space in the proxy server. Therefore, we push objects one by one according to the sorted order until the storage constraint of

proxy server i is reached.

As is shown in figure 28, we assume that object L is the first object that cannot be pushed into proxy server i subjected to a storage constraint of i. If objects can be divided into pieces, pushing $\{$object 1, object 2,..., object $(L-1)\}$ and a fraction of object L will provide the smallest total cost

$$\Delta_{mn} - \sum_{j=1}^{L-1} f_{ij} - \frac{c_i - \sum_{j=1}^{L-1} s_j}{s_L} f_{iL} \tag{6.11}$$

which is described in Figure 29. However, objects cannot be partitioned in our push-pull optimization problem. Thus, the optimum result of our optimization problem cannot surpass that of the fractional optimization problem. Suppose $OptSet$ is the object set of the optimal solution for non-fractional optimization problem, the weighted total cost of this set is

$$\Delta_{mn} - \sum_{j \in OptSet} f_{ij} \tag{6.12}$$

that will not be smaller than the cost in Eq. (6.11).

According to our algorithm, if $\sum_{j=1}^{L-1} f_{ij} \geq f_{iL}$, object 1, object 2,..., object $(L-1)$ will be pushed into the proxy server i; otherwise, object L will be pushed into the proxy server i. Then, we have either $\sum_{j=1}^{L-1} f_{ij} \geq \frac{1}{2} \sum_{j \in OptSet} f_{ij}$ or $f_{iL} \geq \frac{c_i - \sum_{j=1}^{L-1} s_j}{s_L} f_{iL} \geq \frac{1}{2} \sum_{j \in OptSet} f_{ij}$ Therefore, the weighted total cost of our algorithm is

$$\min\{\Delta_{mn} - \sum_{j=1}^{L-1} f_{ij}, \Delta_{mn} - f_{iL}\} \tag{6.13}$$

from which the upper bound of our algorithm can be derived as

$$\Delta_{mn} - \frac{1}{2} \sum_{j \in OptSet} f_{ij} \tag{6.14}$$

□

We now discuss the time and space complexity of the proposed algorithm. The algorithm computes $PushSet_i$ for each proxy server $i \in 1, 2, \ldots, m$. In each iteration, ratios r_{ij} are sorted in $O(nlog(n))$ time. Therefore, the total time complexity of the approximation algorithm is $O(mnlog(n))$.

On the other hand, $O(n)$ storage space is needed in order to sort the ratios and record the $PushSet_i$ for each proxy server $i \in 1, 2, \ldots, m$. However, because iterations are executed serially, the $O(n)$ storage space for sorting can be reclaimed in each iteration. Meanwhile, considering m proxy servers, the space required for m $PushSet_i$ is $O(mn)$. Thus, the total space complexity of the proposed approximation algorithm is $O(mn)$. Note that the approximation algorithm can be further improved with the upper bound as $\Delta_{mn} - (1 - \varepsilon) \sum_{j \in OptSet} f_{ij}$, where $\varepsilon > 0$, but with an increased time complexity of $O(mnlog(\frac{1}{\varepsilon}) + m\frac{1}{\varepsilon^4})$, and an increased space complexity of $O(mn + m\frac{1}{\varepsilon^3})$ as proved in [72].

Finally, driven by the requirement of offloading the work of origin server and backbone networks, the proposed approximation algorithm can be implemented in a distributed manner as depicted in Algorithm 7. The Distributed Traffic-Latency-Minimization (DTLM) algorithm is running on each proxy server to enable proxy servers to dynamically adjust the distribution of replica so that economically and efficiently server the content users' requirements without burdening the origin server.

As presented in Algorithm 7, each proxy server i first calculates the $PushSet_i$ that includes the objects to be pushed on proxy server i, based on the assumption that the

Algorithm 7 DTLM approximation algorithm - runs on each proxy server

Initialize the distance d_{ij} for each object j as the distance from origin server to local;
Initialize the location of each object j as origin server;
Calculate the f_{ij} and r_{ij} for each object j;
Sort r_{ij} in descending order and record corresponding indices in array h;
Calculate the $PushSet_i$ according to r_{ij} and current d_{ij};
Update the location for objects in $PushSet_i$ as local;
Inform cooperative-proxy server about current $PushSet_i$;
While (receive $PushSet_{i'}$ from cooperative proxy server i')
    For each objects k in received cooperate-proxy server's $PushSet_{i'}$;
        If distance from proxy server i' to local is nearer than d_{ij};
            update d_{ij} as the distance from proxy server i' to local;
            record the location of object k as proxy server i';
        End if
    End for
    For each objects j
        If (Location is proxy server i') AND (Not in $PushSet'_i$)
            Update the distance d_{ij} as the distance from origin server to local;
            Update the location of object j as origin server;
        End if
    End for
    Recalculate the f_{ij} and r_{ij} for each object j;
    Recalculate the $PushSet_i$ according to updated r_{ij} and current d_{ij};
    Inform cooperate-proxy server updated $PushSet_i$;
End while

nearest replica is on the origin server. After that, proxy server i informs its cooperative proxy servers about $PushSet_i$ and meanwhile notified by its cooperative proxy servers about their $PushSet'_i$. Then proxy server i may update the distance d_{ij} between the nearest replica of object j and proxy server i if j is in $PushSet'_i$, and recomputes a new $PushSet_i$ by using updated distance d_{ij}. By continuously exchanging the $PushSet_i$ with the cooperative proxy server and recompute the $PushSet_i$ based on $PushSet'_i$ received from cooperative proxy server, proxy server i can gradually approach the optimal solution that has a minimum weighted total cost of the push-pull network. The space complexity of DTLM is $O(n)$ on each proxy server. Limited rounds of control messages are exchanged only among neighbors with their lists of objects. Upon receiving messages from neighbors, $O(nlog(n))$ of the time complexity is spent.

6.3 Evaluations

In this section, we conduct extensive performance evaluations of our proposed approximation algorithms, TLM, and its distributed version, DTLM, using both simulations with parameters from practices and experiments on a real network.

6.3.1 Simulations

We first describe the parameters used for simulations. In our simulation, a proxy server i is randomly endowed with a different storage capacity c_i, the mean of which is set to 25% of the total object size to obtain an ideal CDN utility and hit ratio [103]. Also, each object is associated with a size s_j that is retrieved from real .avi files, which range from 1.28 MB to 41.8 GB. Each object has its probability of being requested in each area,

Table 11: Parameter Setting for Simulations

Parameter	Values
m	Number of proxy servers, $m = 10$
c_i	$\sim$ normal distribution $N(0.25 * j$GB, 1GB$^2)$
n	Varies in the range of $[100, 200, \ldots, 1000]$
s_j	Sizes of real media files, range in [1.28MB 41.800GB]
p_{ij}	$\sim$ Zipf distribution $Z(1, n)$
α	0.5
d_{ij}	$\sim$ normal distribution $N(10$ hops, 5 hops$^2)$. 15 ms per hop.
λ_i	$\sim$ normal distribution $N(200$ requests, 100 requests$^2)$

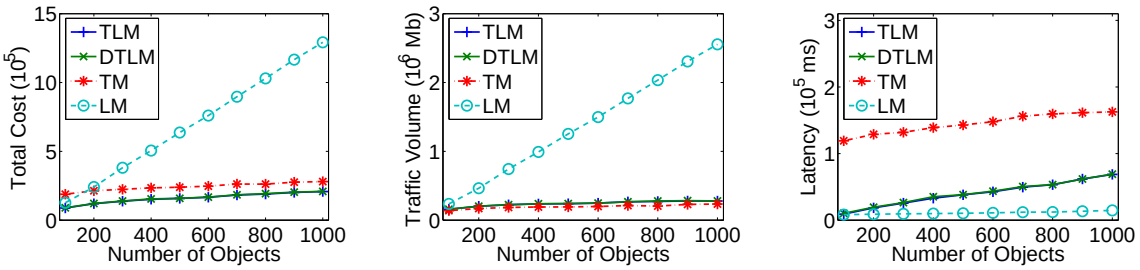

(a) Total cost (b) Traffic overhead (c) Latency overhead

Figure 30: Comparison for varied number of objects (simulation with real object sizes)

following a Zipf distribution. In particular, the probability of object j to be demanded in area i is $\frac{1/k_{ij}}{H_{n,1}}$.[1] The cost coefficient α in (6.4) is set to balance the traffic volume and latency requirements. In Figures 30 and 31, we set α as 0.5 so that the requirements of traffic volume and latency are of equal weights. We then show how α can be used for different requirements in Figure 32. The parameters used in this simulation are described in Table 11.

[1] k is the rank of the decreasing probability list of objects, out of $[1, n]$, where n is the number of objects. $H_{n,1}$ is the nth harmonic number. $H_{n,1} = 1 + 1/2 + 1/3 + ... + 1/n$.

We compare the performance of the proposed algorithm with other existing algorithms that minimize traffic volume – referred to as the Traffic-Minimization (TM) algorithm – as in [18], and that minimize latency – referred to as the Latency-Minimization (LM) algorithm – as in [67], respectively. In [18], the objects are replaced dynamically with the highest global utility in the proxy servers that can be referred to as a pull-based scheme; meanwhile, in a push-based scheme such as [67], the objects are replicated according to their popularity and transmission distance.

Figures 30 (a), (b) and (c) compare the total cost of the traffic overhead and the latency overhead of three algorithms, respectively, as the number of objects increases. We have varied the total number of objects ranging from 100 to 1000 as in [65, 67, 74, 107].

In Figure 30 (a), we observe the total cost of the proposed algorithm, TLM, and the compared algorithms, BM and LM. It shows that the proposed TLM and DTLM uses the lowest cost, and outperforms BM and LM algorithms that consider traffic volume or latency individually, especially as the demand increases. When we investigate the individual performance of traffic and latency, the proposed TLM and DTLM algorithm achieves a good tradeoff between traffic volume and latency, and is closer to the lowest, as shown in Figures 30 (b) and (c). We observe that, TLM performs slightly better than DTLM. That is because the origin server has the complete knowledge of the placements of each object's replica; while proxy servers in DTLM only have limited knowledge shared from neighbors. On the other hand, there is no significant improvement of TLM, since network issues such as packet loss and queueing delay are not captured in the simulations. Therefore, we further examine the performance of TLM and DTLM in a real test platform,

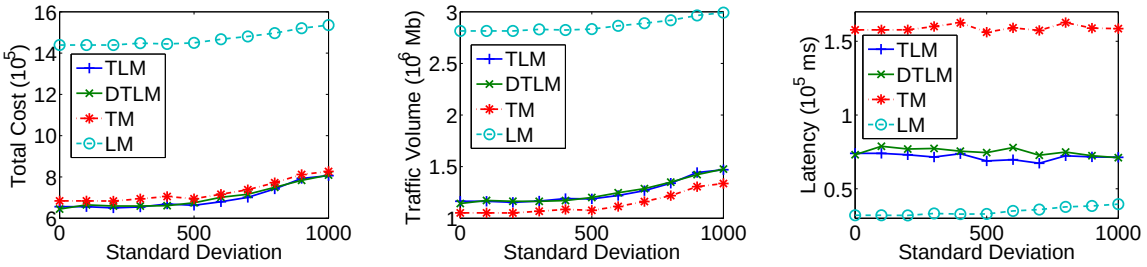

(a) Total cost (b) Traffic overhead (c) Latency overhead

Figure 31: Comparison for varied standard deviation of object sizes (simulation with synthetic object sizes)

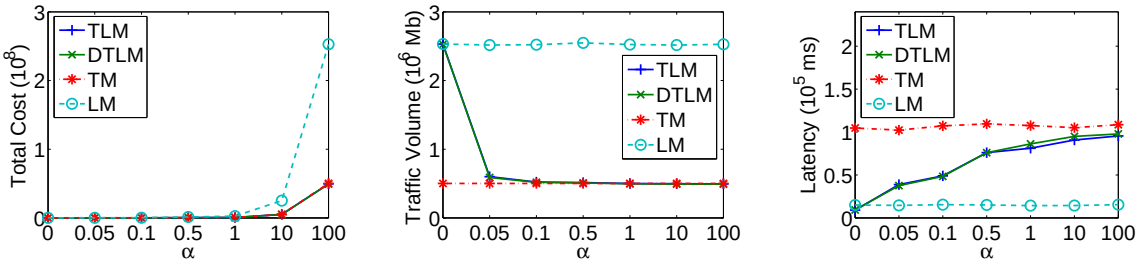

(a) Total cost (b) Traffic overhead (c) Latency overhead

Figure 32: Comparison for varied balance parameter α (simulation with real object sizes)

Planetlab.

We further investigate the impact of the variance of object size in Figures 31 (a), (b), and (c). Object sizes in this group of experiments are randomly selected from a normal distribution $N(1$ GB, Va MB$^2)$, where Va varies from [0, 1000]. As observed in Figure 31 (c), when the standard deviation increases, latency cost by LM steadily increases. This poses less impact on TLM and DTLM.

In addition, the impact of balance parameter α is presented in Figures 32 (a), (b)

Table 12: Parameter Setting for Planetlab Experiments

Parameter	Values
m	Number of proxy servers, $m = 10$
c_i	$\sim$ normal distribution $N(0.25 * j$GB, 1GB$^2)$
n	Varies in the range of $(100, 200, \ldots, 1000)$
s_j	Size of real media files, range in [1.28MB 41.800GB]
p_{ij}	$\sim$ Zipf distribution $Z(1, n)$
α	0.05
d_{ij}	Real distances between Planetlab sites
λ_i	$\sim$ normal distribution $N(200$ requests, 100 requests$^2)$

and (c). As exhibited in Figures 32 (b) and (c), when α is set to 0, TLM and DTLM are reduced to simply minimize latency while when α is approaching infinite, TLM and DTLM will simply minimize traffic volume. However, the weighted total costs of TLM and DTLM are always the least compared with BM and LM.

6.3.2 Experiments

In order to validate the efficiency and effectiveness under a more realistic environment, we also evaluate our algorithm on Planetlab testbed [90]. Furthermore, for realistic purpose, we employ real object sizes instead of randomly assigning them as we do in the simulation portion. Object sizes are obtained from a search engine by searching media objects. As in simulations, the experiments are implemented with 1 origin server and 10 proxy servers, and the network topology is presented in Figure 33. The distance between servers are derived from real RTT times between these 11 Planetlab sites. The other parameter settings, such as proxy servers' storage ability, popularity and request number in each area are the same with those in the simulations.

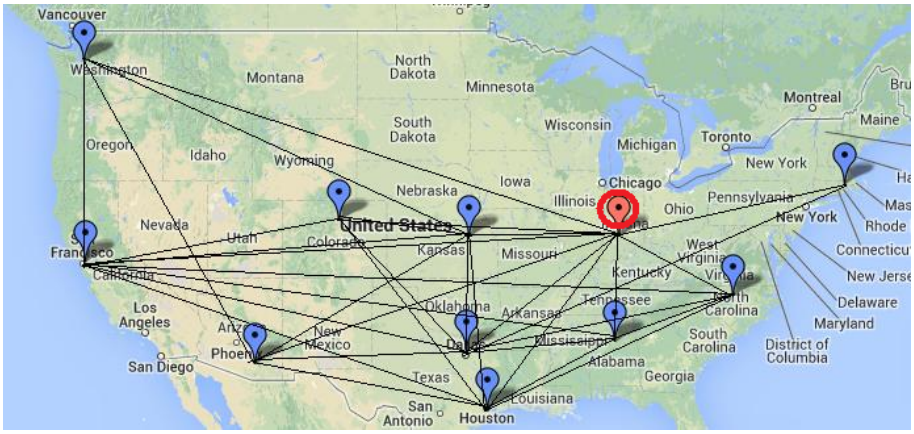

Figure 33: Locations for the origin server and proxy servers: the mark in the circle indicates the location for the origin server; and the remain sites are all proxy servers. Each proxy server is connected to origin server and its cooperative proxy servers. Proxy servers may pull objects from the origin server or a closer proxy server.

As in the evaluation with simulations, we have studied the total cost, the traffic overhead, and the latency overhead of three algorithms in Figures 34 (a), (b) and (c), respectively, as the number of objects increases from 100 to 1000. The balanced coefficient α is set to 0.05 to enforce the traffic volume and latency work in the same order. We summarize the parameters in experiments in Table 12.

As shown in Figure 34 (a), both TLM and DTLM outperform LM and BM algorithms in the total cost that considers both traffic volume and latency. DTLM performs a little worse than TLM, since it may not find the most proper replica location for every object. Furthermore, as depicted in Figures 34 (b) and (c), we find that our TLM and DTLM algorithms can find a good tradeoff between latency and traffic volume consumption, which conforms to the observations we have made from the simulations. The differences in the values of total cost, traffic, and latency consumption in simulation and

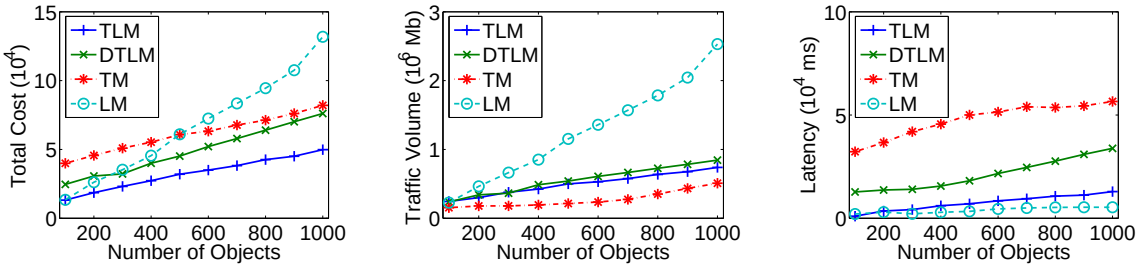

(a) Total cost (b) Traffic overhead (c) Latency overhead

Figure 34: Comparison for varied number of objects (Planetlab experiments with real object sizes)

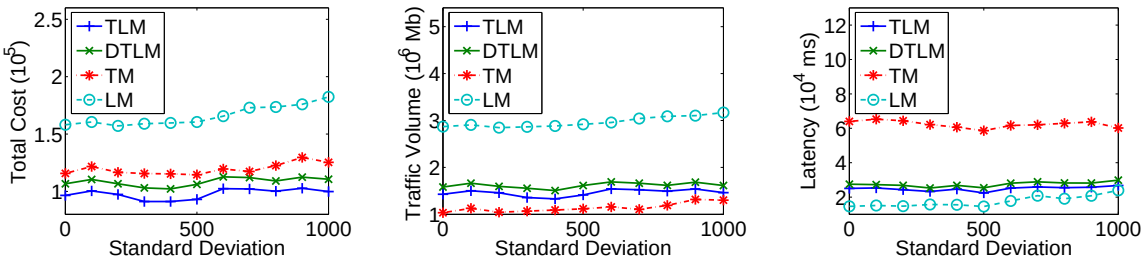

(a) Total cost (b) Traffic overhead (c) Latency overhead

Figure 35: Comparison for varied standard deviation of object sizes (Planetlab experiments with synthetic object sizes)

experiments come from the object sizes and distance settings.

The impact of size variance is also examined on Planetlab as presented in Figures 35 (a), (b) and (c). The number of objects is 1000 as used in [65, 67, 74, 107], and the storage limitation for each proxy server is 250 GB. The size of objects follows normal distribution with mean 1 GB, and standard deviation varies from 0 to 1 GB^2. As shown in Figure 35 (c), as standard deviation varies, the latency consumed by the LM algorithm increases, while the latency of the other three algorithms stays stable.

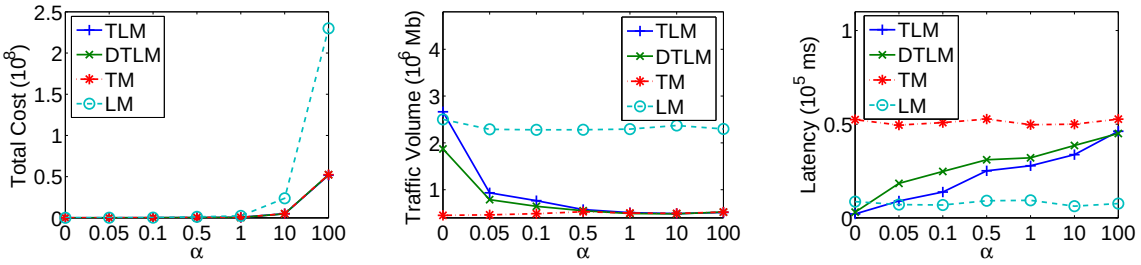

(a) Total cost (b) Traffic overhead (c) Latency overhead

Figure 36: Comparison for varied balance parameter α (Planetlab experiments with real object sizes)

We further investigate the impact of balance parameter α in Figures 36 (a), (b) and (c). As presented in Figures 36 (a), (b) and (c), α can be used to balance the impact of latency and traffic volume requirements. Especially, TLM and DTLM can be reduced to simply minimize latency or traffic volume by setting α to 0 or a very large value (e.g. 100), respectively.

6.4 Summary

We have studied the problem of content placements that determines which objects should be pushed to which proxy servers and which should be pulled on demand for an optimal content delivery over cloud storage. To the best of our knowledge, our work is the first to consider both bandwidth usage in the network and latency for the optimization of content delivery using cloud storage services. We have modeled and formulated this

push-pull content delivery problem, and proved that it is NP-complete using the Knapsack problem. We have developed an approximation algorithm named Traffic-Latency-Minimization (TLM) for our push-pull optimization problem. Theoretical analysis indicates that the upper bound of the TLM algorithm is $\Delta_{mn} - \frac{1}{2}\sum_{j \in OptSet} f_{ij}$ comparing that the optimal solution can achieve $\Delta_{mn} - \sum_{j \in OptSet} f_{ij}$, where Δ_{mn} is the weighted total cost for a simple pull strategy and f_{ij} denotes the saved cost by pushing object j to proxy server i. The time complexity of our TLM algorithm is $\Theta(mnlog(n))$, while the space complexity is $O(mn)$. In our model, we have made system parameters such as the storage capacity, the number of requests, object request probability, and object size to be dynamic rather than constant. We have further implemented a distributed algorithm for our TLM algorithm named DTLM and compared our TLM and DTLM algorithms with other existing algorithms with simulations and experiments. We have also shown that our approximation algorithm, both in a centralized and a distributed manners outperforms them, reaching near the minimum cost of both latency and bandwidth.

Several related challenges need to be addressed before deploying into a real content distribution system. Relevant future work would include developing an accurate on-the-fly estimation scheme for the demands, the methods for short and long-term optimal cache dimensioning and placements, and content delivery based on different Service Level Agreements.

CHAPTER 7

CONCLUSIONS AND FUTURE WORK

This dissertation focus on energy efficient resource allocation for virtual network service in cloud data centers. New models are proposed and studied to minimize the cost in resource allocation for virtual networks, virtual machines and cloud storage services while persevering QoS requirements of network services. We consider practical constraints and demands, such as time evolving workload of virtual services and available physical resources, practical DC topologies. In addition,green physical nodes that enables sleep/awake mode are employed to improve energy efficiency in data centers.

For the energy efficient virtual network embedding, we plan possible future migration in advance, and minimize the total energy consumption including both operation cost and potential future migration cost. An efficient and practical virtual network embedding algorithm (TMAE-VNE) and an Ant Colony Optimization based memory efficiency algorithm have been developed to determine the initial embedding and future migration for a virtual networks considering its predictable demands. Extensive comparisons with existing VNE algorithms validated the improvements of the proposed algorithms in energy saving and acceptance ratio under various scenarios.

In addition, container based virtual machine embedding and resource allocation attracts more attentions as its light weight and efficiency. Driven by the advantages of

container based VM, we proposed a novel framework to provision resources for virtual network services utilizing container based VM. In our framework, we separated the resource management and job execution for the network services into two kinds of containers named as pallet container and execution container. We further designed a cost efficiency resource allocation model and corresponding algorithm to solve this problem. Compared with static Hypervisor based VM placement, evaluations validated that container based resource allocation improves the acceptance ratio and cost efficiency.

Finally, we studied content placement problem with the optimization goal to minimize the bandwidth usage in the network and latency experienced by final users. We modeled the push-pull content delivery problem and proved its hardness. Later an approximate algorithm has been designed and developed with guaranteed bound. We implemented the algorithm in a distributed manner as well as a centralized manner and compared them with existing algorithms through simulations and experiments on planetlab.

Resource allocation is one of the most essential problem in cloud computing. As the development of cloud computing and the advent of new techniques, such as the utilization of fiber optic in data centers, multi-regional electricity markets, edge cloud and mobile cloud, new challenges and new opportunities would be brought to resource allocation problem. These new scenarios will be further explored and taken into consideration in the future.

REFERENCE LIST

[1] 15% Growth Forecast for North America Colocation Market 2014. http://www.datacenterdynamics.com/focus/archive/2014/01/15-growth-forecast-north-america-colocation-market-2014-0.

[2] Akamai. http://www.akamai.com/.

[3] Al-Fares, M., Loukissas, A., and Vahdat, A. A scalable, commodity data center network architecture. In Proceedings of the ACM SIGCOMM 2008 conference on Data communication (New York, NY, USA, 2008), SIGCOMM '08, ACM, pp. 63–74.

[4] Almeida, J. M., Eager, D. L., Vernon, M. K., and Wright, S. J. Minimizing delivery cost in scalable streaming content distribution systems. IEEE Trans. Multimedia 6, 2 (2004), 356–365.

[5] Amazon Simple Storage Service (Amazon S3). http://aws.amazon.com/s3/.

[6] Amokrane, A., Zhani, M., Langar, R., Boutaba, R., and Pujolle, G. Greenhead: Virtual Data Center Embedding across Distributed Infrastructures. Cloud Computing, IEEE Transactions on 1, 1 (Jan 2013), 36–49.

[7] Andersen, D. G. Theoretical approaches to node assignment. Computer Science Department (2002), 86.

[8] Arlitt, M. Characterizing web user sessions. ACM SIGMETRICS Performance Evaluation Review 28, 2 (2000), 50–63.

[9] at Scale, G. G. C. E. https://static.googleusercontent.com/media/www.google.com/en//green/pdfs/g green-computing.pdf.

[10] Baev, I., Rajaraman, R., and Swamy, C. Approximation algorithms for data placement problems. SIAM J. Computing 38, 4 (2008), 1411–1429.

[11] Baev, I. D., and Rajaraman, R. Approximation algorithms for data placement in arbitrary networks. Proc. 12th Annu. ACM-SIAM Symp. Discrete algorithms (SODA) (2001), 661–670.

[12] Barham, P., Dragovic, B., Fraser, K., Hand, S., Harris, T., Ho, A., Neugebauer, R., Pratt, I., and Warfield, A. Xen and the Art of Virtualization. SIGOPS Oper. Syst. Rev. 37, 5 (Oct. 2003), 164–177.

[13] Barroso, L. A., and Hölzle, U. The case for energy-proportional computing. IEEE computer 40, 12 (2007), 33–37.

[14] Bash, C. E., Patel, C. D., and Sharma, R. K. Dynamic thermal management of air cooled data centers. In Thermal and Thermomechanical Phenomena in Electronics Systems, 2006. ITHERM'06. The Tenth Intersociety Conference on (2006), IEEE, pp. 8–pp.

[15] Beck, M., Moore, T., and Plank, J. S. An End-to-end Approach to Globally Scalable Network Storage. In ACM SIGCOMM Computer Communication Review (2002), vol. 32, ACM, pp. 339–346.

[16] Bednarcik, E., Tresh, M., and Jackson, B. Data Center Air Routing System, Oct. 26 2009. US Patent App. 12/605,992.

[17] Blum, C., and Roli, A. Metaheuristics in Combinatorial Optimization: Overview and Conceptual Comparison. ACM Comput. Surv. 35, 3 (Sept. 2003), 268–308.

[18] Borst, S., Gupta, V., and Walid, A. Distributed caching algorithms for content distribution networks. Proc. IEEE INFOCOM (2010), 1–9.

[19] Botero, J., Hesselbach, X., Duelli, M., Schlosser, D., Fischer, A., and de Meer, H. Energy Efficient Virtual Network Embedding. Communications Letters, IEEE 16, 5 (May 2012), 756–759.

[20] Box, V. https://www.virtualbox.org/wiki/Downloads.

[21] Broberg, J., Buyya, R., and Tari, Z. MetaCDN: Harnessing 'Storage Clouds' for high performance content delivery. J. Network and Computer Applications 32, 5 (2009), 1012–1022.

[22] Cai, Z., Liu, F., Xiao, N., Liu, Q., and Wang, Z. Virtual Network Embedding for Evolving Networks. In IEEE Global Tele. Conf. (GLOBECOM) (2010), pp. 1–5.

[23] Cao, W., Wang, H., and Liu, L. An Ant Colony Optimization Algorithm for Virtual Network Embedding. In Algorithms and Architectures for Parallel Processing,

vol. 8630 of Lecture Notes in Computer Science. Springer International Publishing, 2014, pp. 299–309.

[24] Chaisiri, S., Lee, B., and Niyato, D. Optimal virtual machine placement across multiple cloud providers. IEEE Asia-Pacific Services Computing Conf. (2009), 103–110.

[25] Chakinala, R., Kumarasubramanian, A., Laing, K., Manokaran, R., Rangan, C., and Rajaraman, R. Playing push vs pull: models and algorithms for disseminating dynamic data in networks. Proc. 8th Annu. ACM Symp. Parallelism in algorithms and architectures (2006), 244–253.

[26] Chang, X., Wang, B., Liu, J., Wang, W., and Muppala, J. Green Cloud Virtual Network Provisioning Based Ant Colony Optimization. In Proceedings of the 15th Annual Conference Companion on Genetic and Evolutionary Computation (New York, NY, USA, 2013), GECCO '13 Companion, ACM, pp. 1553–1560.

[27] Chen, G., He, W., Liu, J., Nath, S., Rigas, L., Xiao, L., and Zhao, F. Energy-aware server provisioning and load dispatching for connection-intensive internet services. In Proceedings of the 5th USENIX Symposium on Networked Systems Design and Implementation (2008), USENIX Association, pp. 337–350.

[28] Chen, Y., Qiu, L., Chen, W., L.Nguyen, and R.H.Katz. Efficient and adaptive web replication using content clustering. IEEE J. Selected Areas in Communications 21, 6 (2003), 979–994.

[29] Cheng, X., Su, S., Zhang, Z., Wang, H., Yang, F., Luo, Y., and Wang, J. Virtual Network Embedding Through Topology-aware Node Ranking. SIGCOMM Comput. Commun. Rev. 41, 2 (Apr. 2011), 38–47.

[30] Chiu, Y., and Eun, D. On the Performance of Content Delivery under Competition in a Stochastic Unstructured Peer-to-Peer Network. IEEE Trans. Parallel and Distributed Systems 21, 10 (2010), 1487–1500.

[31] Chowdhury, M., Rahman, M. R., and Boutaba, R. ViNEYard: virtual network embedding algorithms with coordinated node and link mapping. IEEE/ACM Trans. Netw. 20, 1 (Feb. 2012), 206–219.

[32] Chowdhury, N. M. K., and Boutaba, R. A survey of network virtualization. Computer Networks 54, 5 (2010), 862 – 876.

[33] Chowdhury, N. M. K., Rahman, M. R., and Boutaba, R. Virtual network embedding with coordinated node and link mapping. In INFOCOM 2009, IEEE (2009), IEEE, pp. 783–791.

[34] Chu, R., Xiao, N., Chen, L., and Lu, X. A Push-based Prefetching for Cooperative Caching RAM Grid. In Parallel and Distributed Systems, 2007 International Conference on (2007), vol. 2, IEEE, pp. 1–8.

[35] Docker. https://www.docker.com/.

[36] Dorigo, M., and Stützle, T. Ant Colony Optimization. Bradford Company, Scituate, MA, USA, 2004.

[37] Dropbox. https://www.dropbox.com/.

[38] Drutskoy, D., Keller, E., and Rexford, J. Scalable network virtualization in software-defined networks. Internet Computing, IEEE 17, 2 (2013), 20–27.

[39] EC2, A. http://aws.amazon.com/ec2/.

[40] ESXi, V. https://www.vmware.com/products/esxi-and-esx/overview.

[41] Fajjari, I., Aitsaadi, N., Pujolle, G., and Zimmermann, H. VNE-AC: Virtual Network Embedding Algorithm Based on Ant Colony Metaheuristic. In Communications (ICC), 2011 IEEE International Conference on (June 2011), pp. 1–6.

[42] Fajjari, I., Aitsaadi, N., Pujolle, G., and Zimmermann, H. VNR Algorithm: A Greedy Approach for Virtual Networks Reconfigurations. In Global Tele. Conf. (GLOBECOM), 2011 IEEE (2011), pp. 1–6.

[43] Fan, X., Weber, W.-D., and Barroso, L. A. Power provisioning for a warehouse-sized computer. In ACM SIGARCH Computer Architecture News (2007), vol. 35, ACM, pp. 13–23.

[44] Felter, W., Ferreira, A., Rajamony, R., and Rubio, J. An updated performance comparison of virtual machines and linux containers. technology 28 (2014), 32.

[45] Feng, C., Li, B., and Li, B. Understanding the performance gap between pull-based mesh streaming protocols and fundamental limits. Proc. IEEE INFOCOM (2009).

[46] Fischer, A., Beck, M., and de Meer, H. An approach to energy-efficient virtual network embeddings. In Integrated Network Management (IM 2013), 2013 IFIP/IEEE International Symposium on (May 2013), pp. 1142–1147.

[47] Fischer, A., Botero, J., Beck, M., De Meer, H., and Hesselbach, X. Virtual Network Embedding: A Survey. Communications Surveys Tutorials, IEEE PP, 99 (2013), 1–19.

[48] Fuerst, C., Schmid, S., and Feldmann, A. Virtual network embedding with collocation: benefits and limitations of pre-clustering. In 2nd IEEE International Conference on Cloud Networking (2013), IEEE.

[49] Ge, C., Sun, Z., and Wang, N. A survey of power-saving techniques on data centers and content delivery networks. Communications Surveys & Tutorials, IEEE 15, 3 (2013), 1334–1354.

[50] Gill, P., Arlitt, M., Li, Z., and Mahanti, A. Youtube traffic characterization: a view from the edge. In Proceedings of the 7th ACM SIGCOMM conference on Internet measurement (2007), ACM, pp. 15–28.

[51] Google. http://www.google.com/green/bigpicture/references.html.

[52] Google Cloud Storage. https://developers.google.com/storage/.

[53] Greenberg, A., Hjalmtysson, G., Maltz, D. A., Myers, A., Rexford, J., Xie, G., Yan, H., Zhan, J., and Zhang, H. A Clean Slate 4D Approach to Network Control and Management. SIGCOMM Comput. Commun. Rev. 35, 5 (Oct. 2005), 41–54.

[54] Guan, X., and Choi, B.-Y. Push or Pull?: Toward Optimal Content Delivery. In Communications (ICC), 2011 IEEE International Conference on (2011), IEEE, pp. 1–5.

[55] Guan, X., and Choi, B.-Y. Push or pull? Toward optimal content delivery using cloud storage. Journal of Network and Computer Applications 40 (2014), 234–243.

[56] Guan, X., Choi, B.-Y., and Song, S. Topology and migration-aware energy efficient virtual network embedding for green data centers. In Computer Communication and Networks (ICCCN), 2014 23rd International Conference on (Aug 2014), pp. 1–8.

[57] Guan, X., Choi, B.-Y., and Song, S. Topology and migration-aware energy efficient virtual network embedding for green data centers. In Computer Communication and Networks (ICCCN), 2014 23rd International Conference on (2014), IEEE, pp. 1–8.

[58] Guan, X., Choi, B.-Y., and Song, S. Energy Efficient Virtual Network Embedding for Green Data Centers using Data Center Topology and Future Migration. Computer Communications (2015).

[59] Guan, X., Wan, X., Choi, B.-Y., and Song, S. Ant Colony Optimization Based Energy Efficient Virtual Network Embedding.

[60] Haβinger, G., and Hartleb, F. Content delivery and caching from a network provider's perspective. Computer Networks 55, 18 (2011), 3991 – 4006.

[61] Han, D., Andersen, D., Kaminsky, M., Papagiannaki, D., and Seshan, S. An Access Network Architecture for Neighborhood-scale Multimedia Delivery. Tech. rep., Tech. Rep. CMU-CS-10-128, Carnegie Mellon University, School of Computer Science, 2010.

[62] Inführ, J., and Raidl, G. R. Introducing the virtual network mapping problem with delay, routing and location constraints. In Network Optimization. Springer, 2011, pp. 105–117.

[63] Jain, S., Kumar, A., Mandal, S., Ong, J., Poutievski, L., Singh, A., Venkata, S., Wanderer, J., Zhou, J., Zhu, M., Zolla, J., Hölzle, U., Stuart, S., and Vahdat, A. B4: Experience with a Globally-deployed Software Defined WAN. SIGCOMM Comput. Commun. Rev. 43, 4 (Aug. 2013), 3–14.

[64] Joshi, Y., and Kumar, P. Energy efficient thermal management of data centers. Springer Science & Business Media, 2012.

[65] Kamiyama, N., Mori, T., Kawahara, R., Harada, S., and Hasegawa, H. Analyzing influence of network topology on designing ISP-operated CDN. Telecommun Systems (Sep. 2011), 1–6.

[66] Kanagavelu, R., Lee, B.-S., Le, N. T. D., Mingjie, L. N., and Aung, K. M. M. Virtual machine placement with two-path traffic routing for reduced congestion in data center networks. Computer Communications 53 (2014), 1–12.

[67] Kangasharju, J., Roberts, J., and Ross, K. W. Object replication strategies in content distribution networks. Computer Communications 25, 4 (2002), 376–383.

[68] Kaplan, J. M., Forrest, W., and Kindler, N. Revolutionizing data center energy efficiency. Tech. rep., Technical report, McKinsey & Company, 2008.

[69] Khan, A., Yan, X., Tao, S., and Anerousis, N. Workload characterization and prediction in the cloud: A multiple time series approach. In Network Operations and Management Symposium (NOMS), 2012 IEEE (2012), IEEE, pp. 1287–1294.

[70] Koomey, J. Growth in data center electricity use 2005 to 2010. The New York Times 49, 3 (2011).

[71] Korupolu, M. R., Plaxton, C. G., and Rajaraman, R. Placement algorithms for hierarchical cooperative caching. Proc. 10th Annu. ACM-SIAM Symp. Discrete algorithms (SODA) (1999), 586–595.

[72] Lawler, E. Fast approximation algorithms for knapsack problems. 18th Annu. Symp. Foundations of Computer Science (1977), 206–213.

[73] Lee, K.-P., and Chen, H.-L. Analysis of energy saving potential of air-side free cooling for data centers in worldwide climate zones. Energy and Buildings 64 (2013), 103–112.

[74] Leong, D., Ho, T., and Cathey, R. Optimal content delivery with network coding. 43rd Annu. Conf. Information Sciences and Systems (CISS) (Mar. 2009), 414–419.

[75] Limelight. http://www.limelight.com/.

[76] Lin, C., Leu, M., Chang, C., and Yuan, S. The study and methods for cloud based CDN. IEEE Int. Conf. Cyber-Enabled Distributed Computing and Knowledge Discovery (2011), 469–475.

[77] Lischka, J., and Karl, H. A virtual network mapping algorithm based on subgraph isomorphism detection. In Proc. 1st ACM workshop on Virtualized infrastructure systems and architectures (New York, NY, USA, 2009), VISA '09, ACM, pp. 81–88.

[78] Liu, Z., Zhang, Q., Zhani, M. F., Boutaba, R., Liu, Y., and Gong, Z. DREAM-S: Dynamic resource allocation for MapReduce with data skew. In Integrated Network Management (IM), 2015 IFIP/IEEE International Symposium on (2015), IEEE, pp. 18–26.

[79] Machine, K. K. V. http://www.linux-kvm.org/page/Main_Page.

[80] Madhyastha, H., Anderson, T., Krishnamurthy, A., Spring, N., and Venkataramani, A. A structural approach to latency prediction. Proc. 6th ACM Internet Measurement Conf. (IMC) (2006), 99–104.

[81] Malone, C. G. Airflow distribution control system for usage in a raised-floor data center, May 8 2007. US Patent 7,214,131.

[82] Natarajan, S., and Wolf, T. Security issues in network virtualization for the future Internet. In Computing, Networking and Communications (ICNC), 2012 International Conference on (Jan 2012), pp. 537–543.

[83] Open Compute Project. Energy efficiency. http://opencompute.org/about/energy-efficiency, 2011.

[84] our customers, D. https://www.docker.com/customers.

[85] Overview, X. P. S. http://wiki.xen.org/wiki/Xen_Project_Software_Overview.

[86] Overview-NetworkX. http://networkx.github.io/.

[87] Pages, A., Perello, J., Spadaro, S., and Junyent, G. Strategies for Virtual Optical Network Allocation. Communications Letters, IEEE 16, 2 (2012), 268–271.

[88] pantheon. Energy Efficiency Are containers the electric cars of computing. https://pantheon.io/platform/energy-efficiency.

[89] Papagiannaki, K., Taft, N., Zhang, Z.-L., and Diot, C. Long-term forecasting of Internet backbone traffic: observations and initial models. In INFOCOM

2003. Twenty-Second Annual Joint Conference of the IEEE Computer and Communications. IEEE Societies (2003), vol. 2, pp. 1178–1188 vol.2.

[90] Planetlab. http://www.planet-lab.org/.

[91] Platform, G. C. https://cloud.google.com/products/.

[92] Qian, H., Surapaneni, C. S., Dispensa, S., and Medhi, D. Service management architecture and system capacity design for PhoneFactor¡ªA two-factor authentication service. In Integrated Network Management, 2009. IM'09. IFIP/IEEE International Symposium on (2009), IEEE, pp. 73–80.

[93] Radha, S., Saira Bhanu, S., and Gopalan, N. P. Remote Memory Management and Prefetching Techniques for Jobs in Grid. In Semantics, Knowledge and Grid, 2006. SKG '06. Second International Conference on (Nov.), pp. 24–24.

[94] Raghavan, B., Vishwanath, K., Ramabhadran, S., Yocum, K., and Snoeren, A. C. Cloud Control with Distributed Rate Limiting. SIGCOMM Comput. Commun. Rev. 37, 4 (Aug. 2007), 337–348.

[95] Raghavendra, R., Ranganathan, P., Talwar, V., Wang, Z., and Zhu, X. No power struggles: Coordinated multi-level power management for the data center. In ACM SIGARCH Computer Architecture News (2008), vol. 36, ACM, pp. 48–59.

[96] Rosa, R., Esteve Rothenberg, C., and Madeira, E. Virtual data center networks embedding through Software Defined Networking. In Network Operations and Management Symposium (NOMS), 2014 IEEE (May 2014), pp. 1–5.

[97] Salesforce. http://www.salesforce.com/.

[98] Sang, A., and qi Li, S. A predictability analysis of network traffic. Computer Networks 39, 4 (2002), 329 – 345.

[99] Server, M. V. http://www.microsoft.com/windowsserversystem/virtualserver/.

[100] Services, M. A. C. C. P. . https://azure.microsoft.com/.

[101] Simarro, J., Moreno-Vozmediano, R., Montero, R., and Llorente, I. Dynamic placement of virtual machines for cost optimization in multi-cloud environments. IEEE Int. Conf. High Performance Computing and Simulation (HPCS) (2011), 1–7.

[102] Soltesz, S., Pötzl, H., Fiuczynski, M. E., Bavier, A., and Peterson, L. Container-based operating system virtualization: a scalable, high-performance alternative to hypervisors. In ACM SIGOPS Operating Systems Review (2007), vol. 41, ACM, pp. 275–287.

[103] Stamos, K., Pallis, G., Vakali, A., and Dikaiakos, M. D. Evaluating the utility of content delivery networks. ACM Proc. 4th edition of the UPGRADE-CN Workshop on Use of P2P, GRID and agents for the (2009), 11–20.

[104] State of the Data Center 2011. http://www.emersonnetworkpower.com/en-US/About/NewsRoom/Pages/2011DataCenterState.aspx.

[105] Su, A., Choffnes, D., Bustamante, F., and Kuzmanovic, A. Relative network positioning via CDN redirections. Int. Conf. Distributed Computing Systems (ICDCS) (2008), 377–386.

[106] Survey, . D. C. I. https://journal.uptimeinstitute.com/2014-data-center-industry-survey/.

[107] Tan, B., and Massoulie, L. Optimal Content Placement for Peer-to-Peer Video-on-Demand Systems. Networking, IEEE/ACM Transactions on (2012), 14.

[108] Tao, F., Zhang, L., and Laili, Y. Configurable Intelligent Optimization Algorithm: Design and Practice in Manufacturing. Springer Publishing Company, Incorporated, 2014.

[109] Thompson, K., Miller, G., and Wilder, R. Wide-area Internet traffic patterns and characteristics. Network, IEEE 11, 6 (1997), 10–23.

[110] Touch, J. The lsam Proxy Cache - A Multicast Distributed Virtual Cache. In Computer Networks and ISDN Systems (1998).

[111] Trinh, T., Esaki, H., and Aswakul, C. Quality of service using careful overbooking for optimal virtual network resource allocation. In Electrical Engineering/Electronics, Computer, Telecommunications and Information Technology (ECTI-CON), 2011 8th International Conference on (2011), pp. 296–299.

[112] Triukose, S., Wen, Z., and Rabinovich, M. Content delivery networks: how big is big enough? ACM SIGMETRICS 37 (Oct. 2009), 59–60.

[113] Triukose, S., Wen, Z., and Rabinovich, M. Measuring a commercial content delivery network. ACM Proc. 20th Int. Conf. World Wide Web (WWW) (2011), 467–476.

[114] Wang, J.-B., Chen, M., Wan, X., and Wei, C. Ant-Colony-Optimization-Based Scheduling Algorithm for Uplink CDMA Nonreal-Time Data. Vehicular Technology, IEEE Transactions on 58, 1 (Jan 2009), 231–241.

[115] Wang, Y., Keller, E., Biskeborn, B., van der Merwe, J., and Rexford, J. Virtual routers on the move: live router migration as a network-management primitive. In ACM SIGCOMM Comp. Commun. Rev. (2008), vol. 38, ACM, pp. 231–242.

[116] we do it, G. D. C. E. H. https://www.google.com/about/datacenters/efficiency/internal/.

[117] Webb, M., et al. SMART 2020: Enabling the low carbon economy in the information age. The Climate Group. London 1, 1 (2008), 1–1.

[118] Wei, G., Vasilakos, A. V., Zheng, Y., and Xiong, N. A game-theoretic method of fair resource allocation for cloud computing services. The journal of supercomputing 54, 2 (2010), 252–269.

[119] Wei, Q., Veeravalli, B., Gong, B., Zeng, L., and Feng, D. CDRM: A cost-effective dynamic replication management scheme for cloud storage cluster. IEEE Int. Conf. Cluster Computing (CLUSTER) (2010), 188–196.

[120] Willinger, W., Paxson, V., and Taqqu, M. S. Self-similarity and heavy tails: Structural modeling of network traffic. A practical guide to heavy tails: statistical techniques and applications 23 (1998), 27–53.

[121] Workday. http://www.workday.com/.

[122] Xiao, Z., Song, W., and Chen, Q. Dynamic resource allocation using virtual machines for cloud computing environment. Parallel and Distributed Systems, IEEE Transactions on 24, 6 (2013), 1107–1117.

[123] Xu, D., Kulkarni, S. S., Rosenberg, C., and Chai, H.-K. Analysis of a CDN–P2P Hybrid Architecture for Cost-effective Streaming Media Distribution. Multimedia Systems 11, 4 (2006), 383–399.

[124] Yu, M., Yi, Y., Rexford, J., and Chiang, M. Rethinking virtual network embedding: substrate support for path splitting and migration. SIGCOMM Comput. Commun. Rev. 38, 2 (Mar. 2008), 17–29.

[125] Yuan, D., Yang, Y., Liu, X., and Chen, J. A data placement strategy in scientific cloud workflows. Future Generation Computer Systems 26, 8 (2010), 1200 – 1214.

[126] Zelkowitz, M. Advances in Computers. Academic Press, 2005.

[127] Zelkowitz, M. V. Advances in Computers. vol. 82. Elsevier, 2011.

[128] Zhang, B., Kreitz, G., Isaksson, M., Ubillos, J., Urdaneta, G., Pouwelse, J. A., and Epema, D. Understanding user behavior in spotify. In IEEE INFOCOM (2013).

[129] Zhang, M., Zhang, Q., Sun, L., and Yang, S. Understanding the power of pull-based streaming protocol: Can we do better? IEEE J. Selected Areas in Communications 25, 9 (2007), 1678.

[130] Zhang, X., Chen, X., and Phillips, C. Achieving effective resilience for QoS-aware application mapping. Computer Networks 56, 14 (2012), 3179 – 3191.

[131] Zhou, R., Wang, Z., McReynolds, A., Bash, C. E., Christian, T. W., and Shih, R. Optimization and control of cooling microgrids for data centers. In Thermal and Thermomechanical Phenomena in Electronic Systems (ITherm), 2012 13th IEEE Intersociety Conference on (2012), IEEE, pp. 338–343.

[132] Zhu, Y., and Ammar, M. H. Algorithms for Assigning Substrate Network Resources to Virtual Network Components. In INFOCOM (2006), pp. 1–12.

VITA

Xinjie Guan received her B.S. degrees from Southeast University in 2006. In August 2009, she joined the Ph.D. program in University of Missouri-Kansas City (UMKC) with Telecommunications and Computer Networking (TCN) as her coordinating discipline, and Computer Science as her co-discipline. Her got her M.S. degrees from UMKC in 2014. Her research interests include network optimization, network traffic measurement, analysis and modeling, cloud computing and software defined networks. During her Ph.D. study, she interned at the Service Integration Lab of NTT in Japan and Huawei Innovation Center in USA for researches on large scale traffic measurement, and future network architecture, respectively. She received a fellowship from NSF/GENI to attend the first GENI summer camp at RIT, June 2012 and received a GENI travel grant for GEC16, 2013. She was the winner of Grace Hopper MINK WIC Poster contest, and received an ACM-W travel grant to attend the 2014 Grace Hopper Celebration of Women in Computing, 2013. She has received UMKC Women's Council Graduate Assistance Fund Scholarship, 2014 and 2015, respectively. One of her paper was selected as the track best paper of ICCCN 2014, and fast track to Elsevier Computer Communications.